

HOM findings and HOM induced power in the superconducting linac of the intense pulsed proton accelerator

SNS/AP TECHNICAL NOTE

Number 10

Sang-ho Kim¹, Marc Doleans¹,

Ronald Sundelin
TJNAF

August 29, 2001

¹)Spallation Neutron Source Project
Oak Ridge National Laboratory
Oak Ridge, TN 37830

Technical note (Draft)

**HOM findings and HOM induced power
in the superconducting linac of the intense pulsed
proton accelerator**

(HOM findings, HOM properties, HOM Power
& damping requirement in SCL of SNS)

Sang-ho Kim, Marc Doleans, and *Ronald Sundelin

SNS/ORNL
*SNS/Jlab

August, 2001

ABSTRACT

Higher order modes (HOM's) of monopoles, dipoles, quadrupoles and sextupoles in $b=0.61$ and $b=0.81$ 6-cell superconducting cavities for the Spallation Neutron Source (SNS) project, have been found up to about 3 GHz and their properties such as R/Q, trapping possibility, etc have been figured out in concerning with the manufacturing imperfection.

Main HOM related issues are the beam instabilities and the HOM induced power especially from TM monopoles. The analysis for the beam instability from HOM showed that it is not an issue in SNS [1, 2].

The time structure of SNS beam has three different time scales of pulses, which are micro-pulse, midi-pulse and macro-pulse. Each time structure will generate resonances. When a mode places near these resonance frequencies, the induced voltage could be large and accordingly the resulting HOM power, too. In order to understand the effects from such a complex beam time structure on the mode excitation and resulting HOM power, analytic expressions are developed. With these analytic expressions, the induced HOM voltage and HOM power were calculated by assuming external Q for each HOM. The results and understandings from this analysis are presented in this technical note.

The purpose of the present study is to determine specific higher order mode (HOM) damping requirements for both betas in order to deal in an acceptable fashion with HOM power generated.

I. INTRODUCTION

Two main HOM related issues were concerned. One is the beam instabilities in both transverse and longitudinal directions, and the other is HOM induced power. In order to investigate these effects on the SNS, a systematic studies explained in Figure I-1 are done.

HOM's are found with the MAFIA eigen value solver [1] and HOM properties such as frequencies, R/Q's, field profiles, mode trapping possibilities, etc. are investigated. The effects on the HOM induced voltages from the multi-time structure of the beam in SNS SC linac are studied extensively. With these HOM information and induced voltages from the SNS beam time structure, the beam instability simulations and the HOM induced power analysis were carried out. The bunch tracking simulations for both transverse and longitudinal direction showed that the beam instabilities are not main concerning in SNS if the external quality factor Q_{ex} for each mode is less than 10^8 , the loaded cavity Q for each non-pi fundamental mode has the expected value, and the expected cavity-to-cavity frequency variation is present [2], [3]. These works correspond to the open boxes in Figure 1.

The SNS beam has three different time structures of the beam pulses, which are micro-pulse, midi-pulse and macro-pulse. Each time structure will generate resonance. In order to understand the effects from such a multi-time structure of the beam on the mode excitation and the resulting HOM power, analytic expressions are developed.

The main objective of this work is to determine whether the HOM coupler is required or not, and to provide damping levels for each HOM if the HOM coupler is required. In this technical note, the gray colored parts in Figure 1 are covered.

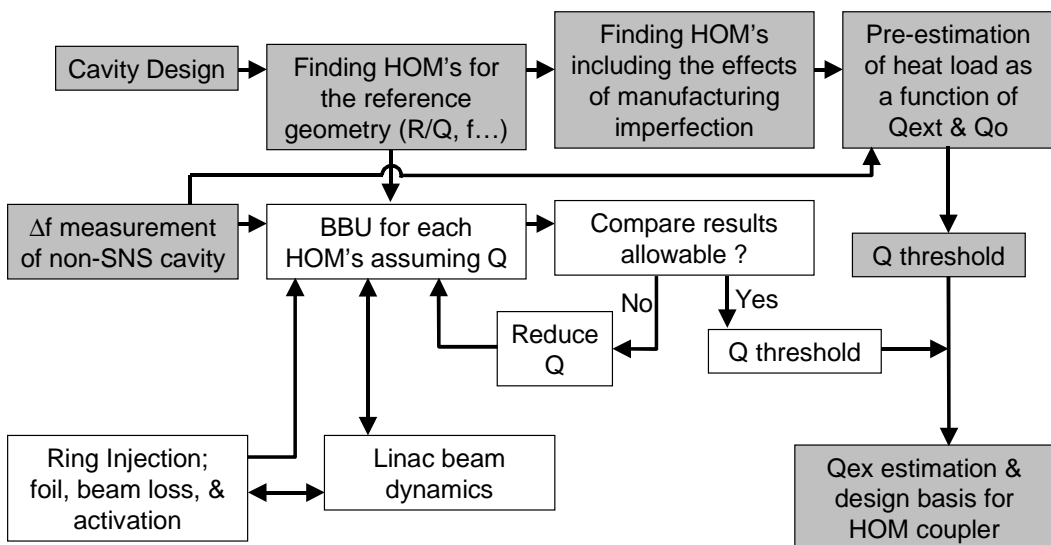


Figure I-1. Block diagram of HOM analysis

II. HOM FINDINGS and THEIR PROPERTIES

HOM's of monopoles, dipoles, quadrupoles and sextupoles are found up to about 3 GHz with MAFIA eigen-value solver for both medium ($\beta=0.61$) and high beta ($\beta=0.81$) cavities. The beam pipe diameter is 3 inches and the corresponding cutoff frequencies of the waveguide modes for this beam pipe are TE11; 2.324GHz, TM01; 3.036 GHz, TE21; 3.855 GHz, and TE01/TM11; 4.837 GHz. TM-monopoles and TE-dipoles above their cutoff frequencies will propagate in the beam pipes which are normal conducting material (stainless steel) and it will provide significant damping. This phenomenon is shown in section II-3 and in Appendix B and C. And the mode impedances decrease with their frequencies as shown in Figure II-3 and in Appendix B and C. So the mode findings up to about 3 GHz in the SNS 805 MHz SC cavity are enough for both beam instability analysis and HOM power analysis which is especially for the TM-monopoles.

Since the beam instability due to the HOM induced voltage is not an issue in SNS SC linac [1], [2] and the their cutoff frequencies are higher than 3 GHz except TE dipole, the multipoles (dipole, quadrupole, sextupole) findings are done with the single cavity model in which the conical ends are attached at both ends. The TM monopoles are analyzed in detail since the other main issue of HOM is the HOM power from the TM monopoles and the their HOM properties are quite sensitive at the frequency near cutoff frequency or higher. All data are summarized in Appendices. Here major considerations devoted to finding of HOM are described.

II-1. Benchmarking

TM monopoles from the MAFIA and the SUPERFISH are compared in order to find the proper input condition and to confirm the further MAFIA results (see. Appendix A). Both results agree well.

II-2. R/Q definitions

The R/Q used here is effective one that is seen by the particle, which is defined;

- TM-monpoles

$$\frac{R}{Q} = \frac{\left| \int E_z(z) \exp(i\omega z/v) dz \right|^2}{\omega U} \text{ in Ohm (For more details about this definition, see Appendix A)}$$

- Dipoles, quadrupoles and sextupoles

$$\frac{R}{Q} = \frac{c^2 \left| \int \nabla_r E_z \exp(i\omega_n z/v) dz \right|^2}{\omega_n^3 U} \text{ in Ohm.}$$

In order to have the general expression of the R/Q for the multipoles (dipoles, quadrupoles and sextupoles), the radial gradient of the axial electric fields are examined, that are shown in Figure II-1 to II-3. The index numbers around axis are close to 1, 2, and 3 for dipole, quadrupole and sextupole respectively. Hereafter the R/Q's for the multipoles are evaluated at the position of 1 cm from the axis and their units are Ohm, Ohm/cm² and Ohm/cm⁴ for dipole, quadrupole and sextupoles respectively. When the R/Q's at certain radial position is needed, one can have the corresponding R/Q by multiplying square and fourth power of that radial position for quadrupole and sextupole respectively.

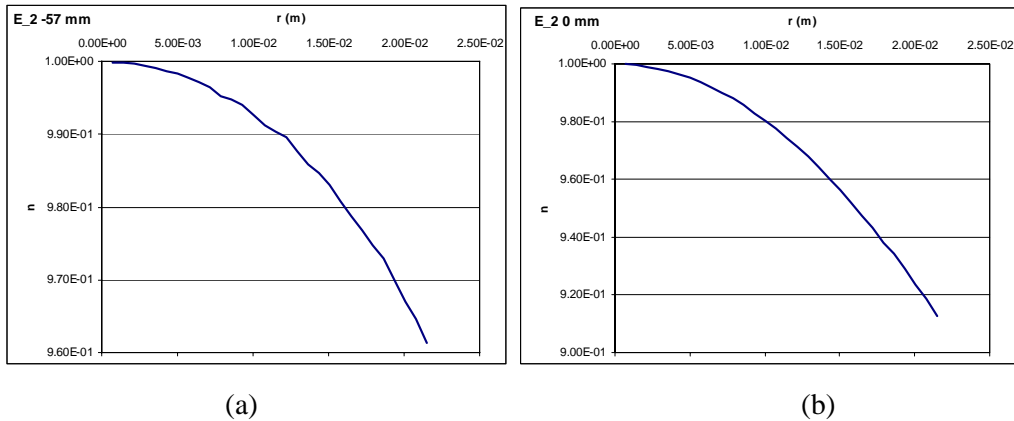


Figure II-1. Typical examples of the radial gradient of the axial electric field ($E_z \propto r^n$) for the dipole. (a) at the equator plane (b) at the iris plane of the cavity.

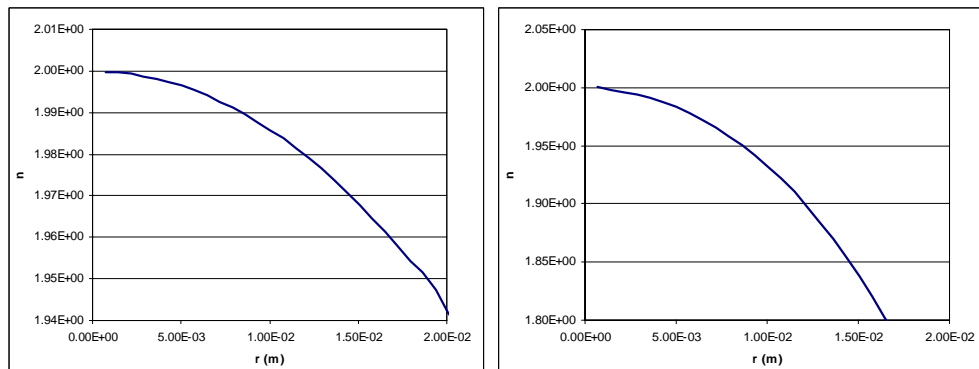


Figure II-2. Typical examples of the radial gradient of the axial electric field ($E_z \propto r^n$) for the quadrupole. (a) at the equator plane (b) at the iris plane of the cavity.

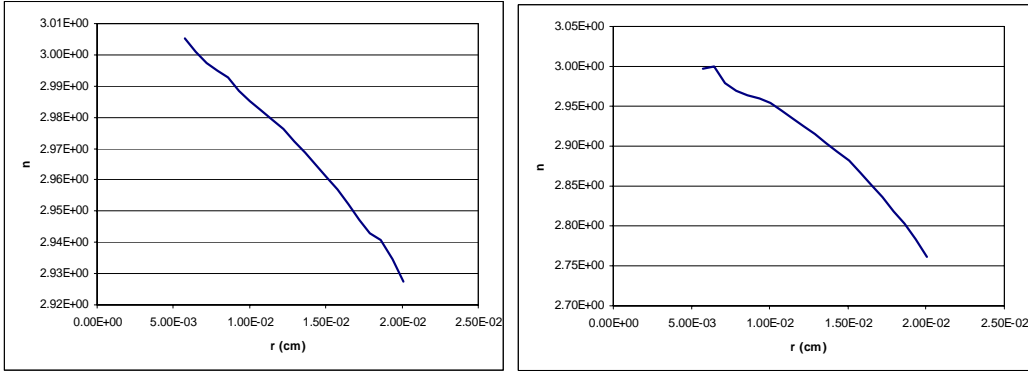


Figure II-3. Typical examples of the radial gradient of the axial electric field ($E_z \propto r^n$) for the sextupole. (a) at the equator plane (b) at the iris plane of the cavity.

II-3. HOM findings

All details are summarized in Appendix B and C. Here some considerations throughout the HOM finding procedures are explained with typical results as examples.

First, forty TM-monopoles, forty-five dipoles, thirty quadrupoles and twenty sextupoles, and their R/Q's as a function of beta are found with the single cavity modeling in which the conical ends are attached at both ends in order to eliminate any artificial impedance for both medium and high beta cavity. Figure II-4 shows some examples of TM-monopoles and their R/Q's as a function of the particle velocity.

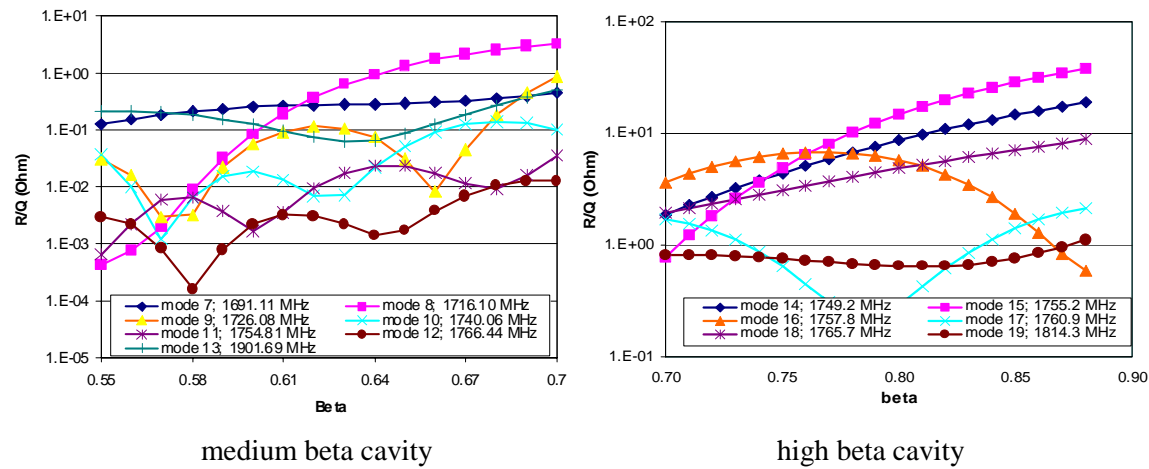


Figure II-4. Examples of TM-monopoles and their R/Q's as a function of particle velocity.

And Figure II-5 and II-6 are plots of the maximum R/Q's for each mode in the particle velocity ranges of both beta cavities. Generally the R/Q decreases with increasing the frequency and the azimuthal degree of the mode.

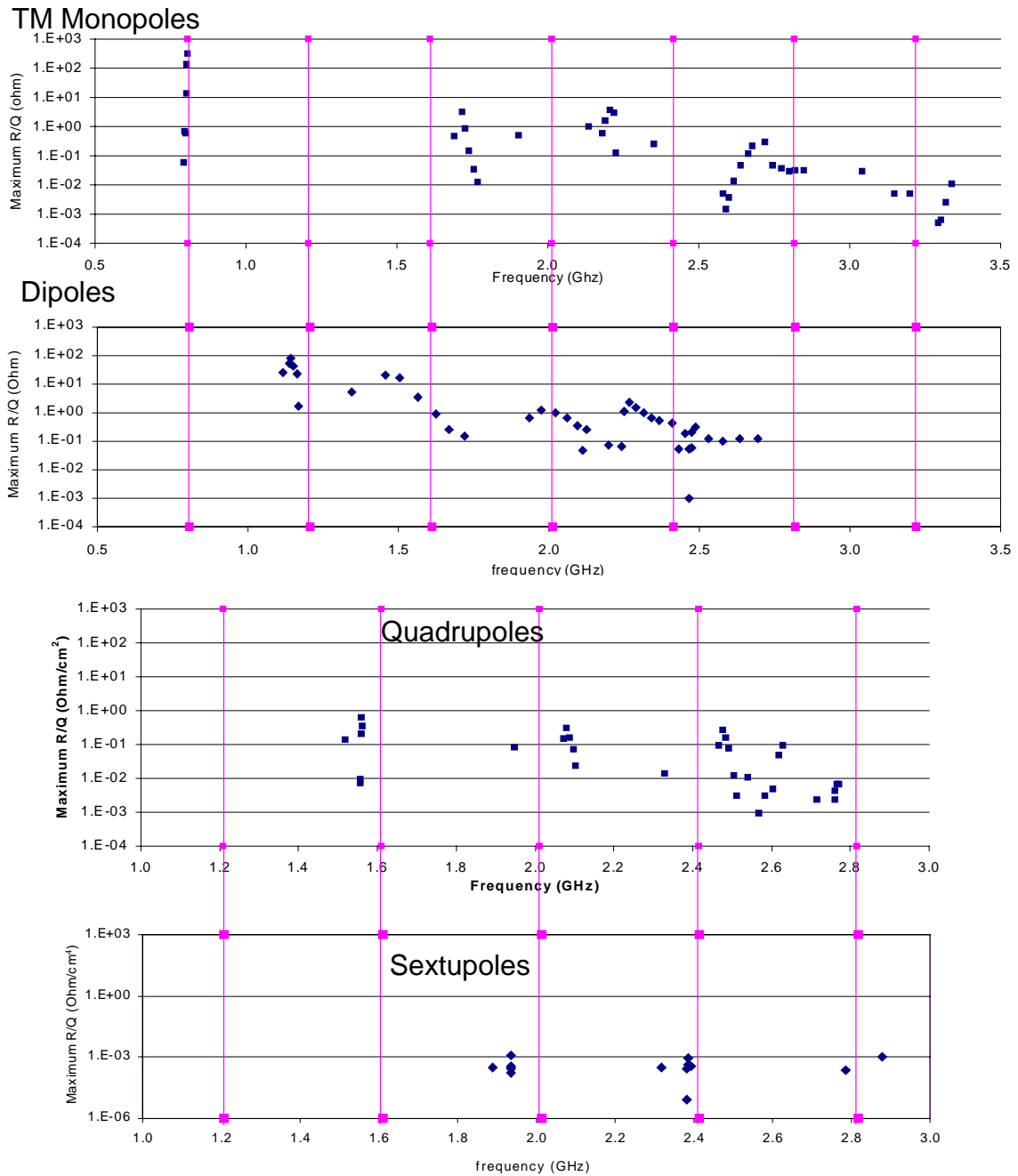
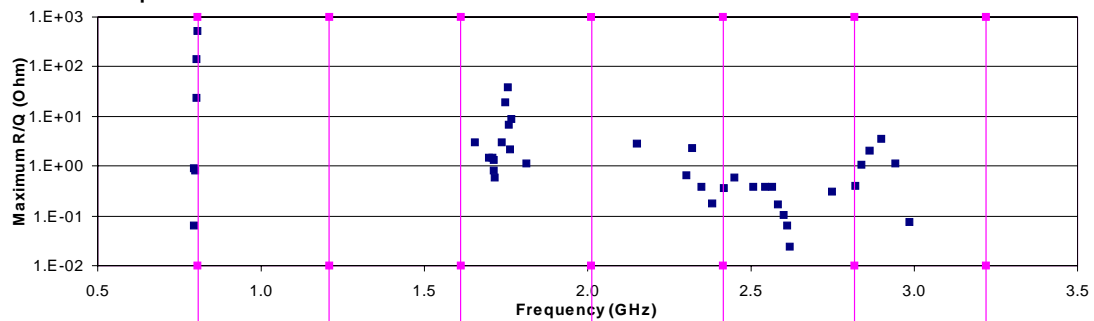
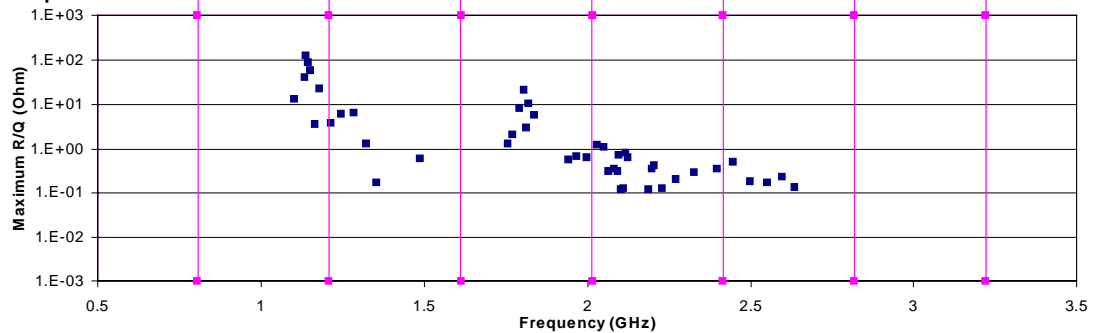


Figure II-5. Maximum R/Q's of medium beta cavity for each mode in the ranges of particle velocity from beta=0.55 to beta=0.7 (single cavity analysis results)

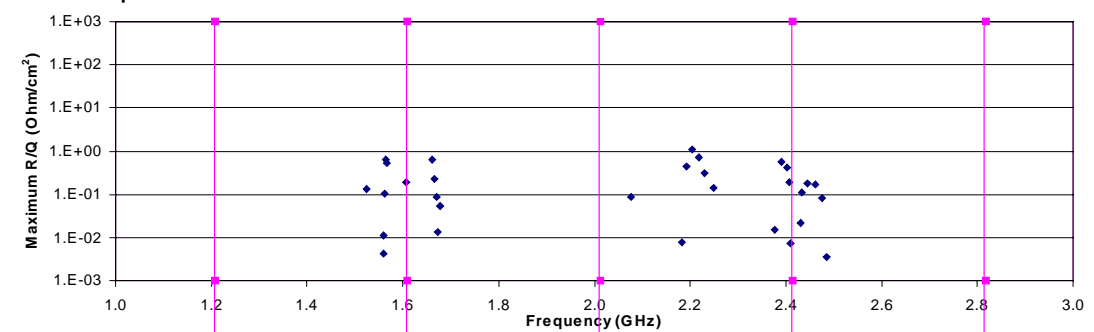
TM Monopoles



Dipoles



Quadrupoles



Sextupoles

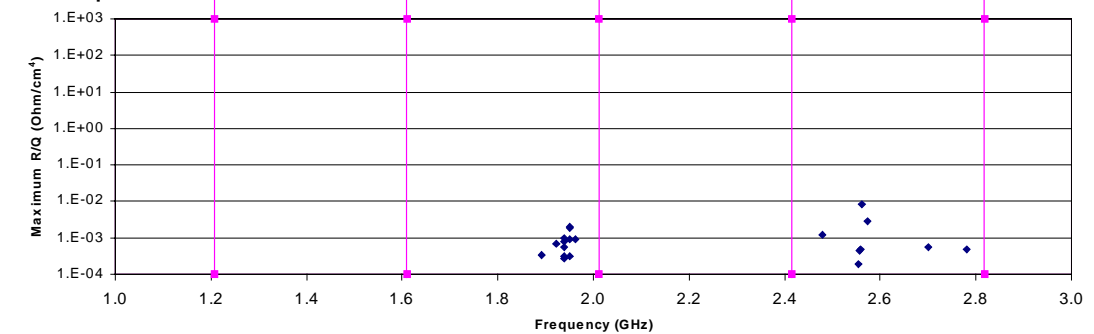


Figure II-6. Maximum R/Q's of high beta cavity for each mode in the ranges of particle velocity from beta=0.7 to beta=0.88 (single cavity analysis results)

For the modes confined well in a cavity, affections of the boundary shape or condition to the HOM electromagnetic properties are quite small. Figure II-7 is an example of this kind of mode. The field shapes are almost identical and the difference in R/Q is negligible.

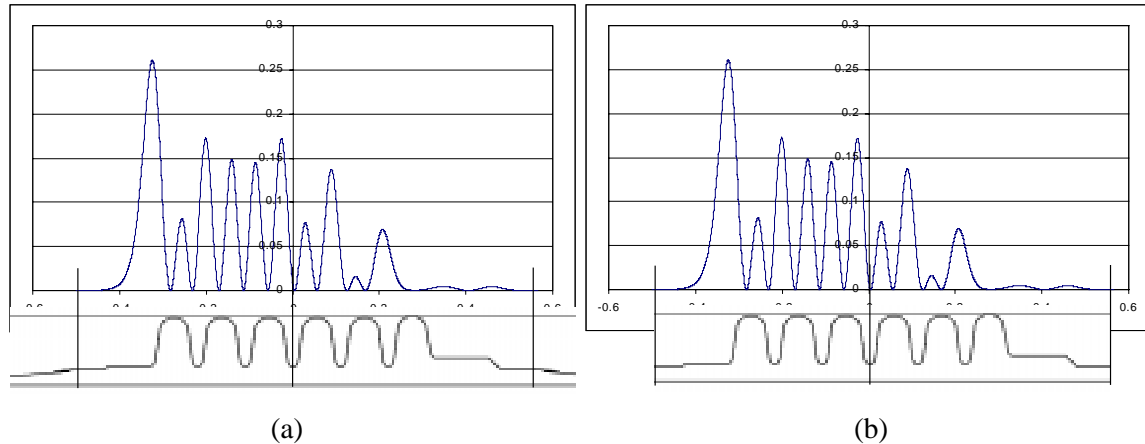


Figure II-7. Plots of the square of the axial electric field on axis for two different boundary conditions. Example of the boundary condition comparison of the well-confined mode (medium beta cavity TM monopole mode 19). (a) conical end boundary, (b) terminated with electric field normal condition.

But the dependencies on the beam pipe length and the boundary condition could be significant for the beam pipe modes, the propagation modes, or the coupled modes between the cavity modes and beam pipe modes, which results in the artificial impedance when the electric field normal boundary condition is applied to the end-side boundary and gives rise to an overestimation of R/Q. In the other hand, artificial suppressing of the field with the conical end boundary could give rise to underestimation of R/Q's.

Table II-1 and II-2 summarize the TM monopoles found with the boundary terminated by the electric field normal condition and the conical end boundary. The frequencies are very close but the some modes show big discrepancies in R/Q's, which are marked with red or gray. The gray-colored modes are not realistic one (This will be explained later). When the beam pipe length varies, the R/Q's change in the electrically terminated boundary condition. That means there are artificial developments of the mode impedances. In the other hand, when the field exists in the beam pipe, the conical end boundary could suppress the field that places at the ends. In this case the conical end boundary could give rise to an underestimation of R/Q.

In order to clarify these modes that are unclear with the single-cavity analysis, one-cryostat superstructure analyses are done especially for the TM-monopoles.

Table II-1. Comparisons of the boundary shape and condition of the SNS medium beta cavity

mode no.	electric boundary		conical end		Differences of R/Q
	frequency Hz	max R/Q Ohm	frequency Hz	max R/Q Ohm	$ e-c /c \times 100 \%$
1	7.93795E+08	0.0721	7.93795E+08	0.0603	19.53
2	7.96049E+08	0.5851	7.96049E+08	0.6896	15.15
3	7.99111E+08	0.7142	7.99111E+08	0.5842	22.25
4	8.02090E+08	12.6903	8.02090E+08	13.3786	5.14
5	8.04189E+08	130.5981	8.04189E+08	131.2810	0.52
6	8.05005E+08	303.9157	8.05005E+08	304.9984	0.35
7	1.69143E+09	0.4538	1.69111E+09	0.4528	0.21
8	1.71679E+09	3.1641	1.71610E+09	3.1914	0.85
9	1.72672E+09	0.8545	1.72608E+09	0.8763	2.48
10	1.74080E+09	0.1399	1.74006E+09	0.1415	1.07
11	1.75569E+09	0.0329	1.75481E+09	0.0351	6.16
12	1.76737E+09	0.0132	1.76644E+09	0.0129	1.89
13	1.90186E+09	0.5231	1.90169E+09	0.4999	4.63
14	2.13509E+09	1.0666	2.13500E+09	1.0225	4.32
15	2.17888E+09	0.4659	2.17910E+09	0.6016	22.55
16	2.19113E+09	1.5279	2.19122E+09	1.5503	1.44
17	2.20604E+09	3.6427	2.20608E+09	3.6322	0.29
18	2.21909E+09	2.9242	2.21909E+09	2.9434	0.65
19	2.22665E+09	0.1304	2.22694E+09	0.1291	1.04
20	2.35116E+09	0.3444	2.35078E+09	0.2483	38.71
21	2.58237E+09	0.0164	2.58197E+09	0.0050	228.06
22	2.59120E+09	0.0067	2.59046E+09	0.0014	364.40
23	2.60162E+09	0.0167	2.60096E+09	0.0036	364.26
24	2.61758E+09	0.0304	2.61692E+09	0.0136	123.30
25	2.63887E+09	0.0986	2.63831E+09	0.0482	104.37
26	2.66652E+09	0.2606	2.66595E+09	0.1209	115.61
27	2.67872E+09	0.4958	2.67867E+09	0.2237	121.63
28	2.71944E+09	0.1916	2.71875E+09	0.2830	32.30
29	2.74571E+09	0.2378	2.74541E+09	0.0460	417.48
30	2.77449E+09	0.2431	2.77443E+09	0.0363	569.53
31	2.80099E+09	0.2606	2.80098E+09	0.0283	822.41
32	2.82068E+09	0.1756	2.82063E+09	0.0307	471.47
33	2.84209E+09	1.8099	2.84821E+09	0.0321	5538.71
34	3.03196E+09	4.7290	3.04294E+09	0.0298	15749.93
35	3.11635E+09	12.7983	3.14895E+09	0.0051	250146.68
36	3.15884E+09	17.4399	3.20072E+09	0.0049	352733.99
37	3.29305E+09	0.0763	3.29303E+09	0.0005	14602.73
38	3.30336E+09	0.4657	3.30321E+09	0.0007	71400.90
39	3.32204E+09	1.7741	3.32019E+09	0.0026	68233.45
40	3.34418E+09	4.3834	3.33724E+09	0.0112	39129.69

%% The R/Q's of electric boundary in red color depends on their beam pipe length in the model

Table II-1. Comparisons of the boundary shape and condition of the SNS high beta cavity

	electric boundary		conical end		Differences of R/Q
mode no.	frequency Hz	max R/Q Ohm	frequency Hz	max R/Q Ohm	e-c /c*100 %
1	7.93629E+08	0.0593	7.93629E+08	0.0663	10.55
2	7.95869E+08	1.0403	7.95869E+08	0.9241	12.57
3	7.98919E+08	0.6815	7.98919E+08	0.8047	15.32
4	8.01954E+08	25.6890	8.01954E+08	24.0066	7.01
5	8.04172E+08	145.4552	8.04172E+08	145.2854	0.12
6	8.04979E+08	516.3855	8.04979E+08	517.3664	0.19
7	1.65461E+09	2.9357	1.65457E+09	2.9940	1.95
8	1.69950E+09	1.5177	1.69962E+09	1.5155	0.14
9	1.70721E+09	1.4723	1.70749E+09	1.4677	0.32
10	1.71022E+09	1.3263	1.71052E+09	1.3168	0.72
11	1.71332E+09	0.7985	1.71370E+09	0.8277	3.52
12	1.71528E+09	0.6689	1.71563E+09	0.5969	12.06
13	1.73666E+09	3.0292	1.73695E+09	3.0718	1.39
14	1.74890E+09	19.5418	1.74926E+09	18.9111	3.34
15	1.75467E+09	37.2318	1.75522E+09	37.6973	1.23
16	1.75734E+09	6.6906	1.75780E+09	6.8309	2.05
17	1.76052E+09	2.0674	1.76088E+09	2.1532	3.98
18	1.76545E+09	8.9015	1.76567E+09	8.8147	0.98
19	1.81358E+09	0.6737	1.81342E+09	0.7512	10.32
20	2.14683E+09	2.3852	2.14631E+09	2.4904	4.22
21	2.30150E+09	0.6177	2.30243E+09	0.6209	0.51
22	2.31987E+09	1.9746	2.32069E+09	2.0407	3.24
23	2.34637E+09	0.3636	2.34716E+09	0.3387	7.36
24	2.37863E+09	0.1402	2.37932E+09	0.1665	15.77
25	2.41399E+09	0.3232	2.41457E+09	0.3474	6.99
26	2.44504E+09	0.5185	2.44580E+09	0.5682	8.76
27	2.49832E+09	0.1575	2.49981E+09	0.3800	58.57
28	2.54152E+09	0.2511	2.54140E+09	0.2416	3.94
29	2.56223E+09	0.2248	2.56249E+09	0.3643	38.29
30	2.58161E+09	0.1191	2.58186E+09	0.1544	22.86
31	2.59821E+09	0.0515	2.59817E+09	0.0650	20.74
32	2.61033E+09	0.0269	2.61004E+09	0.0369	26.88
33	2.61721E+09	0.0166	2.61678E+09	0.0072	128.78
34	2.73843E+09	0.7535	2.73812E+09	0.3300	128.33
35	2.81447E+09	0.8800	2.81596E+09	0.4117	113.77
36	2.82887E+09	1.1891	2.83079E+09	1.0048	18.34
37	2.85618E+09	1.9617	2.85801E+09	1.8934	3.60
38	2.89234E+09	2.9933	2.89410E+09	3.0068	0.45
39	2.93255E+09	4.2102	2.93447E+09	1.2030	249.96
40	2.97395E+09	2.3066	2.97638E+09	0.0583	3855.78

%% The R/Q's of electric boundary in red color depends on their beam pipe length in the model

Figure II-8 shows the squares of axial electric field on axis from three different runs. Here we can see the artificially developed electric field and also field profile itself is modified by the fact of the unrealistic boundary condition in (b).

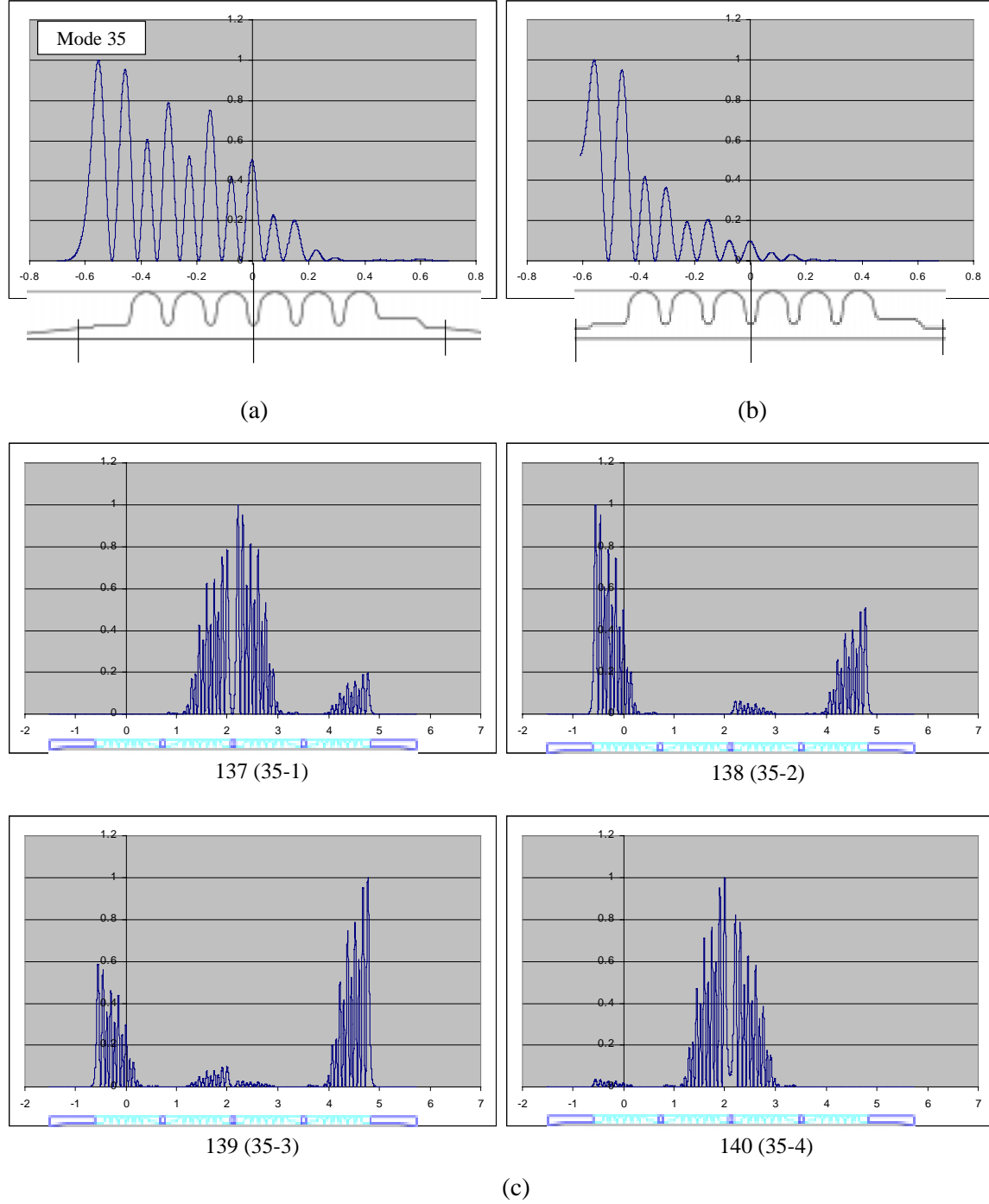


Figure II-8. Plots of the square of the axial electric field on axis. Example of the boundary condition comparison of the ill-confined mode (high beta cavity TM monopole mode 35). (a) conical end boundary, (b) terminated with electric field normal condition, and (c) super-structure.

In super-structure analysis, the dimensions of each cavity are a little bit different from each other due to the fact of mafia meshing scheme. And the modes that partially have beam pipe mode component would be excited in different way since the cavity is asymmetry and the orientations of the cavities vary. From these two reasons, the four similar modes are normally found with the super-structure model. Table II-3 shows the examples for R/Q comparisons in the high beta cavity among 4-cavity super-structure analysis results and the two single-cavity analysis results with different boundary conditions.

Table II-3. Examples for comparison of R/Q's with super-structure results for high beta cavity.

electric boundary			conical end		super-structure (4 cavities)			one cavity in super-structure	
mode no.	frequency Hz	max R/Q Ohm	frequency Hz	max R/Q Ohm	mode no.	frequency Hz	Max R/Q Ohm	highly excited cavity	Max R/Q Ohm
34	2.73843E+09	0.753455	2.73812E+09	0.329981	133	2.73806E+09	0.504775	4th	0.37894
					134	2.73816E+09	0.694499	2nd	0.32067
					135	2.73833E+09	0.791331	3rd	0.32036
					136	2.73823E+09	0.51047	1st	0.31712
35	2.81447E+09	0.880043	2.81596E+09	0.411669	137	2.81540E+09	0.627341	3rd	0.50162
					138	2.81576E+09	0.643673	1st	0.39224
					139	2.81555E+09	0.543017	4th	0.41592
					140	2.81556E+09	0.804426	2nd	0.73458
36	2.82887E+09	1.189141	2.83079E+09	1.004816	141	2.83064E+09	1.763105	2nd	1.08726
					142	2.83046E+09	1.622125	4th	0.97109
					143	2.83016E+09	2.336633	3rd	1.33939
					144	2.83008E+09	2.226843	1st	0.96477
37	2.85618E+09	1.961684	2.85801E+09	1.893445	145	2.85782E+09	3.621073	2nd	1.96636
					146	2.85752E+09	3.098627	1st	1.94032
					147	2.85719E+09	3.235713	4th	1.81778
					148	2.85730E+09	2.361658	3rd	2.63480
38	2.89234E+09	2.99331	2.89410E+09	3.006771	149	2.89364E+09	3.905259	4th	3.07926
					150	2.89339E+09	3.083761	2nd	4.19912
					151	2.89337E+09	4.08833	1st	3.14343
					152	2.89375E+09	4.761967	3rd	3.04771
39	2.93255E+09	4.210214	2.93447E+09	1.203049	153	2.93384E+09	1.18511	4th	1.11348
					154	2.93391E+09	1.264367	1st	1.03560
					155	2.93351E+09	1.329471	3rd	0.85042
					156	2.93414E+09	1.01928	2nd	1.28965
40	2.97395E+09	2.306584	2.97638E+09	0.058309	157	2.97490E+09	0.055745	2nd	0.55086
					158	2.97548E+09	0.07999	4th	0.16566
					159	2.97604E+09	0.128743	3rd	0.09558
					160	2.97555E+09	0.08836	1st	0.05664

%% The R/Q's of electric boundary depends on their beam pipe length in the model

The R/Q's of super-structure correspond to one cryostat (4 cavities). So generally the maximum of the R/Q's of super-structure would be larger than those of single cavity, which depends on the

transit time. The transit time is a function of the mode frequency, the particle velocity, and the mode frequency. So the comparison with R/Q's along the whole 4-cavity is not fair.

Table II-3 also shows the maximum R/Q's of the highly excited cavity in the super-structure of the high beta cavity in the particle velocity range for the fair comparison. The highly excited cavities are counted from the left in the super-structure model shown in Figure II-8. Most of the modes from the super-structure analysis have very close properties with those from the single cavity analysis with conical ends. But some modes have similar behaviors with those from the electric boundary condition. For example the mode 137, 138, and 139 from the super-structure modeling are same with the mode 35 from the single cavity modeling with conical ends, and the mode 140 is have properties close to the mode 35 from the single cavity modeling with electric boundary. So a single cavity modeling with conical ends is enough for the estimation of HOM properties in most cases (mode 34 or less in the high beta cavity). But the modes, whose frequencies are close to the cutoff frequency, have intermediate R/Q values between those from conical ends boundary and from electric boundary condition.

In medium beta cavity, there's no mode that have similar filed profile with that of electric boundary condition.

II-4. Beam pipe modes between cavities and propagation modes

It is difficult to figure out the beam pipe modes and the propagation modes to the warm section with the results from the single cavity modeling, which could also result in some artificial modes. These kinds of problems are also cleared by the results from the super-structure modeling.

Figure II-9 shows typical examples of beam pipe mode and propagation mode. The beam pipe mode is realistic one trapped between cavities where the stainless steel bellows are. The modes like the bottom of Figure II-9 are propagation modes. The field profile of this propagation mode is not realistic one, it is just artificially created by the confined boundaries. This kind of modes is found at the frequency of cutoff or higher; from mode 100 ($f=3.038326e9$) in medium beta cavity and from mode 165 ($f=3.03902e9$) in high beta cavity. The cutoff frequency of the beam pipe in SNS cavities is $3.036e9$ Hz. (see the Appendix B and C for the field profiles). And also the propagation modes are not a major concern since these modes will damp strongly on the stainless less beam pipes. Some modes have hybrid properties of the beam pipe mode, the propagation mode, and the cavity mode especially in high beta cavity. Anyway these modes locate in the highly damping region intrinsically, which are stainless steel bellows between cavities and stainless steel beam pipes at the end of cryostat or in warm section. In Appendix B and C, the

unloaded Q values, Qo's are summarized. These modes have Qo less than 10^5 that could be used as an upper limit of the Q for the beam instability analysis and the HOM power estimation. These intrinsic damping effects are seen even in the normal cavity modes as shown in Table II-3.

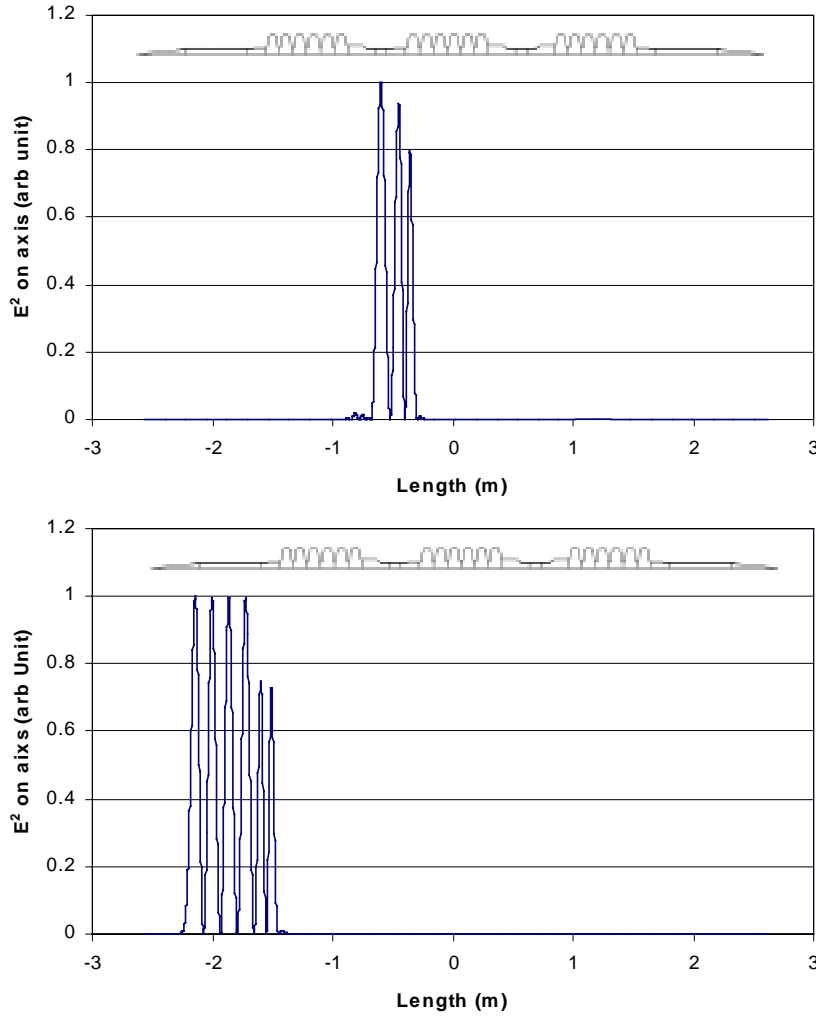


Figure II-9. Examples of the beam pipe mode (top; mode 113, $f=3.1827e9$) and the propagation mode (bottom; mode 114, $f=3.12122e9$) in medium beta super-structure.

The TM monopoles 35 and 36 or higher in medium beta cavity and the TM monopoles 43 or higher in high beta cavity founded with single cavity models are unrealistic modes, those are generated from artificial boundary condition. In Appendix B and C, the modes are compared, that founded from the single cavity model and the super-structure model in terms of frequencies, R/Q's, and axial field profiles.

II-5. Searching of mode trapping

Trapped mode is difficult to extract through the HOM coupler since this mode is confined well in the inner-cell of a cavity, so the coupling with the HOM coupler is very small. Although the coupling strength is related the shape and the orientation of the HOM coupler, the field profiles and strengths of HOM at around the HOM coupler, etc, the following simple criteria are used as a preliminary definition of the trapped mode.

-for monopoles, the stored energy in both end cell and beam pipe combined < 0.1 % of total stored energy

-for multipoles, the stored energy in each end cell and beam pipe < 0.1 % of total stored energy

Two HOM couplers will be attached for each cavity at each end. The multipoles generally have two polarizations in cylindrically symmetry cavity, which is the reason for the criterion of multipole trapping. The possible trapped modes are searched for the perturbed cavity geometry by applying random mechanical manufacturing imperfections also for the reference geometry. The trapping is governed by the original reference cavity geometry. The details are summarized in Appendix D.

There's no TM monopole that satisfies the above tapped mode criterion in both medium and high beta cavity. The modes 15 and 16 of high beta TM monopole are possibly trapped mode.

Among dipoles and quadrupoles, several trapped modes are found. But the most of fields of all these trapped mode of dipole and quadrupoles are placed in the other end cell and beam pipe where the intrinsic damping from normal conducting stainless bellows or beam pipes exists. The Q_o of these trapped modes are less than 10⁸.

Several sextupoles are trapped modes whose fields exist only in inner-cells. The Q_o of these trapped mode will be higher than 10⁸ but the R/Q's are less than 10⁻³ and the modes frequencies are far from the micro pulse beam spectral lines which will be explained in the following chapter.

III. Time Structure of SNS Beam & HOM Induced Voltage

The SNS beam has a time structure shown in figure III-1. Micro-bunches are separated by about 2.5 ns which corresponds to 402.5 MHz. A midi-pulse is composed of about 260 micro bunches and there's about 300 ns gap for the injection to the accumulator ring. The midi-pulse period T_i corresponds to the ring revolution time. About 1000 midi-pulses build up one macro pulse whose repetition rate is 60 Hz. The midi-pulse length would vary depending on the operation condition and the beam energy.

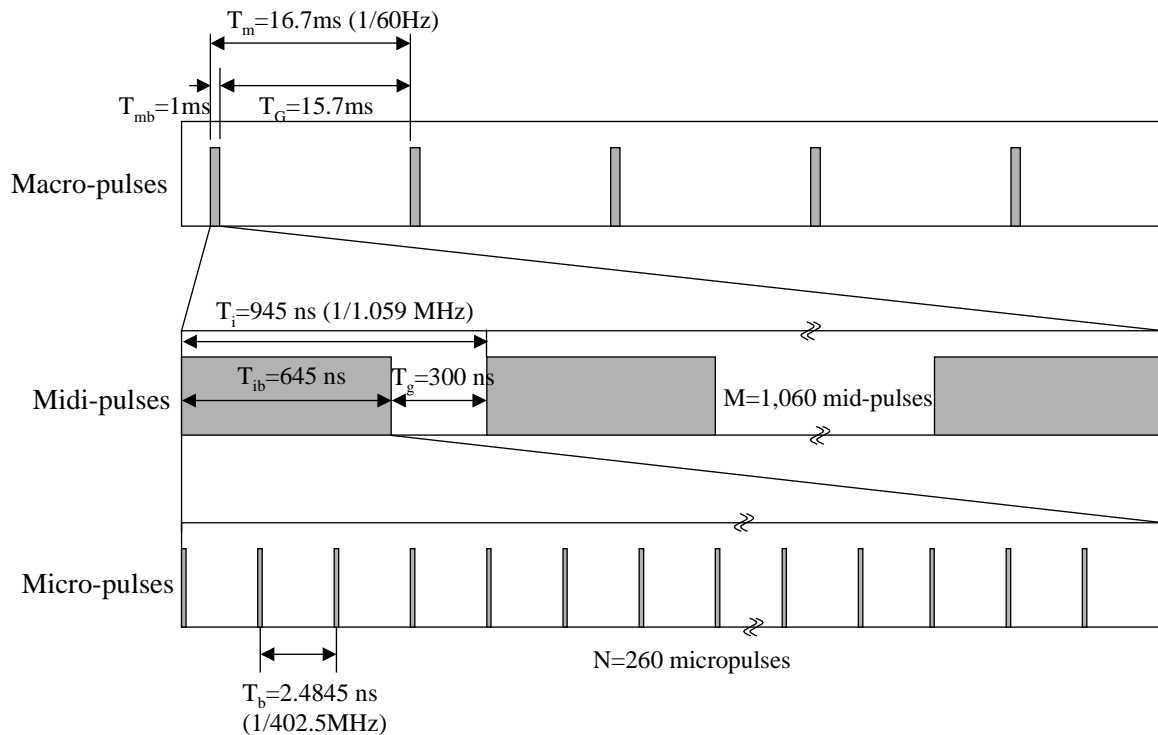


Figure III-1. Time structure of SNS beams in the Linac (The midi-pulse lengths, T_i , T_{ib} , and T_g will vary depending on operation condition and beam energy. This example is for the 1 GeV nominal operation).

As a charge q passes a cavity on axis, monopoles are excited and their induced voltages in the loss-free cavity are;

$$\tilde{V}_q = \frac{\omega_n}{2} \frac{R}{Q} |q| \exp(i\omega_n t) = V_q \exp(i\omega_n t),$$

and the acting voltage back on the charge itself is ;

$$V_{self} = V_q / 2,$$

where ω_n is the HOM frequency, R/Q has same definition in the previous chapter (effective one), q is the point charge and the time t is set to zero when the point charge passes the cavity.

When the decay term is included, the actual voltage behavior in a cavity can be written as;

$$V_q \exp(i\omega_n t) \exp(-t/T_d),$$

where the first exponential term represents the oscillation of HOM with time, the second exponential term corresponds the decay due to losses such as wall loss, outgoing power to the coupler, etc, and the decay time constant T_d is determined by the external Q for each mode having the relation of $T_d = 2Q_{ex}/\omega_n$.

When the beam has single time structure such as the micro-pulses in Figure III-1, the analytic expression is pretty simple [3].

$$V = V_q \sum_{n=0}^{\infty} \exp(in\omega_n T_b - n \frac{T_b}{T_d}) = \frac{V_q}{1 - \exp(i\omega_n T_b - T_b/T_d)}$$

For the gaussian profile bunch, the corresponding induced voltage can be written,

$$\tilde{V}_q = \frac{\omega_n}{2} \frac{R}{Q} Q_b \exp\left(-\frac{\omega_n^2 \sigma_t^2}{2}\right) \exp(i\omega_n t),$$

where Q_b is the total charge in a bunch, $\sigma_z = \beta c \sigma_t$ is the standard deviation of the bunch length. If $\omega_n \ll 1/\sigma_t$, the induced voltage from the gaussian bunch is much smaller than that from a point charge. In the SNS case, $\omega_n < 1/\sigma_t$, for the HOM frequencies less than 3 GHz. For example of $f_n = 2.0$ GHz, and 5 degree of 805 MHz bunch span with the speed of $\beta = 0.9$, the gaussian factor is 0.97, while that is about 0.85 for $f_n = 2.0$ GHz, and 8 degree of 805 MHz bunch span at the speed of $\beta = 0.6$. So the assuming the point charge is not so pessimistic but a little bit conservative. Hereafter, the point charge will be assumed.

The peak macro-pulse beam current in the linac is 38.2 mA, and the average macro-pulse beam current is 26 mA. So the number of H- ions in one bunch is about 5.93e8 and the corresponding charge is about 94.9 pC. The voltage development per R/Q from a single bunch is less than 1 V up to 3 GHz HOM. So the affection from the self-induced voltage is very small, hereafter this will be neglected. Here the peak macro-pulse beam current is assumed to be 52 mA for the future upgrade, which corresponds to 1 GeV, 2 MW beam at the end of SNS linac. The induced voltage per R/Q from a bunch is less than 2 V at this beam current.

The voltage development from the train of bunches passing through a cavity is the superposition of the induced voltage from a single bunch in concerning of the time evolution of the HOM induced voltage. The HOM voltage just after n-th micro bunch passes a cavity can be written;

$$V = V_q \sum_{n=1}^n \exp\{i(n-1)\omega T_b\} \exp\{-(n-1)T_b/T_d\} = V_q \left(\frac{1 - \exp(-nT_b/T_d + i\omega nT_b)}{1 - \exp(-T_b/T_d + i\omega T_b)} \right).$$

The general HOM induced voltage for the time structure of the SNS beam can be expressed like below. Here ω is used as the HOM frequency in order to explain the HOM voltage behavior in the frequency domain instead of ω_n .

- at the time just after k th macro-pulse;

$$A_{N,M,k} = V_q \left(\frac{1 - \exp(-NT_b/T_d + i\omega NT_b)}{1 - \exp(-T_b/T_d + i\omega T_b)} \right) \left(\frac{1 - \exp(-MT_i/T_d + i\omega MT_i)}{1 - \exp(-T_i/T_d + i\omega T_i)} \right) \left(\frac{1 - \exp(-kT_m/T_d + i\omega kT_m)}{1 - \exp(-T_m/T_d + i\omega T_m)} \right)$$

- during the gap between k th and $(k+1)$ th macro-pulses;

$$B_{N,M,k} = A_{N,M,k} \exp(-t/T_d + i\omega t), \quad 0 \leq t < T_g$$

- at the time just after m th midi-pulse in $(k+1)$ th macro-pulse;

$$C_{N,(M,m),k+1} = B_{N,M,k} \exp\{-(mT_i - T_g)/T_d + i\omega(mT_i - T_g)\} \left(\frac{1 - \exp(-NT_b/T_d + i\omega NT_b)}{1 - \exp(-T_b/T_d + i\omega T_b)} \right) \left(\frac{1 - \exp(-mT_i/T_d + i\omega mT_i)}{1 - \exp(-T_i/T_d + i\omega T_i)} \right)$$

- during the gap between m th and $(m+1)$ th midi-pulses in $(k+1)$ th macro-pulse;

$$D_{N,(M,m),k+1} = C_{N,(M,m),k+1} \exp(-t/T_d + i\omega t), \quad 0 \leq t < T_g$$

- at the time just after n th micro-pulse in $(m+1)$ th midi-pulse in $(k+1)$ th macro-pulse;

$$E_{(N,n),(M,m),k+1} = D_{N,(M,m),k+1} \exp\{-(n-1)T_b/T_d + i\omega(n-1)T_b\} \left(\frac{1 - \exp(-nT_b/T_d + i\omega nT_b)}{1 - \exp(-T_b/T_d + i\omega T_b)} \right)$$

- during the gap between n th and $(n+1)$ th micro-pulses in $(m+1)$ th midi-pulse in $(k+1)$ th macro-pulse;

$$F_{(N,n),(M,m),k+1} = E_{(N,n),(M,m),k+1} \exp(-t/T_d + i\omega t), \quad 0 \leq t < T_b.$$

Though the above expressions for the induced voltage have the complex form, but the handling of them is quite simple with the help of the popular mathematical software.

The induced voltage is function of Qex in T_d , frequency ω , time t and R/Q. Other parameters are determined after the time structure of the beam and the beam current are fixed. The R/Q is a property of the HOM and the induced voltage is linearly proportional to the R/Q. So the normalized induced voltage in terms of R/Q is introduced. With this normalized induced voltage, the effect only from the beam time structure can be visualized by exploring the three remaining parameter spaces that are Qex, frequency, and time. The HOM frequency is one of the HOM characteristics, which is explained in previous chapter. The Qex is also the property of the HOM and is determined with the connection of the damping mechanism of the system such as loss on the wall and power flowing out thru the coupler. Now the HOM induced voltage and the HOM power will be explored using the equations introduced before.

Figure III-2 is an example of the envelope of the normalized induced voltage as a function of the time for the different Qex's in steady state. Here 2.8175 GHz, 7th harmonic of micro-bunch frequency is exemplified because of simple and clear shape at these micro-bunch harmonics. The bunch tracking simulation showed there would be no longitudinal instability if the Qex is less than 10^8 [1], which justifies the existence of the steady state or at least the state that is very close to the steady state. The damping is not enough at $Qex=10^8$ during the macro-pulse gap, which indicates there's 60 Hz macro period resonances in addition.

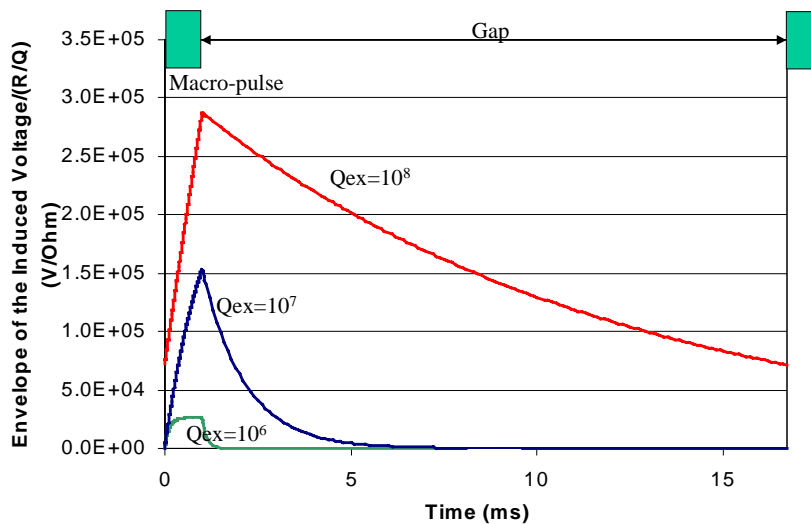


Figure III-2. Envelopes of the normalized induced voltage for the three Qex at the frequency of 2.8175 GHz (7 * 402.5 MHz) in the steady state.

IV. HOM Power

IV-1. HOM power general behavior from the beam time structure

The HOM power dissipated by the beam is

$$P(t) = \frac{V(t)^2}{\left(\frac{R}{Q}\right)\rho_{ex}}.$$

Figure III-3 shows the time evolutions of the normalized HOM power for the four different Q_{ex} 's at the frequency of 2.8175 GHz.

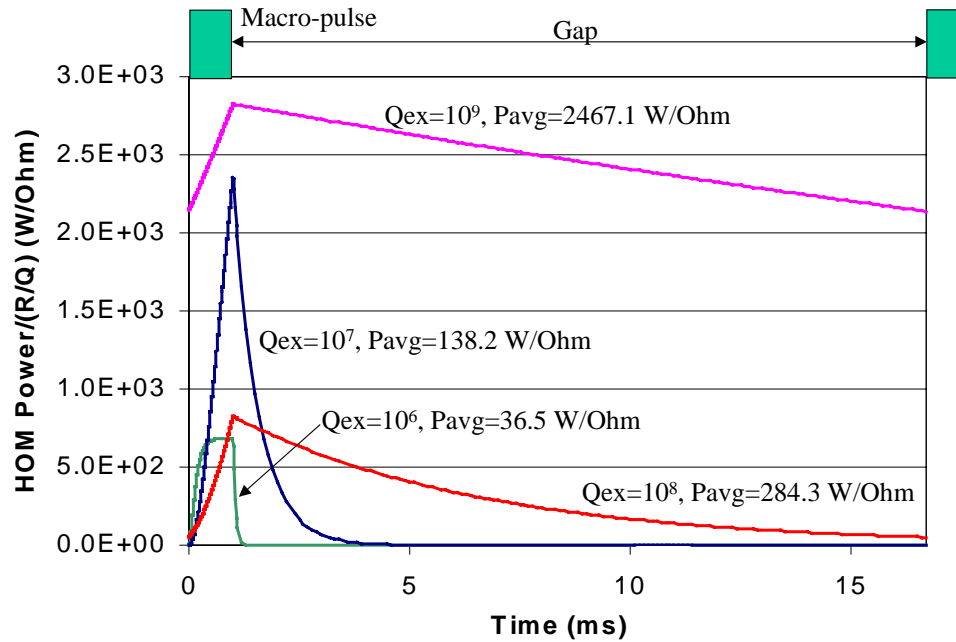


Figure III-3. Normalized HOM power for the four Q_{ex} 's at the frequency of 2.8175 GHz (7 *402.5 MHz) in the steady state.

The time averaged HOM power can be obtained by integrating the $P(t)$ in one period or more,

$$P_{avg} = \frac{1}{T} \int_{t_1}^{t_1+T} P(t) dt .$$

Since the voltage is proportional to the R/Q, the power is also proportional to the R/Q. So the normalized HOM power with respect to the R/Q can be defined again. By defining normalized quantity, the general phenomena that result only from the beam time structure can be seen clearly.

The normalized time-average HOM power is only a function of the Qex and the frequency, which are the HOM properties.

Now the investigation of the HOM power from the beam time structure is much simpler by fixing one parameter. After having this general behavior of the normalized HOM power from the beam time structure as a function of frequency or Qex, getting the actual HOM powers for each mode is straightforward by applying R/Q's those are found in Chapter II.

(1) HOM Power behavior in the frequency space.

Figure IV-4 and 5 are plots of the normalized time-average HOM power from the SNS beam time structure as a function of frequency for $Q_{ex}=10^6$ and 5×10^8 , respectively. Each time structure in Figure III-1 generates resonances or anti-resonances as explained in the Figure 4 and 5.

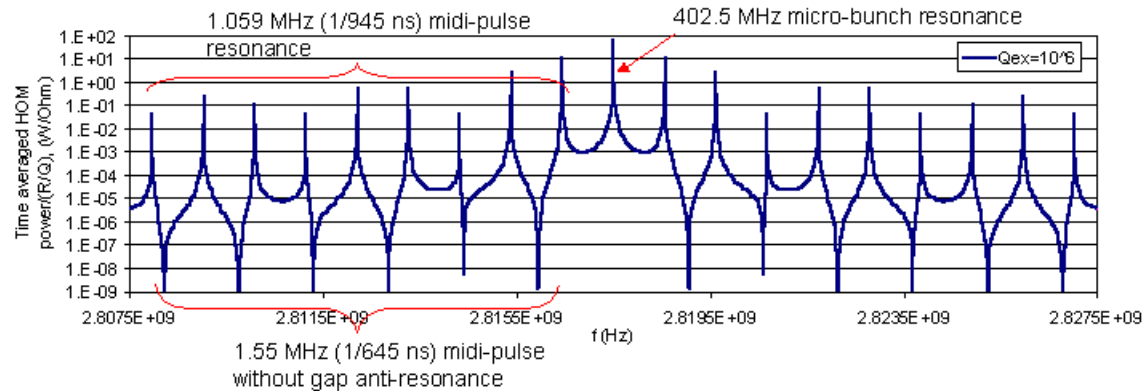


Figure IV-4. The normalized time-average HOM power from the beam time structure of SNS at around 2.8175 GHz at $Q_{ex}=10^6$

Every multiples of micro-bunch frequency give rise to the highest resonance lines. The modes around these frequencies are dangerous even though their R/Q's are small. And the normalized HOM powers at midi-pulse resonance frequencies are determined from the relation of the midi-pulse anti-resonance frequencies and the distances from the micro-pulse main resonance frequency. When the midi-pulse resonance frequencies are closer to the micro-pulse resonance frequencies and farther to the midi-pulse anti-resonance frequencies, the corresponding HOM power is higher. If the Qex is higher than about 10^8 , 60 Hz resonances appear since the damping during the macro-pulse gap is not enough as shown in Figure IV-5. That means the damping time constant $T_d=2Q_{ex}/\omega$ is longer than the macro pulse gap.

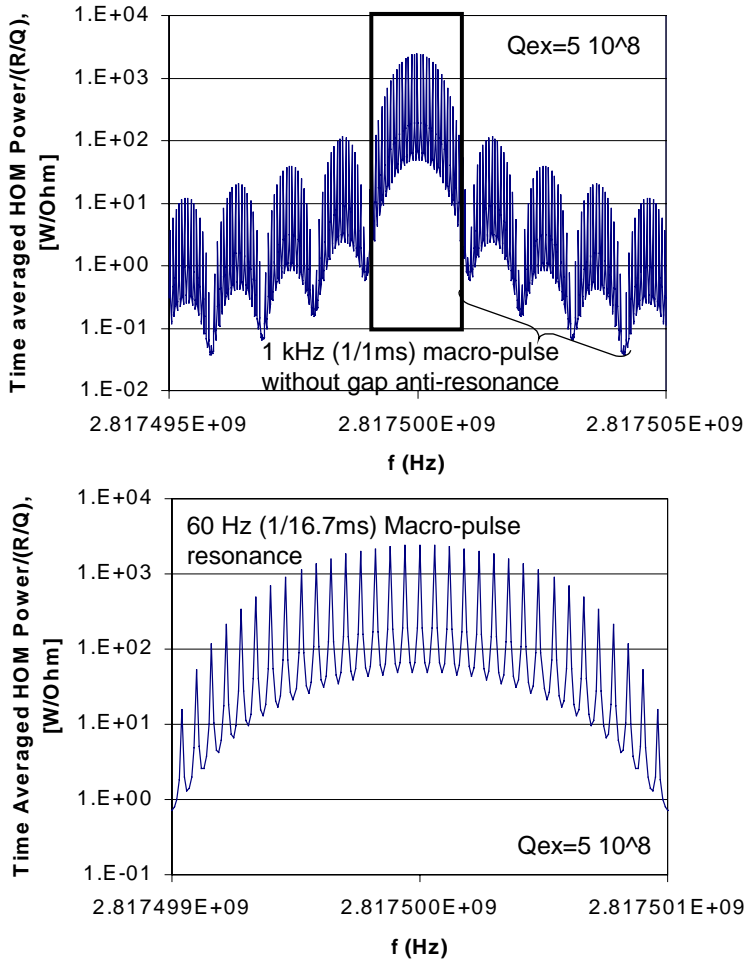


Figure IV-5. The normalized HOM power from the beam time structure of SNS at around 2.8175 GHz at $Q_{ex}=5 \times 10^8$. The bottom is the magnified view of the top.

(2) HOM Power behavior in the Q_{ex} space.

Here the normalized HOM power is explored as a function of Q_{ex} at a fixed frequency. Figure IV-6 are plots of normalized HOM power at the three representative frequencies, which are micro-pulse resonance frequency (a), midi-pulse resonance frequency (b), and off-resonance frequency (c).

When the Q_{ex} is high enough to develop the 60 Hz resonances ($Q_{ex} > \sim 10^8$), the HOM powers increase linearly everywhere in log-log scale. So the Q_{ex} that is higher than 10^8 should be avoided. For example, the frequency span from the every micro-pulse resonance frequency, where the normalized HOM power is higher than 1 W, is about a few tens of MHz at $Q_{ex} \sim 10^8$.

If the power dissipation (~2 W) on the wall from the fundamental acceleration mode is compared, 1 W is not small at all.

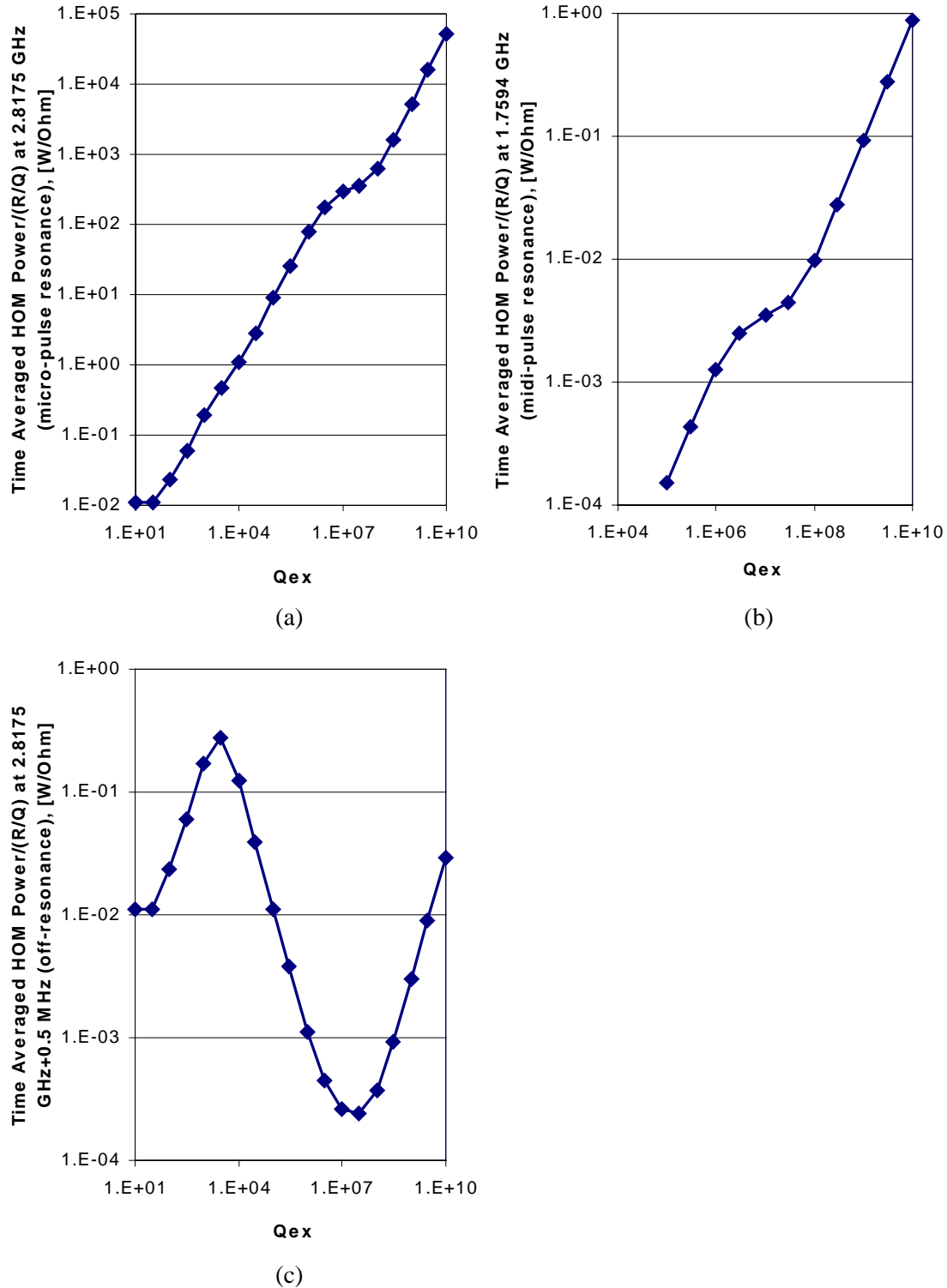


Figure IV-6. HOM power dependencies on the Q_{ex} (a) micro-bunch resonance, (b) midi-pulse resonance, and (c) off resonance

IV-2. Properties of the HOM and the other fundamental passband members frequencies

Before applying calculated HOM frequencies and R/Q's values to the actual HOM power estimation, some precise consideration for the HOM frequency should be done since the frequency dependencies on the HOM power are quite critical as explained before.

The HOM frequency of each cavity is different even for the same mode due to the mechanical imperfection of cavity shape. Actually cavities are tuned to have same fundamental mode frequencies and to satisfy the required field flatness in each cell. But it does not mean the mechanical dimensions are same and each cavity has the same HOM frequency. From the viewpoint of the beam dynamics the cavity-to-cavity HOM frequency spreads reduce the beam dynamics problems. The result from the Cornell University study [1],[4] with tuned fundamental mode is;

$$\sigma = 0.00109 \times |f_n - f_0|$$

where σ is the standard deviation of HOM frequency spread, f_n is the HOM frequency for the reference geometry and f_0 is the fundamental mode frequency. The smaller HOM frequency spread is the severe condition for the beam dynamics.

The 20 % of this nominal HOM frequency spread is used for the beam instability analysis [4].

Another HOM frequency property is the difference between the measured HOM frequency centroids and the calculated HOM frequency of the reference geometry. This information is very important when the beam time structure forms resonance behaviors. Even though one instance probability with which a HOM hits the resonance line is small, the overall probability of hitting the resonance line (beam spectral line) during the whole the machine operation would be large. If the HOM frequency is near the main spectral line and the R/Q of this HOM is large enough, the HOM power generation could damage the cavity in a very short instance.

The measured maximum fractional error from Cornell University [1],[4] is ± 0.00376 for the frequency difference between the measured HOM frequency centroids and the calculated HOM frequency of the reference geometry. In SNS, ± 0.008 is used for the conservative analysis. The larger deviation is worse because the actual HOM frequency centroid may hit the micro-pulse or midi-pulse resonance lines.

And for the other fundamental passband members (non-Pi fundamental modes) this difference is written;

$$\left| \frac{f_{measured} - f_{calculated}}{f_{calculated}} \cdot \frac{f_{\pi-mode}}{f_{\pi-mode} - f_{calculated}} \right| \leq 0.027$$

where $f_{measured}$ is the measured frequency of other fundamental passband member, $f_{calculated}$ is the calculated frequency of other fundamental passband member, $f_{\pi-mode}$ is the Pi-mode frequency.

Here 0.0675 is used instead of 0.027 for the conservative estimation. [4]

The probability that any cavity frequency will fall on a significant beam power spectral line at any instant in time is very small. However, many factors can cause HOM frequencies to move around with time. One of these factors is intentional detuning of a cavity, using the mechanical tuner, when a cavity is to be taken out of service for any reason (e.g., its klystron failed); the "parking" frequency is different every time this is done. If a cavity is warmed up to degas the surface, the HOM frequencies will be different when it is cooled down. Changes in the liquid helium level and liquid helium pressure will have to be compensated by the mechanical tuner, but the HOM frequencies will all be different. Changes in the fundamental voltage, beam bunch phase, beam bunch charge, or beam velocity profile along the linac will require changes in the fundamental detuning angle, which will change all the HOM frequencies. Changes in the linac output energy will change the midi-pulse frequency, which will change many beam spectral line frequencies as shown in Figure IV-7.

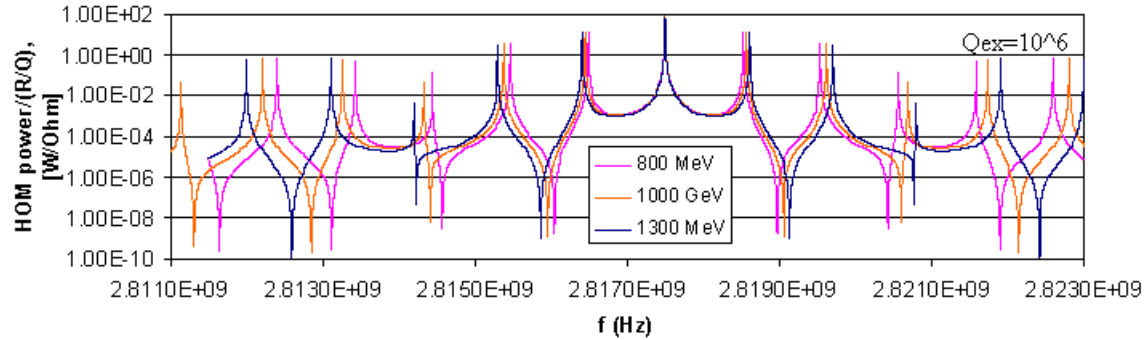


Figure IV-7. HOM power dependencies on the midi-pulse time structure.

Figure IV-8 explains the worst frequency centroid shift with the mode 4 of the medium beta cavity at the Qex values provided by the fundamental power coupler. The line B corresponds to the frequency found using MAFIA. The centroid shift range explained in the previous section is bounded with lines A and B. The HOM powers are plotted for three different beam final energies. One midi-pulse resonance exists in the range at 0.8 GeV operation. This case, the value at this resonance is taken. In the other hand there's not resonance at 1 GeV, 1.3 GeV linac operations. This case the biggest values are at the frequency of C.

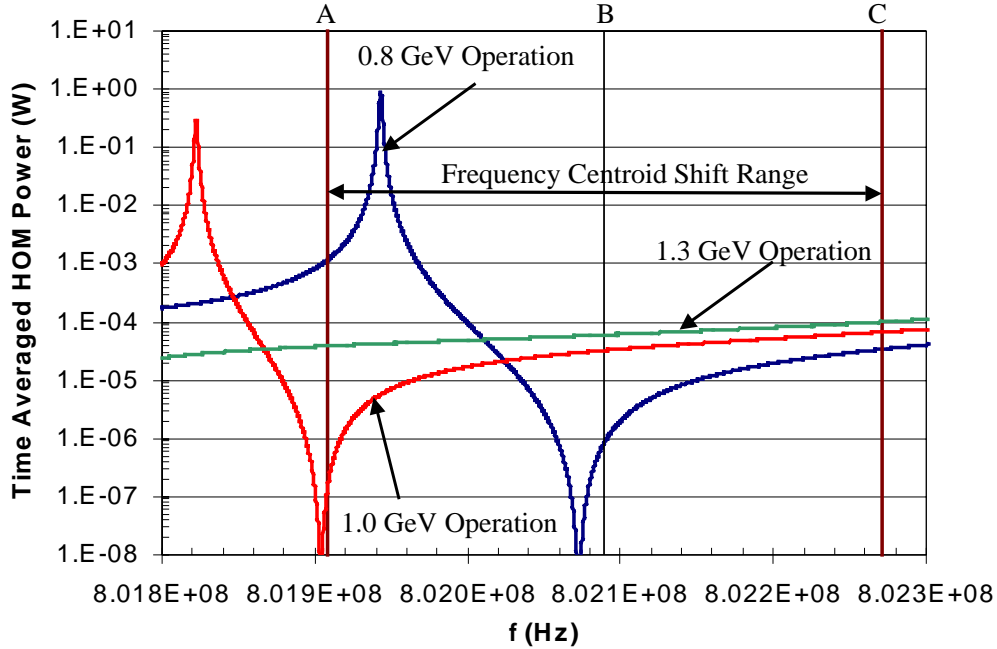


Figure IV-8. Example of the HOM frequency centroid shift for the HOM power estimation. For the other fundamental passband members, it is assumed that the Qex's are provided by the fundamental power coupler. (Qex=470,000, 4th mode, Max R/Q=13.4, medium beta cavity.)

During the 40-year life of a SNS cavity, the probability that it will have a HOM land on an important beam spectral line at least once approaches unity. To have a reliable accelerator, it is imperative that such an event destroys neither the beam properties nor the cavity.

IV-3. HOM power in SNS

As mentioned in the previous section, even though the instant probability at which the HOM frequency may hit the resonance lines is very small, the proper damping scheme or the HOM power-handling scheme should be prepared since the HOM frequency will randomly change with time. The overall probability during the whole machine operation is not negligible and even one hitting of the dangerous resonance lines will result in a critical damage to the cavity or accelerator itself.

After applying the worst HOM frequency centroid shift within the range explained in the previous section, the HOM power of each TM monopole is estimated by inserting the actual R/Q of the SNS cavity of each mode. Whatever the HOM behaviors are in this possible range, the biggest value is taken as the HOM power.

Figure IV-9 and 10 are the time averaged HOM power plots of each TM-monopoles for both beta cavities also after applying the worst frequency centroid shift within the deviation explained in the previous section. The HOM powers of the other fundamental passband members in Figure 11 are calculated with the expected Qex's provided just by the fundamental power coupler since the HOM coupler is usually designed to have a very weak coupling at around the fundamental acceleration frequency.

Three modes of each beta cavity should be damped to the proper level. These are modes 31, 32, 36 in the medium beta cavity, and modes 25, 35, 36 in the high beta cavity. The damping requirement is modest for these dangerous modes of the medium beta cavity. 10^6 or less is tolerable. But the Qex's less than 10^5 are required for these dangerous modes of the high beta cavity.

The 5th fundamental mode of each beta cavity might be also dangerous since it has high R/Q (~ 140) and it is near the 805 MHz. If the midi-pulse resonance frequency is in the centroid shift range of the 5th mode frequency, the HOM power from this mode could be more than 1 kW. But the 5th mode of each beta cavity locates well out of any possible resonance range.

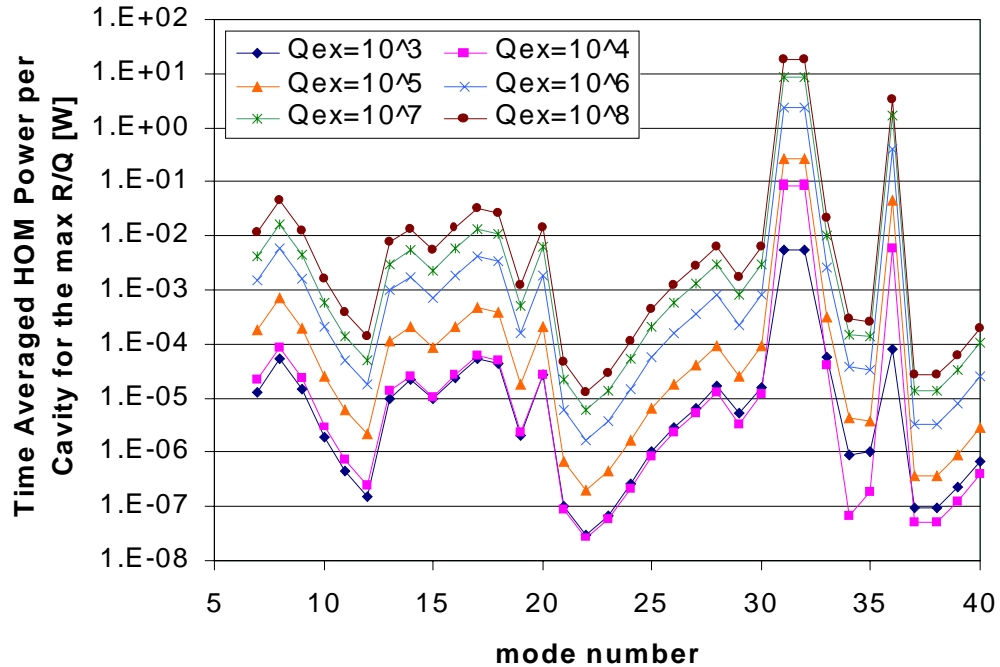
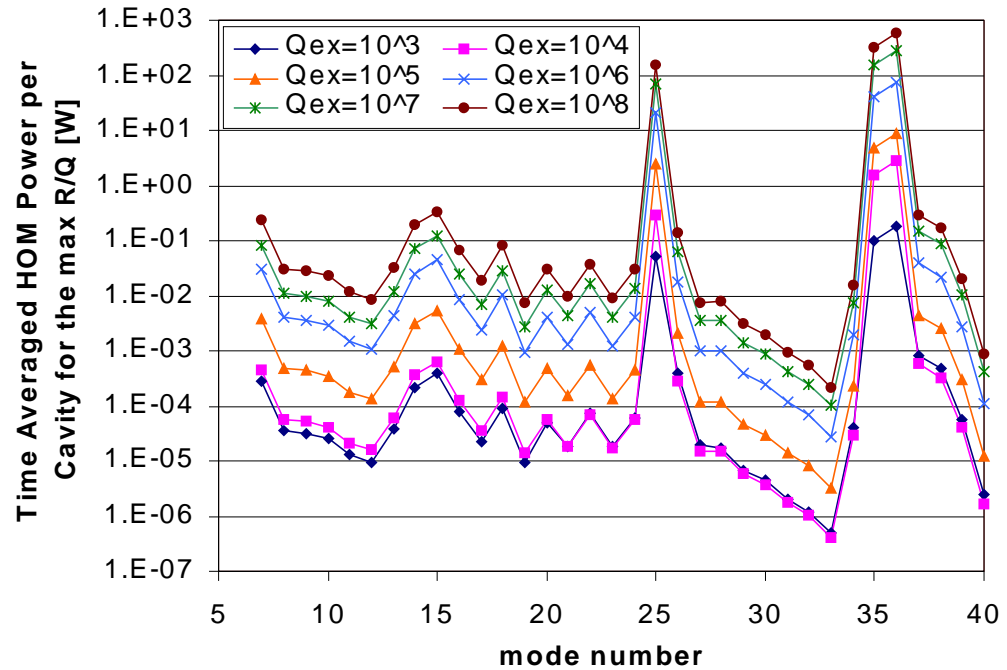
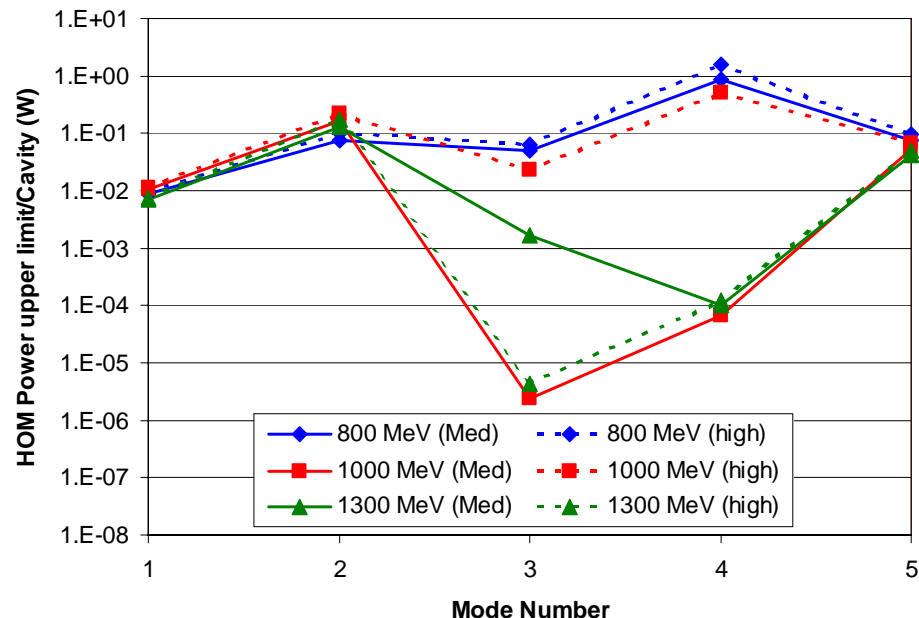


Figure IV-9. HOM power upper limits of the medium beta cavity for each TM-monopoles.
Maximum R/Q's are used in this



estimation.

Figure IV-10. HOM power upper limits of the medium beta cavity for each TM-monopoles.
Maximum R/Q's are used in this



estimation.

Figure IV-10. HOM power of the other fundamental passband members for the different operating energy. Maximum R/Q's within the accelerating ranges are used. The Qex's is estimated by assuming the coupling provided by the fundamental power coupler.

V. Conclusions

- HOM's and their properties are found up to 3 GHz for TM-monopoles, dipoles, quadrupoles and sextupoles.
- With the superstructure modeling, the beam pipe modes and the propagation modes are classified, along with the clarification of some unclear modes in the single cavity modeling.
- General analytic expressions for the multi-time structure beam are developed. Results agree well with the bunch tracking simulation.
- The affection of the beam time structure on the HOM induced voltage and the HOM power developments is fully understood
- HOM powers in SNS SC cavity are estimated by assuming the Qex.
- Damping requirements are established. Three modes for each beta cavity should be damped.

REFERENCES

- [1]. Ronald Sundelin, et al, "SNS HOM Damping Requirements via Bunch Tracking," submitted to PAC2001 Chicago, June 18-22 (2001)
- [2]. Dong-o Jeon, et al, "Transverse Beam Break-up Study of SNS SC Linac," submitted to PAC2001 Chicago, June 18-22 (2001)
- [3]. H. Padamsee, et al, "RF Superconductivity for Accelerators," John Wiley & Sons, New York, (1998)
- [4]. Ron Sundelin, Private communication.

Appendix A. MAFIA results benchmarking with SUPERFISH results for SNS medium beta cavity

MAFIA HOM results are benchmarked with SUPERFISH for TM-monopoles to confirm the MAFIA input conditions and the further multi-pole results of MAFIA.

TABLE A-1. Frequency comparison for TM monopoles of the medium beta cavity

mode	Frequency/Hz	Frequency/MHz	(MAFIA-SF)/SF	f/402.5
	MAFIA	SUPERFISH		
1	7.937953E+08	793.631	0.000207	1.972
2	7.960493E+08	795.931	0.000149	1.978
3	7.991110E+08	799.025	0.000108	1.985
4	8.020895E+08	802.049	0.000050	1.993
5	8.041887E+08	804.211	-0.000028	1.998
6	8.050046E+08	805.001	0.000004	2.000
7	1.691108E+09	1690.804	0.000180	4.202
8	1.716099E+09	1715.861	0.000139	4.264
9	1.726083E+09	1725.947	0.000079	4.288
10	1.740060E+09	1740.079	-0.000011	4.323
11	1.754806E+09	1755.0689	-0.000150	4.360
12	1.766435E+09	1766.814	-0.000215	4.389
13	1.901693E+09	1901.820	-0.000067	4.725
14	2.134996E+09	2134.863	0.000062	5.304
15	2.179098E+09	2179.597	-0.000229	5.414
16	2.191223E+09	2191.858	-0.000290	5.444
17	2.206082E+09	2206.913	-0.000377	5.481
18	2.219091E+09	2220.094	-0.000452	5.513
19	2.226939E+09	2228.132	-0.000535	5.533
20	2.350782E+09	2351.479	-0.000296	5.840
21	2.581966E+09	2581.670	0.000115	6.415
22	2.590456E+09	2590.153	0.000117	6.436
23	2.600957E+09	2600.817	0.000054	6.462
24	2.616924E+09	2616.968	-0.000017	6.502
25	2.638307E+09	2638.547	-0.000091	6.555
26	2.665950E+09	2666.434	-0.000181	6.623
27	2.678670E+09	2679.367	-0.000260	6.655
28	2.718752E+09	2719.439	-0.000253	6.755
29	2.745414E+09	2746.383	-0.000353	6.821
30	2.774434E+09	2775.867	-0.000516	6.893
31	2.800984E+09	2802.882	-0.000677	6.959
32	2.820630E+09	2822.963	-0.000827	7.008
33	2.848207E+09	2848.871	-0.000233	7.076

The TM monopole results from both MAFIA and SUPERFISH are summarized In Table A-1. And the R/Q comparisons are shown in Figure A-1. Since the solving schemes of MAFIA is based on FIM (finite integral method), the meshing element has square shape and the results are more sensitive to the meshing size than those of SUPERFISH which is FEM (finite element

method) code. The proper meshing size is found by varying the number of elements in MAFIA. Here about 600,000 elements is set for the SNS medium beta cavity in the MAFIA input. The agreements between these two codes are very good after having proper meshing size for MAFIA. Basically the axial field profiles of the fundamental passband members and the frequencies are checked. The shunt impedance in R/Q is effective one, that is seen by the particle, which is a function of particle velocity;

$$\frac{R}{Q} = \frac{\left| \int Ez(z) \exp(i\omega z/v) dz \right|^2}{\omega U}, \text{ where } v; \text{ particle velocity, } U; \text{ stored energy of each mode, } \omega;$$

resonance angular frequency of each mode, Ez; axial electric field on the axis.

The integration can be divided into two parts like;

$$\int Ez(z) \exp(i\omega z/v) dz = \int Ez(z) \cos(\omega z/v) dz + i \int Ez(z) \sin(\omega z/v) dz = T + iS$$

This effective R/Q can be written with the similar notation used in SUPERFISH.

$$\frac{R}{Q} = \frac{(Eo \tilde{T} L)^2}{\omega U}, \text{ where } \tilde{T}; \text{ Transit time factor } (|T+iS|), T; \text{ cosine term integration, } S; \text{ sine term}$$

integration, L; the effective cavity length, $3\beta\lambda$ in SNS cavity, and $Eo = \frac{1}{L} \int |Ez(z)| dz$.

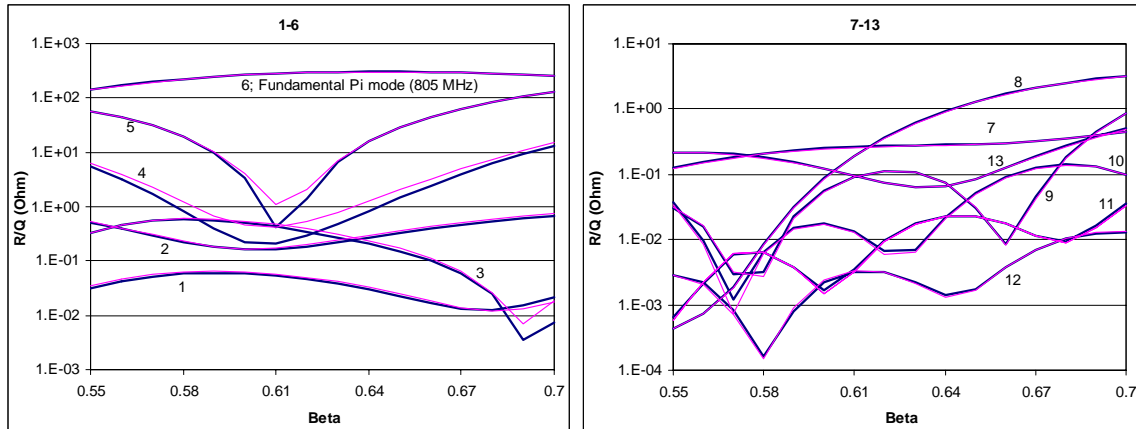


Figure A-1. R/Q comparisons from MAFIA and SUPERFISH (continue)

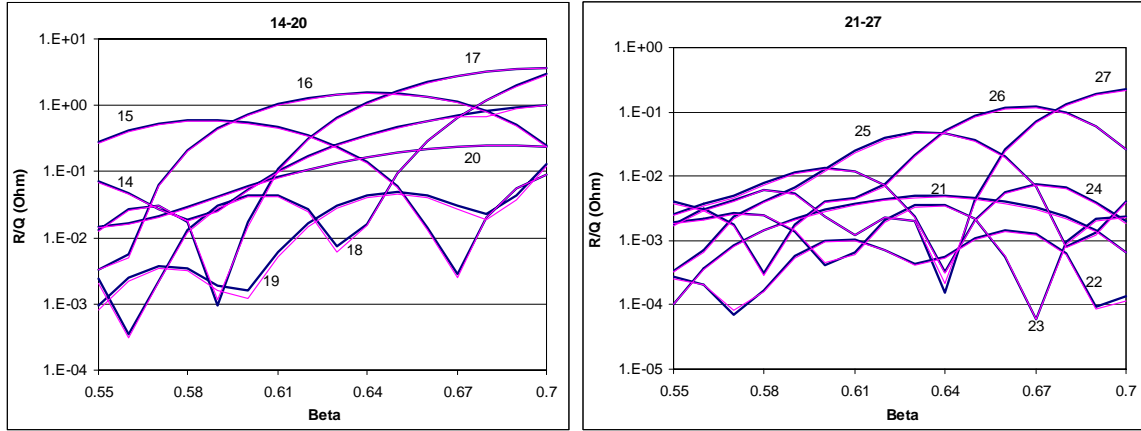


Figure A-1. R/Q comparisons from MAFIA and SUPERFISH.

Figure A-1. R/Q comparisons for TM monopoles (pink lines; SUPERFISH, blue lines; MAFIA). The more detailed R/Q results for each mode is in the following Appendix.

The SUPERFISH results are very stable for the frequencies, fields, etc at the different meshing sizes. But the driving point location in the SUPERFISH input should be chosen at the place where the magnetic field is high enough [??]. Otherwise the solution from SUPERFISH might be far from the realistic one. Figure A-2 explains the effect of the driving. The pink line is the case for the wrong driving point location which placed at the region of weak magnetic field. Just changing the location of the driving point, the pink line moves to the red line in Figure A-2.

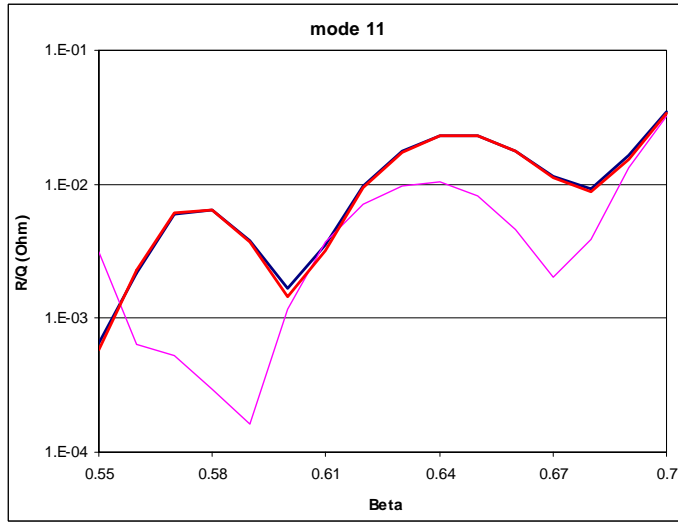
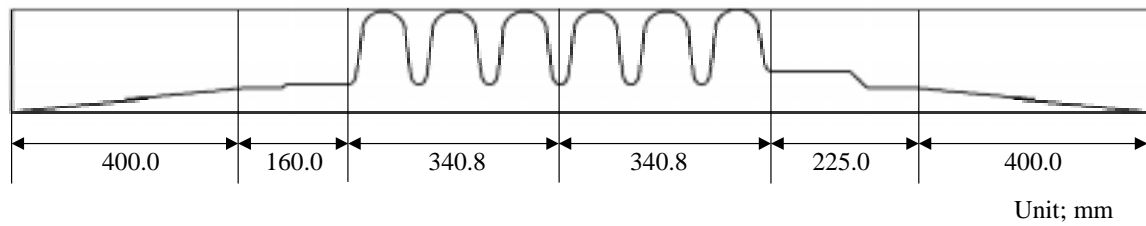


Figure A-2. Effect of driving point location in SUPERFISH (pink line; SUPERFISH results with a wrong driving point location, red line; SUPERFISH results with a correct driving point location, blue line; MAFIA).

Appendix B. SNS medium beta cavity HOM and their properties.



INPUT GEOMETRY

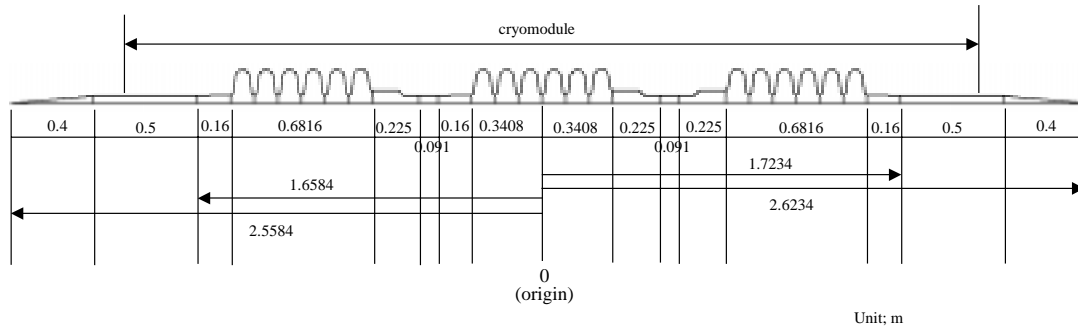


Figure B-1. MAFIA models of the single cavity with conical ends and the super structure (ref. SNS drawing).

Table B-1. TM monopoles and R/Q as a function of the particle velocity of medium beta, single cavity (continue..)

mode	Frequency/Hz	R/Q at beta=							
		0.55	0.56	0.57	0.58	0.59	0.6	0.61	0.62
1	7.93795E+08	0.032258	0.04329	0.052586	0.058466	0.060334	0.058406	0.053412	0.046336
2	7.96049E+08	0.512511	0.395513	0.297638	0.225432	0.180568	0.161395	0.164448	0.185814
3	7.99111E+08	0.333857	0.467467	0.554348	0.58421	0.563391	0.506684	0.430755	0.349855
4	8.02090E+08	5.585858	3.249122	1.729711	0.841041	0.393125	0.222457	0.212178	0.302681
5	8.04189E+08	56.32125	43.66662	30.95896	19.35279	9.874397	3.36103	0.424069	1.43508
6	8.05005E+08	142.064	169.8033	196.9187	222.4263	245.4568	265.3038	281.4336	293.5068
7	1.69111E+09	0.1266	0.15498	0.183296	0.209668	0.232366	0.250223	0.262966	0.271345
8	1.71610E+09	0.000435	0.000752	0.001924	0.008684	0.031586	0.086729	0.192585	0.36488
9	1.72608E+09	0.030793	0.015975	0.003001	0.0032	0.022504	0.056775	0.092546	0.11302
10	1.74006E+09	0.037379	0.009833	0.001187	0.006434	0.015079	0.018152	0.01354	0.006739
11	1.75481E+09	0.00066	0.002174	0.006019	0.006507	0.003804	0.001653	0.003492	0.009731
12	1.76644E+09	0.002885	0.002206	0.000825	0.000164	0.000805	0.002196	0.003223	0.003155
13	1.90169E+09	0.21582	0.21599	0.203318	0.180951	0.153147	0.123682	0.096046	0.074195
14	2.13500E+09	0.069459	0.046938	0.027386	0.018403	0.025819	0.053128	0.101276	0.169026
15	2.17910E+09	0.28123	0.413635	0.527886	0.595110	0.601584	0.551657	0.461822	0.351797
16	2.19122E+09	0.003264	0.005572	0.063544	0.208158	0.441855	0.734066	1.034581	1.293441
17	2.20608E+09	0.013233	0.026569	0.030468	0.017515	0.000957	0.017019	0.11125	0.319771
18	2.21909E+09	0.002365	0.000354	0.002257	0.012906	0.030307	0.044441	0.044022	0.026953
19	2.22694E+09	0.000964	0.002499	0.003769	0.003492	0.001917	0.001623	0.006039	0.016586
20	2.35078E+09	0.01443	0.016471	0.021103	0.029351	0.042073	0.059533	0.081601	0.107739
21	2.58197E+09	0.000103	0.000366	0.000838	0.001461	0.002204	0.003004	0.003787	0.004477
22	2.59046E+09	0.000269	0.000206	7.1E-05	0.000169	0.000579	0.000985	0.001033	0.000721
23	2.60096E+09	0.001892	0.002201	0.002692	0.002477	0.001398	0.00042	0.00065	0.002096
24	2.61692E+09	0.002581	0.003708	0.005004	0.00777	0.011486	0.013621	0.012061	0.007299
25	2.63831E+09	0.000334	0.0007	0.00234	0.004079	0.006553	0.012901	0.024785	0.03885
26	2.66595E+09	0.001778	0.00312	0.001798	0.000309	0.001747	0.004014	0.004567	0.007532
27	2.67867E+09	0.004004	0.003072	0.004272	0.006188	0.005314	0.002347	0.001195	0.002275
28	2.71875E+09	0.000391	0.001803	0.003486	0.003427	0.002649	0.003698	0.007463	0.013806
29	2.74541E+09	0.001718	0.001738	0.000674	0.001887	0.007643	0.017176	0.0288	0.039937
30	2.77443E+09	3.33E-05	0.001452	0.007224	0.01627	0.02573	0.033371	0.03631	0.031511
31	2.80098E+09	0.010745	0.018742	0.024839	0.028133	0.028252	0.023937	0.015411	0.006596
32	2.82063E+09	0.030729	0.024905	0.019182	0.013798	0.008323	0.00348	0.000897	0.00094
33	2.84821E+09	0.007369	0.010667	0.013355	0.015019	0.01568	0.01603	0.016343	0.016311
34	3.04294E+09	0.002068	0.003508	0.004949	0.006032	0.006451	0.005822	0.0047	0.003365
35	3.14895E+09	0.001516	0.001844	0.00213	0.002351	0.002551	0.002616	0.002576	0.002492
36	3.20072E+09	0.000398	0.000342	0.000559	0.000806	0.001398	0.002123	0.002704	0.003661
37	3.29303E+09	7.02E-05	8.83E-05	6.61E-05	2.26E-05	7.68E-06	1.06E-05	2.25E-05	3.95E-05
38	3.30321E+09	0.000277	5.23E-05	1.72E-05	0.000106	0.000108	5.28E-05	2.78E-05	2.73E-05
39	3.32019E+09	0.000198	0.000554	0.000537	0.000251	0.00024	0.000335	0.000362	0.000418
40	3.33724E+09	0.000275	0.000137	0.000137	0.000657	0.000628	0.000348	0.000558	0.00045

Mode 35 and mode 37 and higher; it is not clear with one cavity simulation. See the multi-cavity data

Table B-1. TM monopoles and R/Q's as a function of the particle velocity (medium beta, Single cavity)

mode	Frequency/Hz	R/Q at beta=								
		0.63	0.64	0.65	0.66	0.67	0.68	0.69	0.7	
1	7.93795E+08	0.038221	0.030056	0.022709	0.016929	0.013359	0.012574	0.015121	0.021542	
2	7.96049E+08	0.221653	0.268913	0.325285	0.389062	0.458877	0.533389	0.610977	0.689585	
3	7.99111E+08	0.273585	0.206542	0.149323	0.100397	0.058383	0.024305	0.003558	0.007423	
4	8.02090E+08	0.493767	0.840057	1.441668	2.432061	3.964561	6.199238	9.290856	13.37858	
5	8.04189E+08	6.530935	15.63346	28.4792	44.65545	63.6374	84.82787	107.5904	131.281	
6	8.05005E+08	301.3598	304.9984	304.5699	300.3413	292.6758	281.9943	268.7672	253.4771	
7	1.69111E+09	0.277084	0.282645	0.290876	0.304592	0.32622	0.35756	0.399639	0.452806	
8	1.71610E+09	0.611617	0.930112	1.306858	1.719728	2.141618	2.544201	2.901341	3.191351	
9	1.72608E+09	0.106514	0.073704	0.030897	0.008437	0.045165	0.181067	0.45032	0.87628	
10	1.74006E+09	0.007065	0.02185	0.051872	0.090134	0.124287	0.141455	0.133505	0.101215	
11	1.75481E+09	0.017551	0.022825	0.022759	0.017718	0.011376	0.009234	0.016317	0.035073	
12	1.76644E+09	0.002214	0.001395	0.001762	0.003764	0.00698	0.010336	0.012603	0.01293	
13	1.90169E+09	0.062561	0.065323	0.085767	0.126096	0.187586	0.270722	0.375203	0.499936	
14	2.13500E+09	0.253908	0.352862	0.462441	0.578694	0.697204	0.813432	0.923105	1.022459	
15	2.17910E+09	0.239033	0.137844	0.060075	0.014206	0.002789	0.020528	0.055048	0.090619	
16	2.19122E+09	1.47321	1.550276	1.512775	1.36191	1.116233	0.813548	0.505898	0.247938	
17	2.20608E+09	0.656892	1.112549	1.655868	2.239385	2.801381	3.268961	3.566651	3.632169	
18	2.21909E+09	0.00742	0.016035	0.094736	0.290161	0.647191	1.201687	1.971071	2.943421	
19	2.22694E+09	0.030873	0.043416	0.048415	0.043077	0.030592	0.022822	0.043137	0.129085	
20	2.35078E+09	0.136523	0.165805	0.193455	0.217616	0.236312	0.247247	0.248256	0.238077	
21	2.58197E+09	0.00493	0.004994	0.004656	0.004034	0.003244	0.002349	0.001428	0.000653	
22	2.59046E+09	0.000428	0.000554	0.001061	0.001449	0.001267	0.000622	9.34E-05	0.000135	
23	2.60096E+09	0.003519	0.003595	0.002207	0.000565	5.99E-05	0.000945	0.002149	0.002415	
24	2.61692E+09	0.00232	0.00032	0.002132	0.005613	0.007594	0.006584	0.00385	0.002	
25	2.63831E+09	0.048226	0.047458	0.03642	0.020475	0.00702	0.00081	0.001308	0.004029	
26	2.66595E+09	0.021569	0.050594	0.087338	0.115785	0.120856	0.098639	0.060311	0.026429	
27	2.67867E+09	0.001986	0.000151	0.00448	0.026173	0.071088	0.13279	0.191868	0.223711	
28	2.71875E+09	0.023374	0.036436	0.051279	0.06666	0.086737	0.122371	0.185969	0.283046	
29	2.74541E+09	0.045952	0.042704	0.031291	0.018353	0.010375	0.008546	0.010739	0.019081	
30	2.77443E+09	0.020116	0.008628	0.003685	0.006003	0.010577	0.012631	0.012007	0.011327	
31	2.80098E+09	0.002256	0.003085	0.005354	0.005499	0.003697	0.002721	0.004332	0.007653	
32	2.82063E+09	0.001882	0.001917	0.001164	0.000982	0.001876	0.002952	0.003247	0.002876	
33	2.84821E+09	0.016119	0.016143	0.016493	0.017441	0.0193	0.022131	0.026198	0.032097	
34	3.04294E+09	0.001883	0.001069	0.001487	0.003439	0.007423	0.013376	0.020858	0.029836	
35	3.14895E+09	0.002364	0.00224	0.002202	0.002337	0.002674	0.003243	0.004092	0.005114	
36	3.20072E+09	0.004203	0.004182	0.004128	0.003806	0.003381	0.00327	0.00369	0.004943	
37	3.29303E+09	3.47E-05	2.64E-05	5.43E-05	0.000109	0.00018	0.000281	0.000403	0.000519	
38	3.30321E+09	6.6E-05	0.000152	0.000171	0.000101	8.37E-05	0.000163	0.000292	0.000651	
39	3.32019E+09	0.000384	0.000182	0.000101	0.00034	0.000474	0.00025	0.000541	0.002596	
40	3.33724E+09	0.000387	0.000708	0.000797	0.000373	0.000243	0.002235	0.006643	0.011174	

Mode 35 and mode 37 and higher; it is not clear with one cavity simulation. See the multi-cavity data

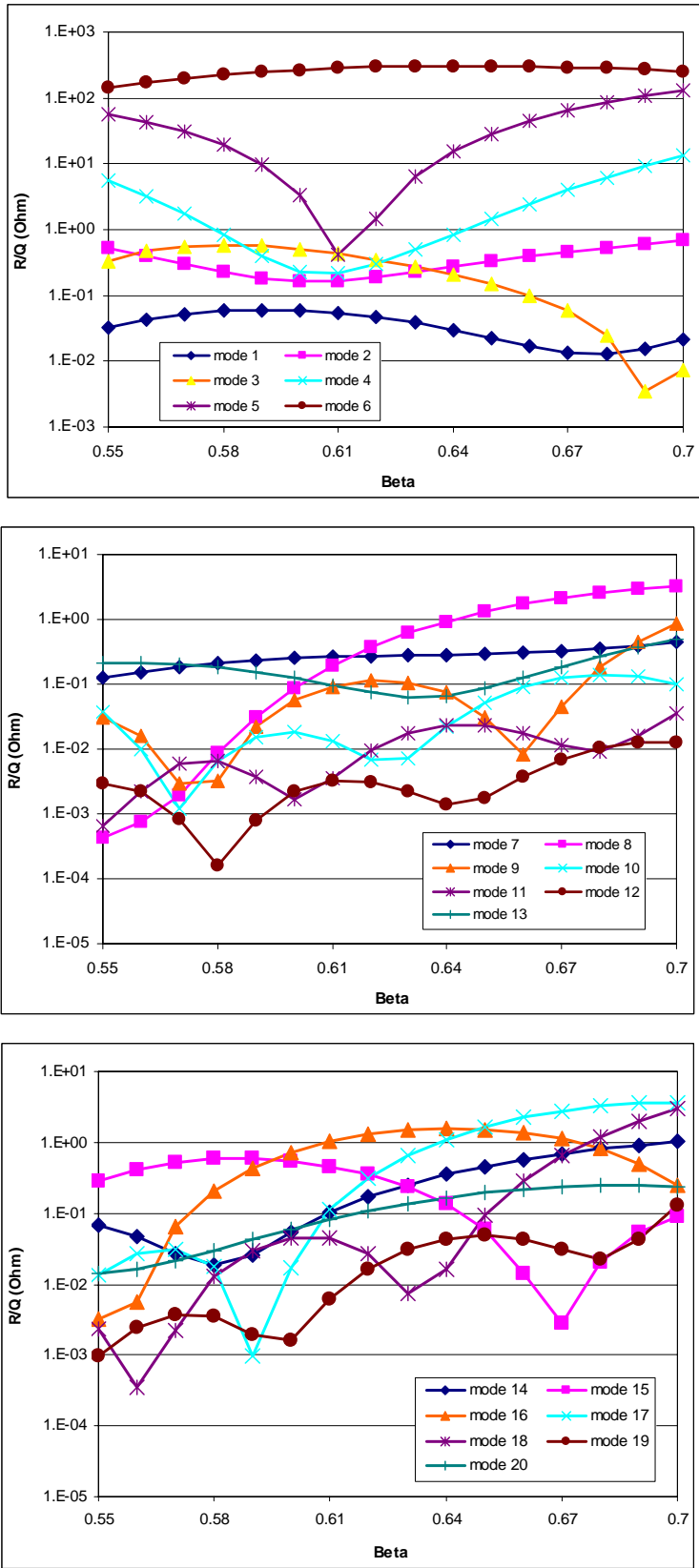


Figure B-2. R/Q 's of TM monopoles (medium beta) (continue...)

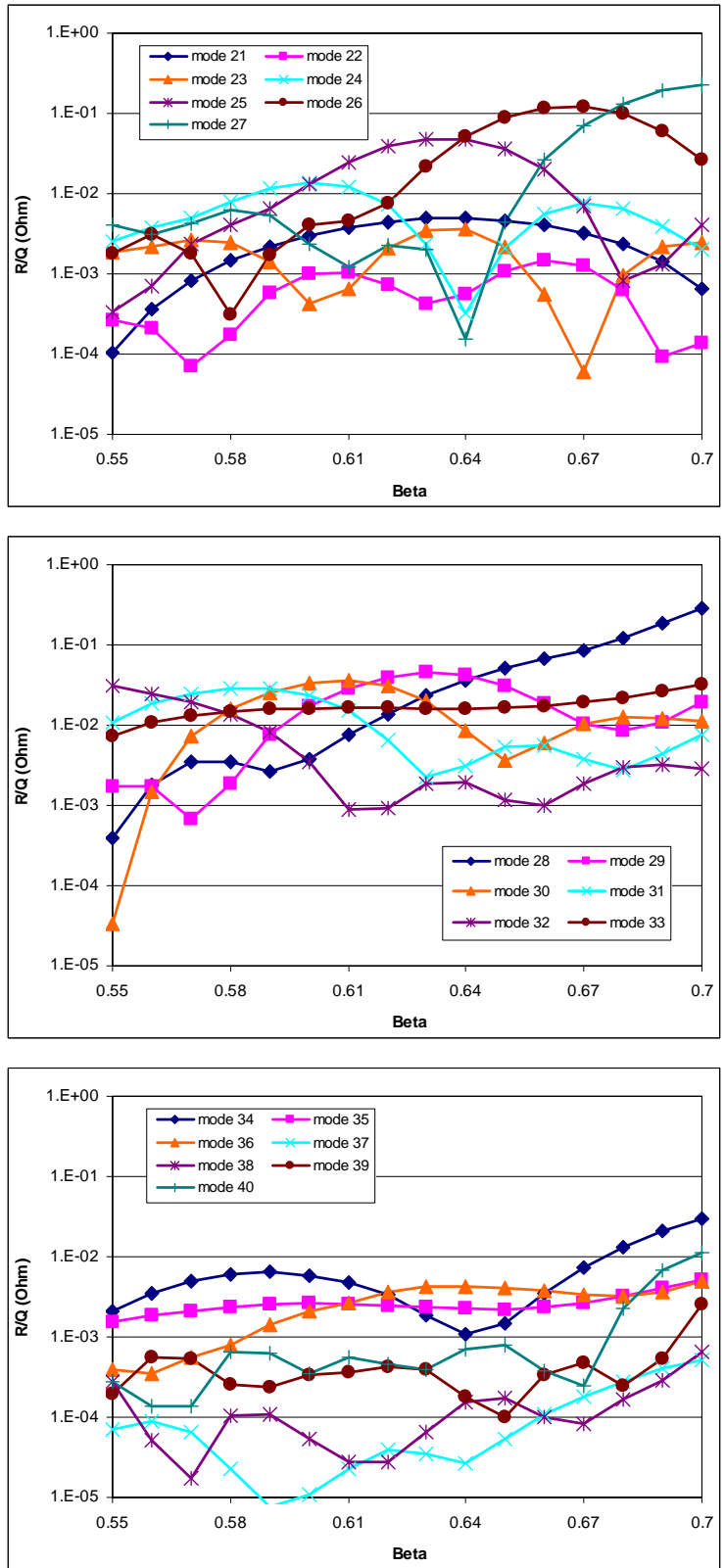


Figure B-2. R/Q 's of TM monopoles (medium beta)

Table B-2. mode comparisons between the results from the single cavity modeling and the super-structure modeling (continue...)

Single cavity	3-cavity superstructure	Single cavity	3-cavity superstructure
	19 1.691303E+09		61 2.581457E+09
7 1.691108E+09	20 1.691454E+09	21 2.581602E+09	
	21 1.691443E+09	2.581966E+09	63 2.581527E+09
	22 1.715823E+09		64 2.590210E+09
8 1.716099E+09	23 1.716056E+09	22 2.589688E+09	
	24 1.716209E+09	2.590456E+09	66 2.589724E+09
	25 1.726205E+09		67 2.600732E+09
9 1.726083E+09	26 1.725969E+09	23 2.600601E+09	
	27 1.726003E+09	2.600957E+09	69 2.600492E+09
	28 1.740227E+09		70 2.616262E+09
10 1.740060E+09	29 1.740065E+09	24 2.616557E+09	
	30 1.739687E+09	2.616924E+09	72 2.616696E+09
	31 1.754448E+09		73 2.638166E+09
11 1.754806E+09	32 1.755052E+09	25 2.637959E+09	
	33 1.754899E+09	2.638307E+09	75 2.638067E+09
	34 1.766813E+09		76 2.666059E+09
12 1.766435E+09	35 1.766518E+09	26 2.665575E+09	
	36 1.766701E+09	2.665950E+09	78 2.665890E+09
	37 1.901895E+09		79 2.678897E+09
13 1.901693E+09	38 1.901785E+09	27 2.679042E+09	
	39 1.901823E+09	2.678670E+09	81 2.679161E+09
	40 2.135203E+09		82 2.718920E+09
14 2.134996E+09	41 2.135178E+09	28 2.718812E+09	
	42 2.135222E+09	2.718752E+09	84 2.718919E+09
	43 2.178146E+09		85 2.745409E+09
15 2.179098E+09	44 2.178870E+09	29 2.745227E+09	
	45 2.178836E+09	2.745414E+09	87 2.745362E+09
	46 2.191084E+09		88 2.774449E+09
16 2.191223E+09	47 2.190850E+09	30 2.774162E+09	
	48 2.190682E+09	2.774434E+09	90 2.774238E+09
	49 2.205667E+09		91 2.800995E+09
17 2.206082E+09	50 2.206053E+09	31 2.800834E+09	
	51 2.205976E+09	2.800984E+09	93 2.800863E+09
	52 2.219116E+09		94 2.820670E+09
18 2.219091E+09	53 2.218722E+09	32 2.820575E+09	
	54 2.218965E+09	2.820630E+09	96 2.820466E+09
	55 2.226603E+09		97 2.848127E+09
19 2.226939E+09	56 2.227074E+09	33 2.847859E+09	
	57 2.227037E+09	2.848207E+09	99 2.847953E+09
	58 2.351619E+09		
20 2.350782E+09	59 2.351817E+09		
	60 2.351783E+09		

Table B-2. mode comparisons between the results from the single cavity modeling and the super-structure modeling

Single cavity	3-cavity superstructure	Single cavity
	100 3.038326E+09	35 3.148949E+09
	101 3.038401E+09	36 3.200717E+09
	102 3.034840E+09	37 3.293028E+09
34 3.042936E+09	103 3.040036E+09	38 3.303212E+09
	104 3.046514E+09	39 3.320185E+09
	105 3.065318E+09	40 3.337244E+09
	106 3.065404E+09	
	107 3.091263E+09	
	108 3.100626E+09	
	109 3.107049E+09	
	110 3.106839E+09	
	111 3.157062E+09	
	112 3.157008E+09	
	113 3.182708E+09	
	114 3.212208E+09	
	115 3.212022E+09	
Mode 36 3.200717E+09	116 3.230296E+09	
	117 3.280371E+09	
	118 3.279687E+09	

red

blue

gray

beam pipe mode (inside cryostat)

propagation mode (or beam pipe mode in the warm section)

Modes founded only from the single cavity modeling (artificial ones formed by the boundary)

Table B-3. Q's only from the damping on the normal conducting beam pipes or bellows in the super-structure modeling.

mode no. (single cavity)	mode no. (super structure)	frequency	Q
27 3	81	2.679161E+09	5.7185E+07
28 1	82	2.718920E+09	6.9102E+07
28 2	83	2.718812E+09	6.7064E+07
28 3	84	2.718919E+09	7.9986E+07
29 1	85	2.745409E+09	4.7636E+07
29 2	86	2.745227E+09	5.1239E+07
29 3	87	2.745362E+09	4.2235E+07
30 1	88	2.774449E+09	2.9858E+07
30 2	89	2.774162E+09	2.2489E+07
30 3	90	2.774238E+09	2.5099E+07
31 1	91	2.800995E+09	1.5660E+07
31 2	92	2.800834E+09	1.6235E+07
31 3	93	2.800863E+09	1.5158E+07
32 1	94	2.820670E+09	1.9979E+07
32 2	95	2.820575E+09	1.8349E+07
32 3	96	2.820466E+09	1.9049E+07
33 1	97	2.848127E+09	7.0954E+05
33 2	98	2.847859E+09	7.1329E+05
33 3	99	2.847953E+09	7.2243E+05
100	100	3.038326E+09	5.8336E+03
101	101	3.038401E+09	5.8331E+03
102	102	3.034840E+09	3.8328E+04
34 1	103	3.040036E+09	5.7948E+04
34 2	104	3.046514E+09	7.4164E+05
105	105	3.065318E+09	6.2183E+03
106	106	3.065404E+09	6.2169E+03
107	107	3.091263E+09	1.2730E+04
108	108	3.100626E+09	1.2352E+04
109	109	3.107049E+09	7.1631E+03
110	110	3.106839E+09	7.1733E+03
111	111	3.157062E+09	8.9036E+03
112	112	3.157008E+09	8.8876E+03
113	113	3.182708E+09	4.4467E+04
114	114	3.212208E+09	8.5669E+03
115	115	3.212022E+09	8.5817E+03
36 1	116	3.230296E+09	3.5576E+04
117	117	3.280371E+09	7.8423E+03
118	118	3.279687E+09	7.8229E+03

red beam pipe mode inside the cryostat

blue propagation mode

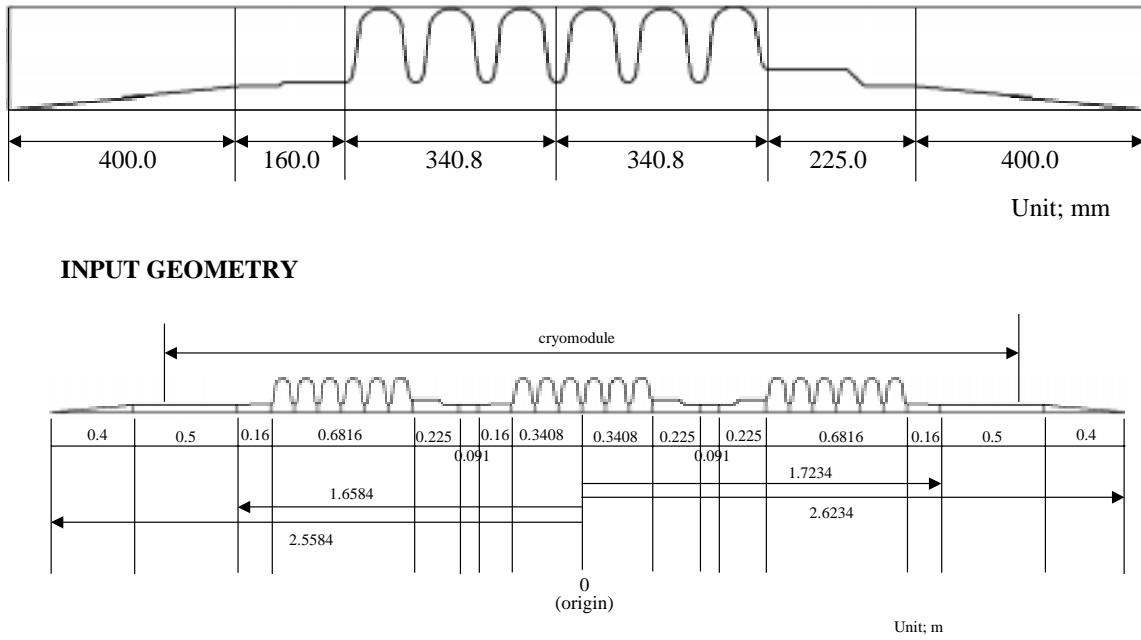


Figure B-3. MAFIA models of the single cavity and the super-structure (ref. SNS drawing).

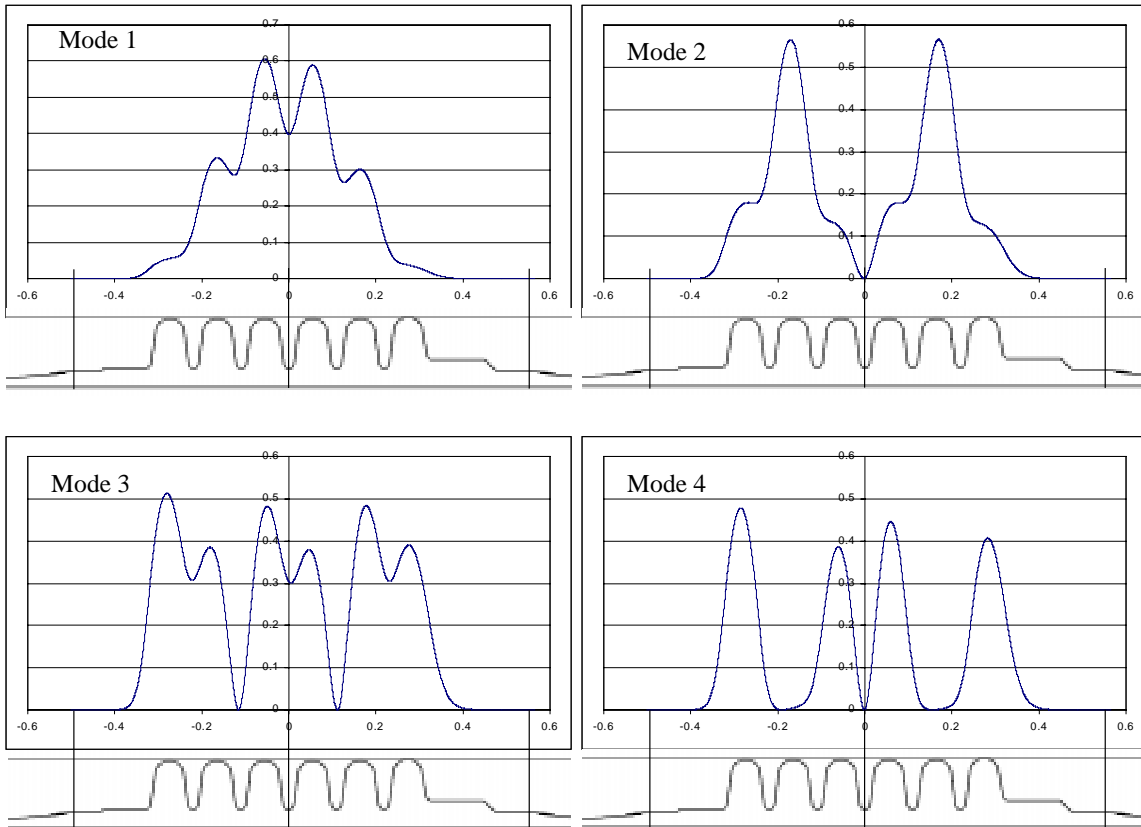


Figure B-4. E_z^2 on the axis of each TM monopoles (continue...)

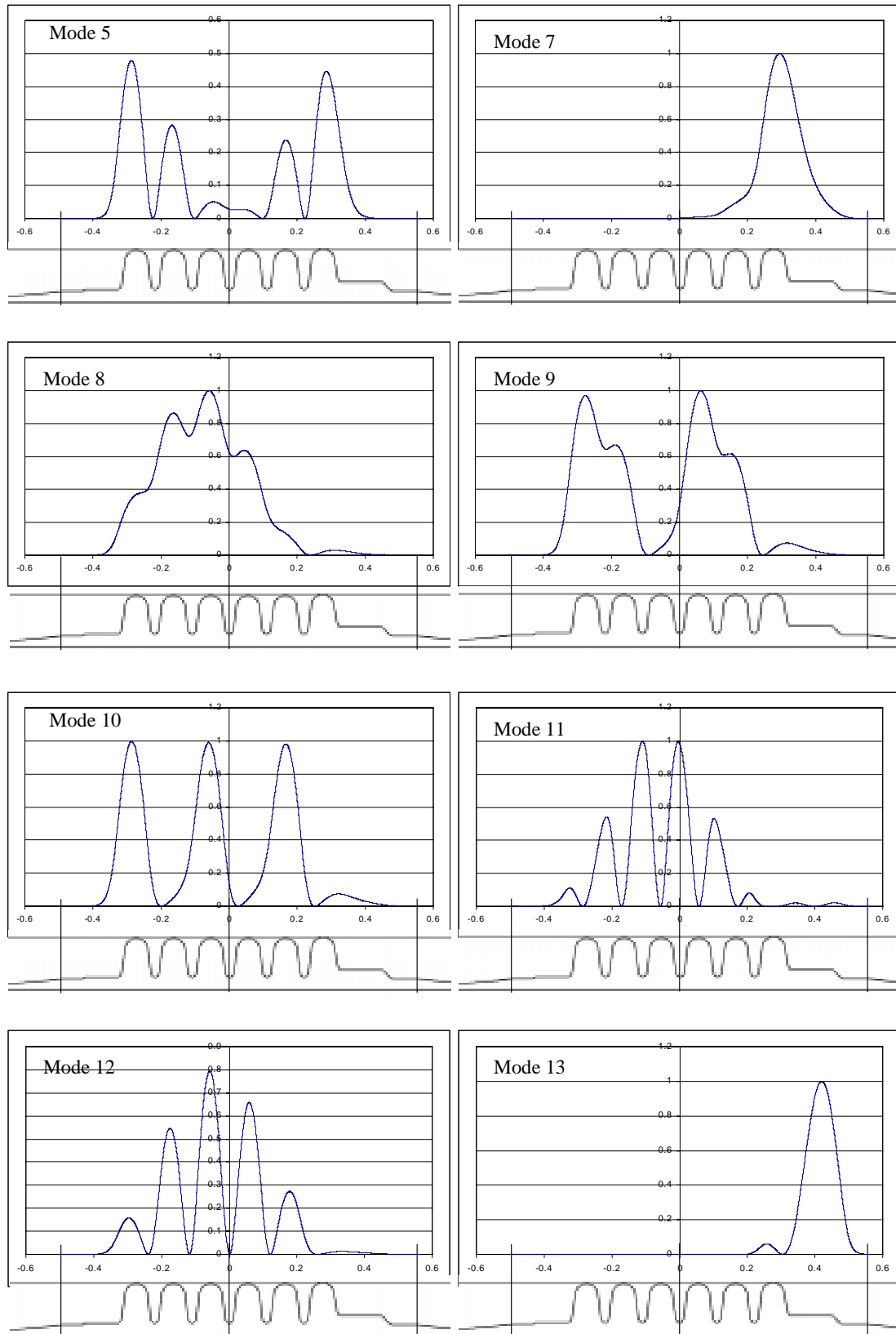


Figure B-4. E_z^2 on the axis of each TM monopoles (continue...)

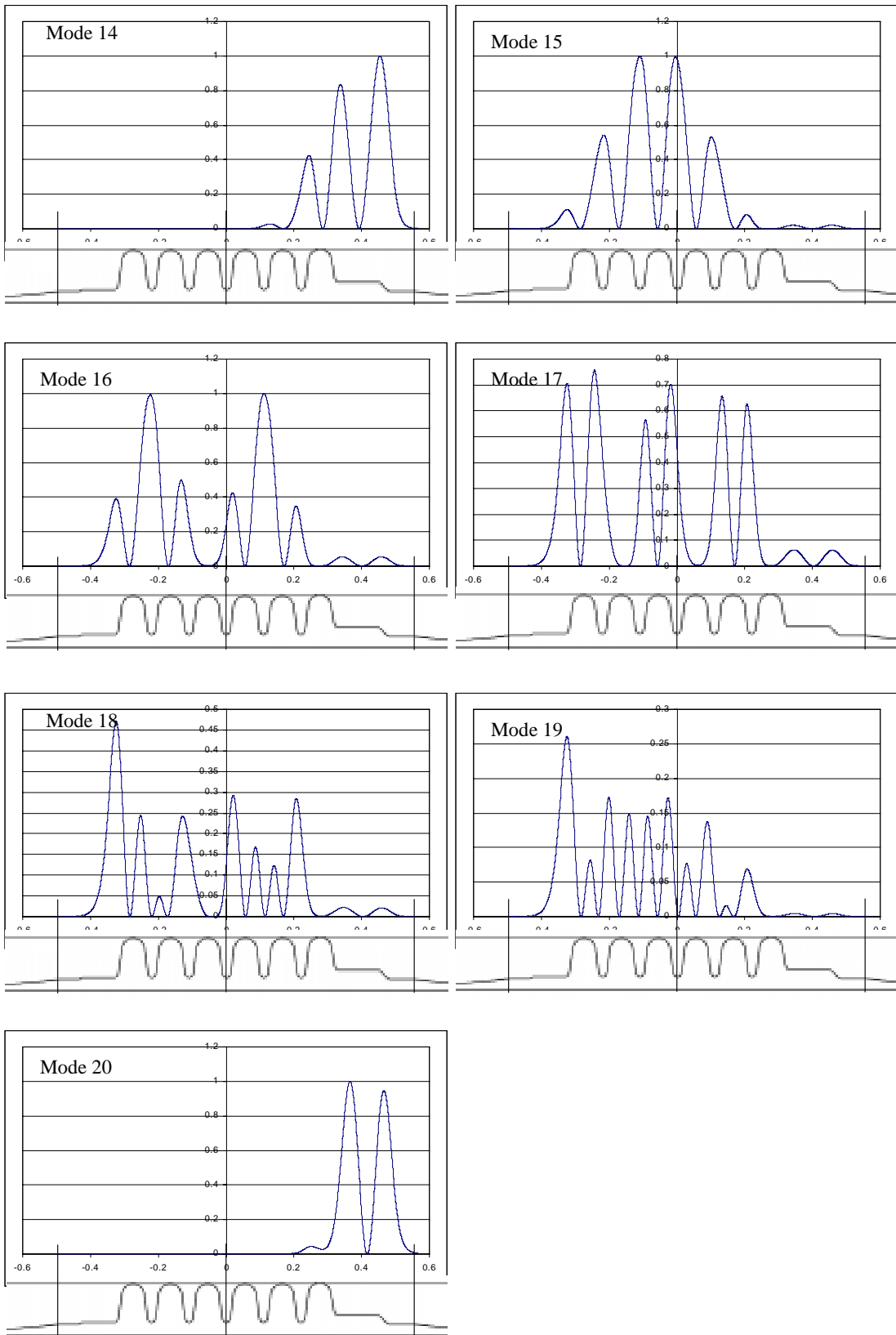


Figure B-4. E_z^2 on the axis of each TM monopoles (continue...)

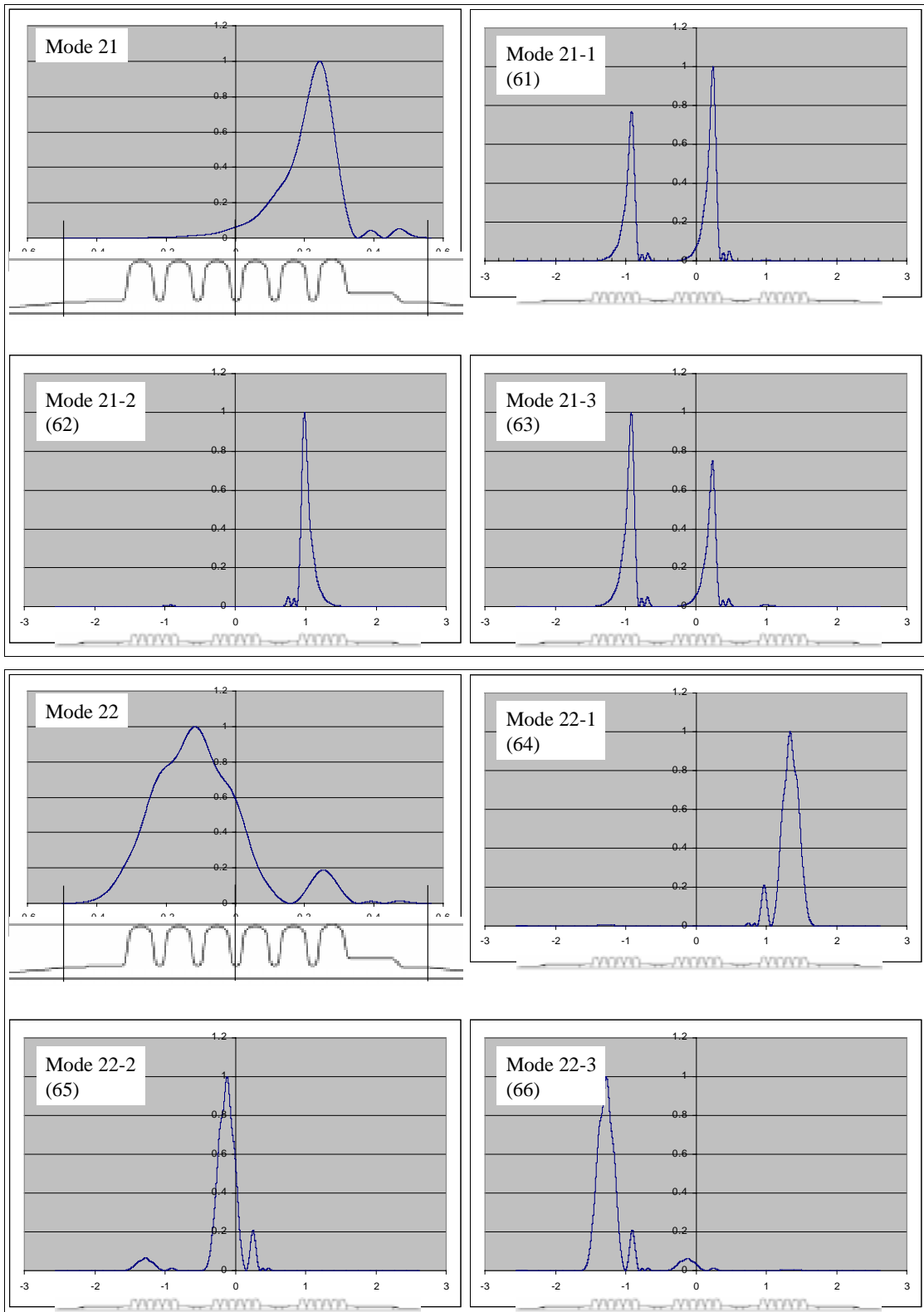


Figure B-4. E_z^2 on the axis of each TM monopoles (continue...)

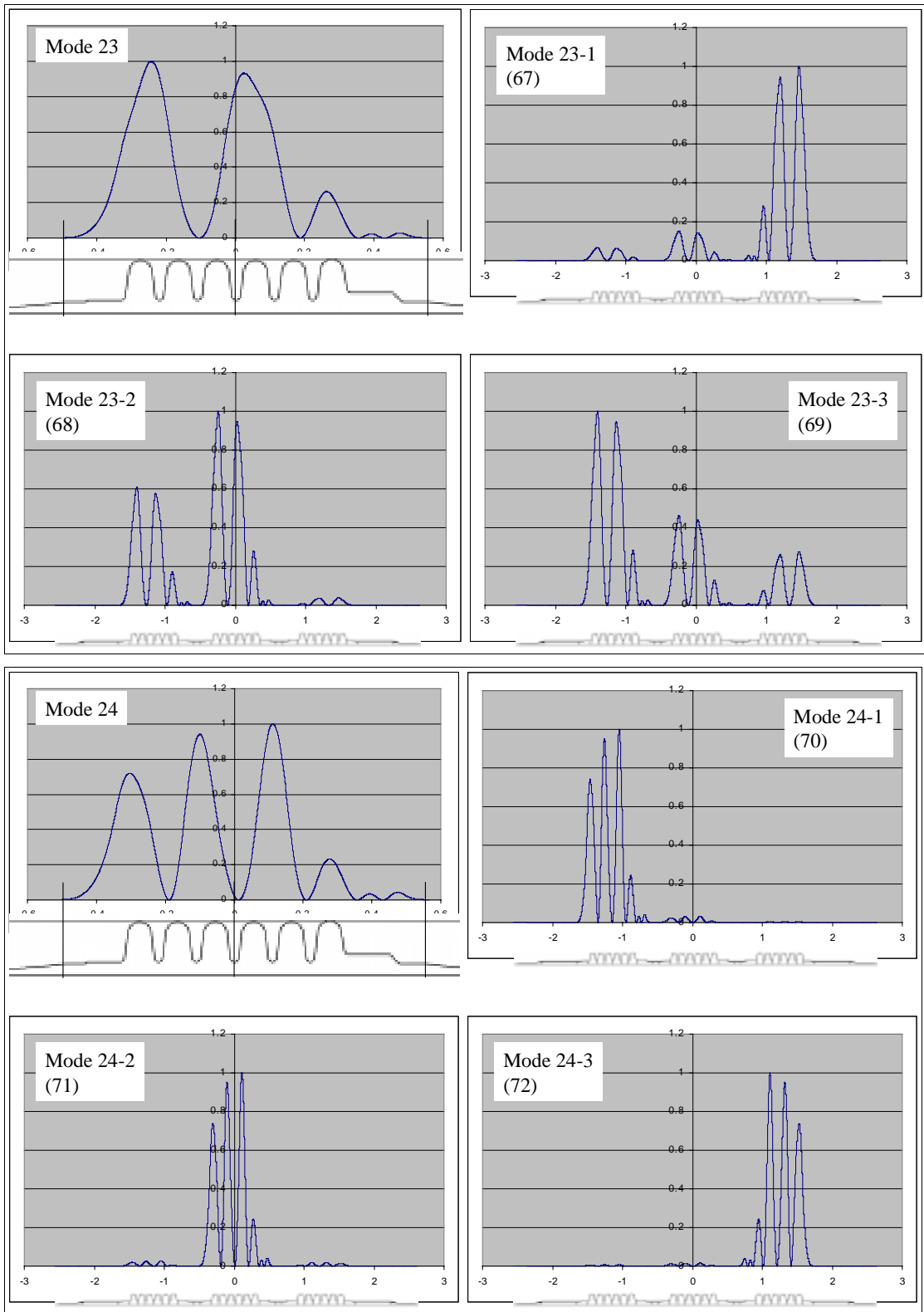


Figure B-4. E_z^2 on the axis of each TM monopoles (continue...)

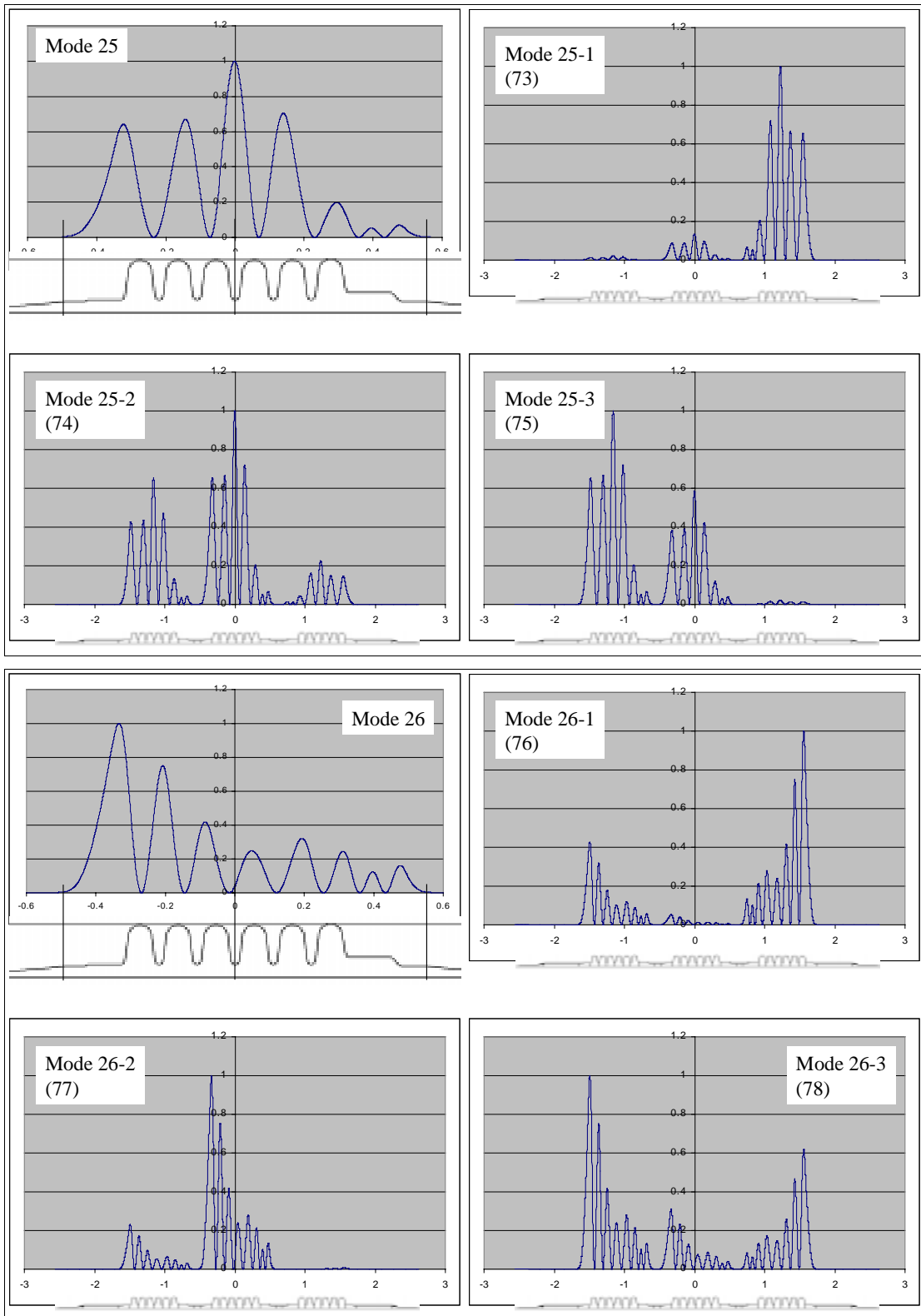


Figure B-4. E_z^2 on the axis of each TM monopoles (continue...)

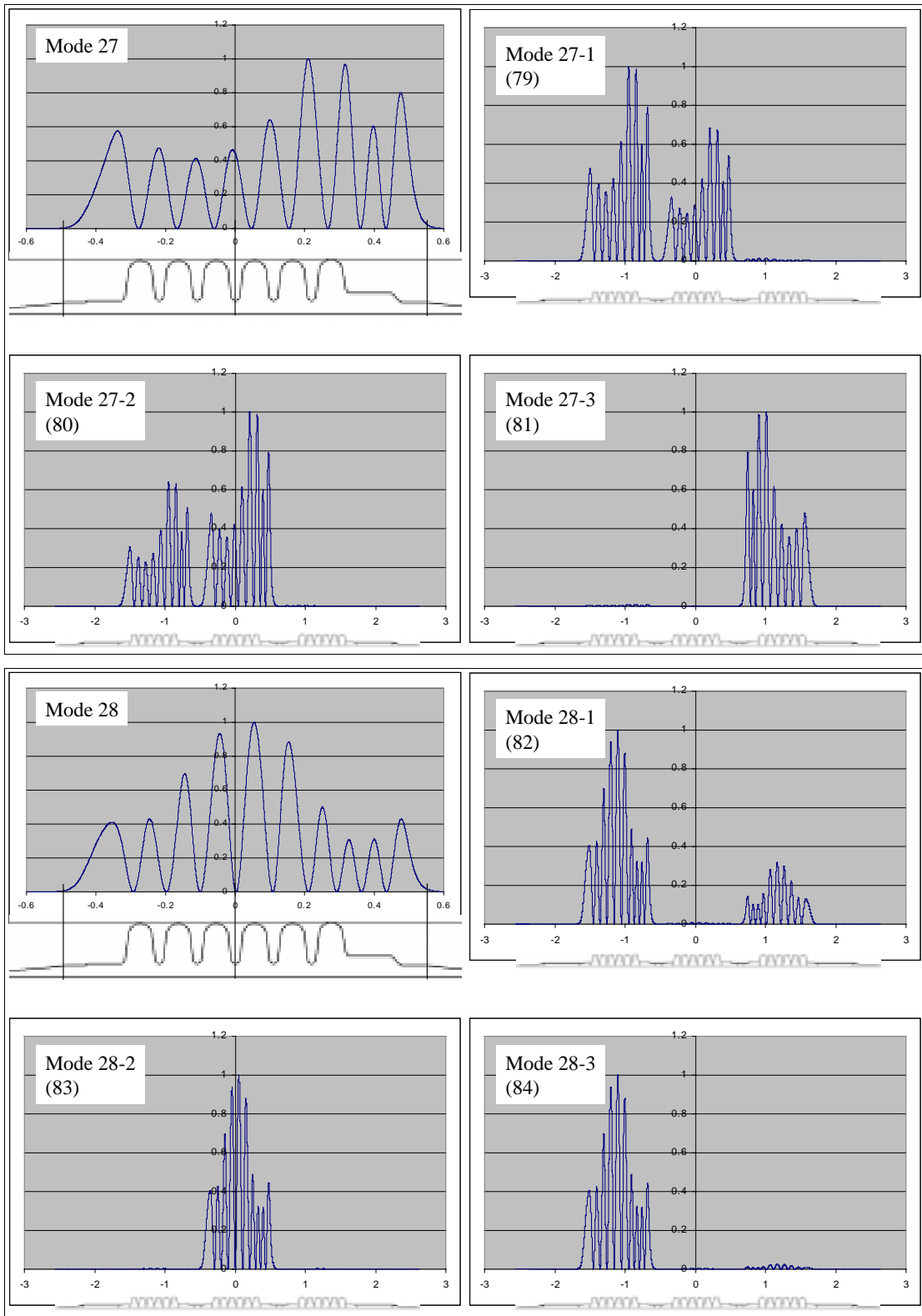


Figure B-4. Ez^2 on the axis of each TM monopoles (continue...)

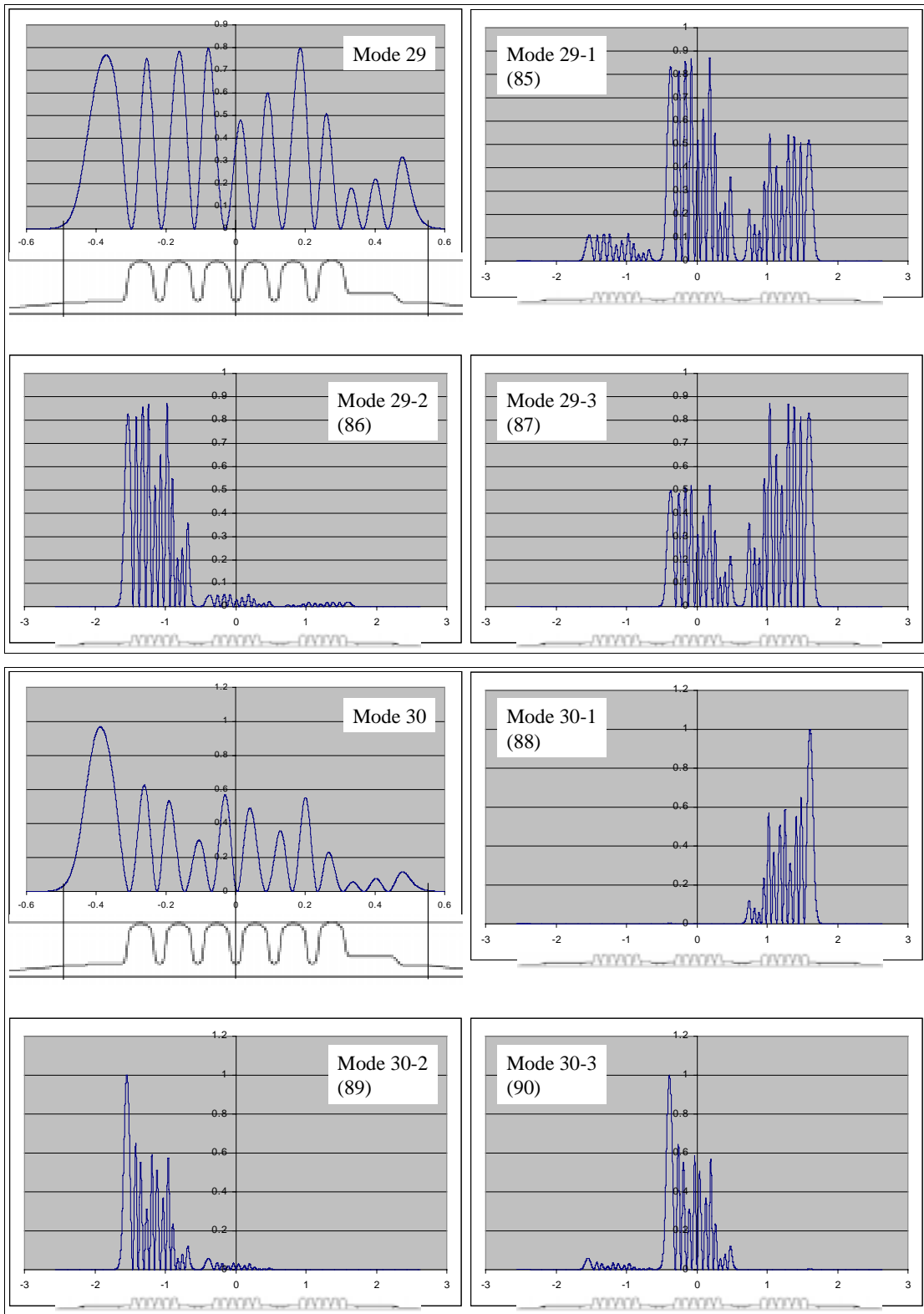


Figure B-4. E_z^2 on the axis of each TM monopoles (continue...)

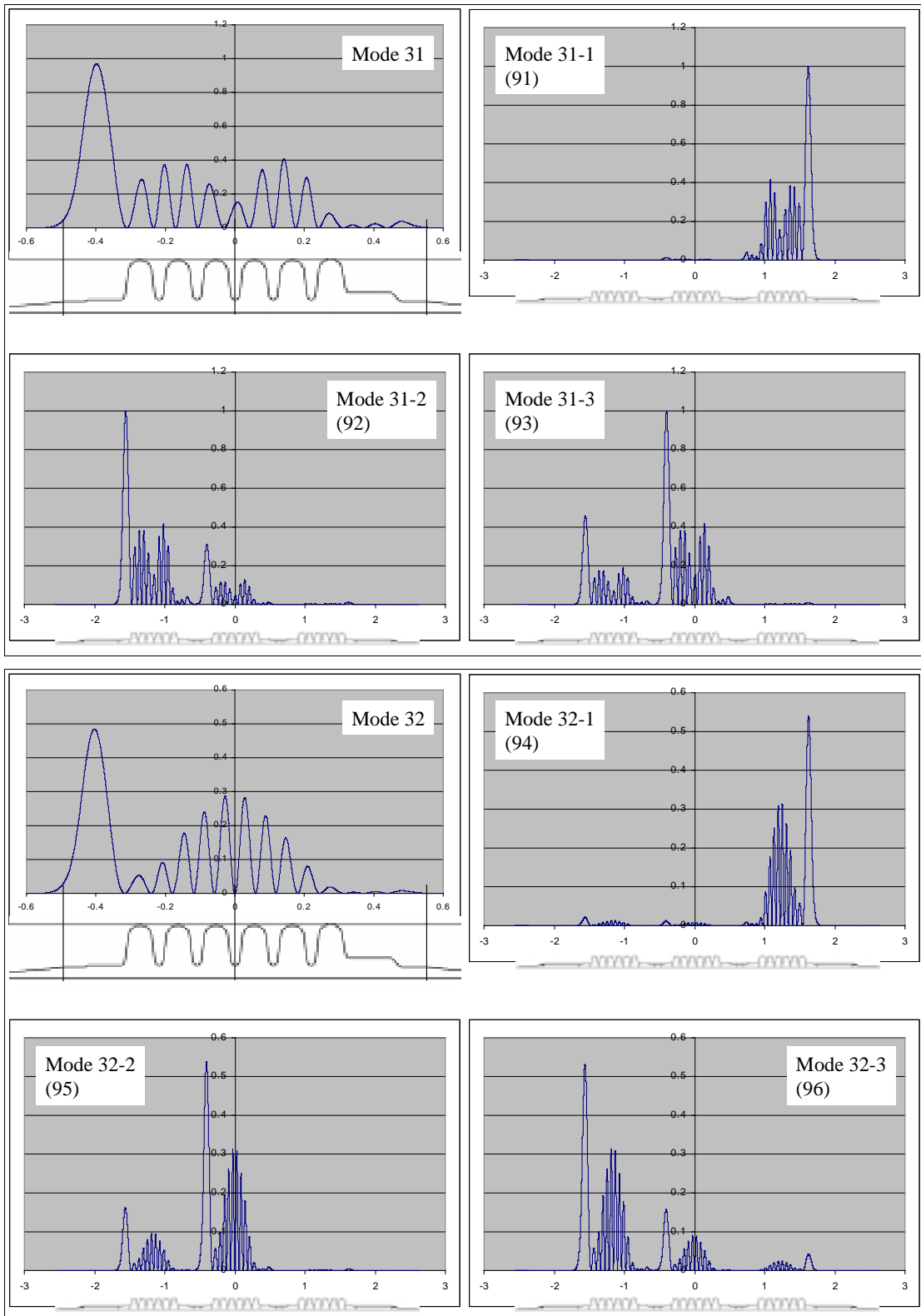


Figure B-4. E_z^2 on the axis of each TM monopoles (continue...)

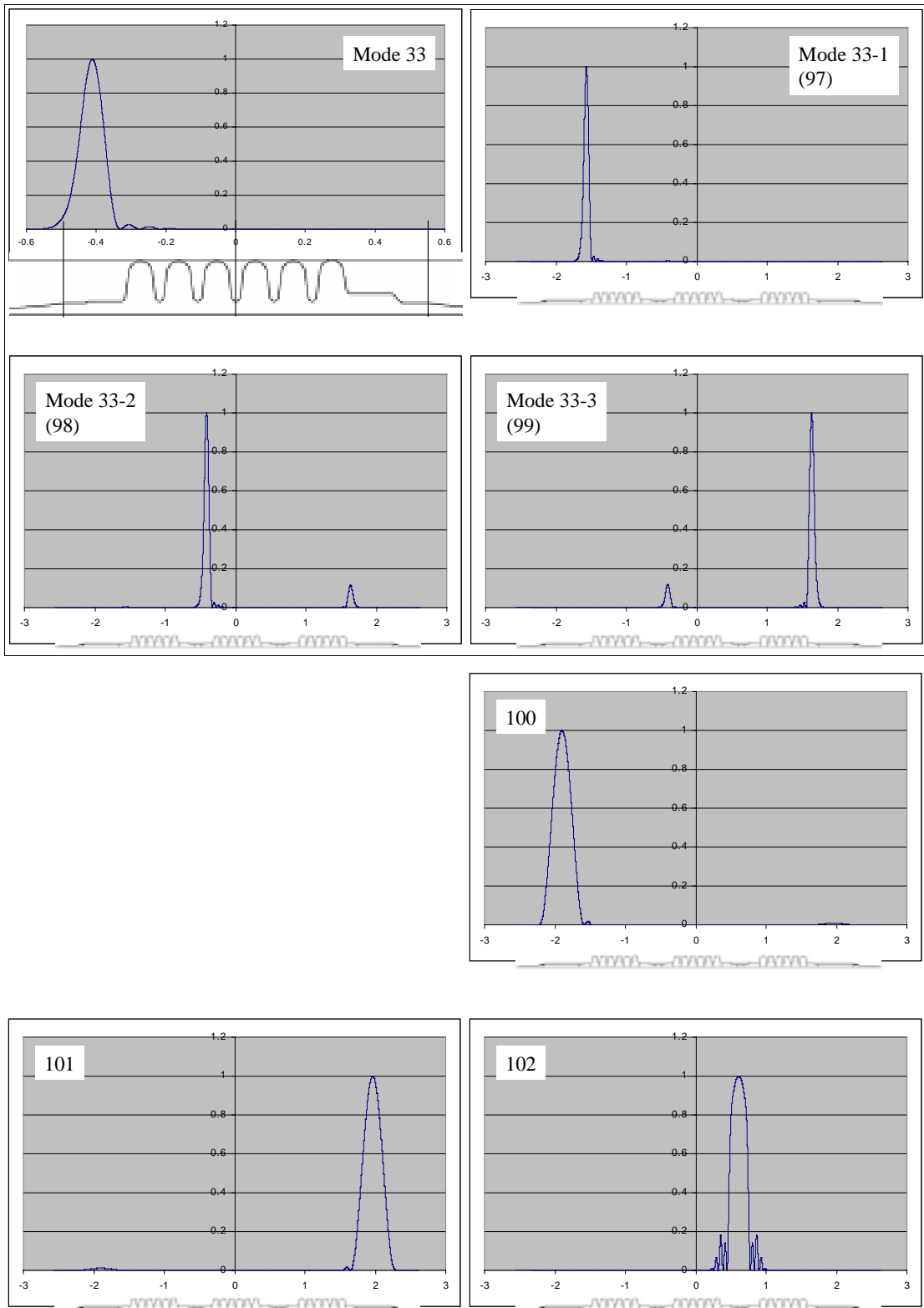


Figure B-4. E_z^2 on the axis of each TM monopoles (continue...)

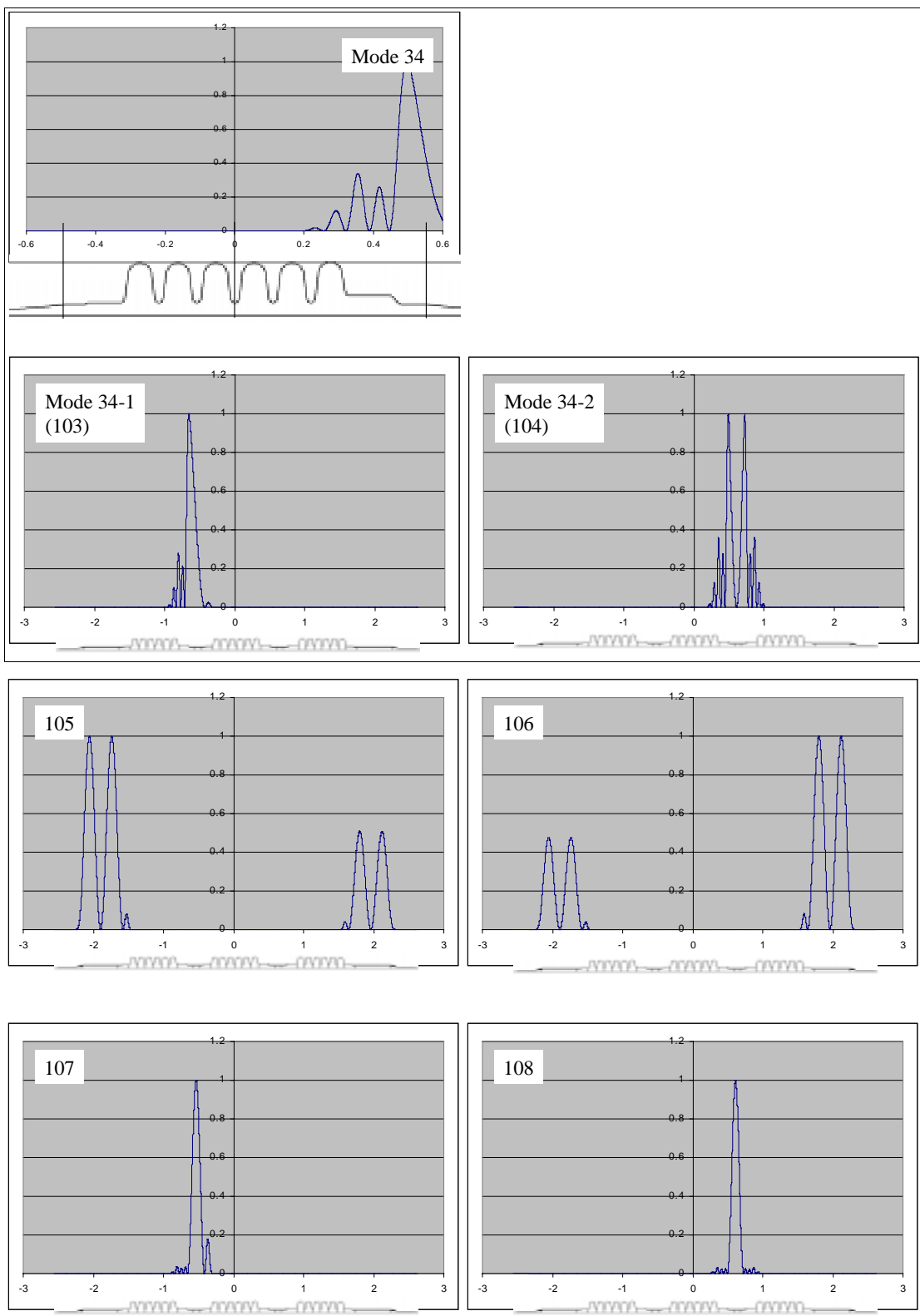


Figure B-4. E_z^2 on the axis of each TM monopoles (continue...)

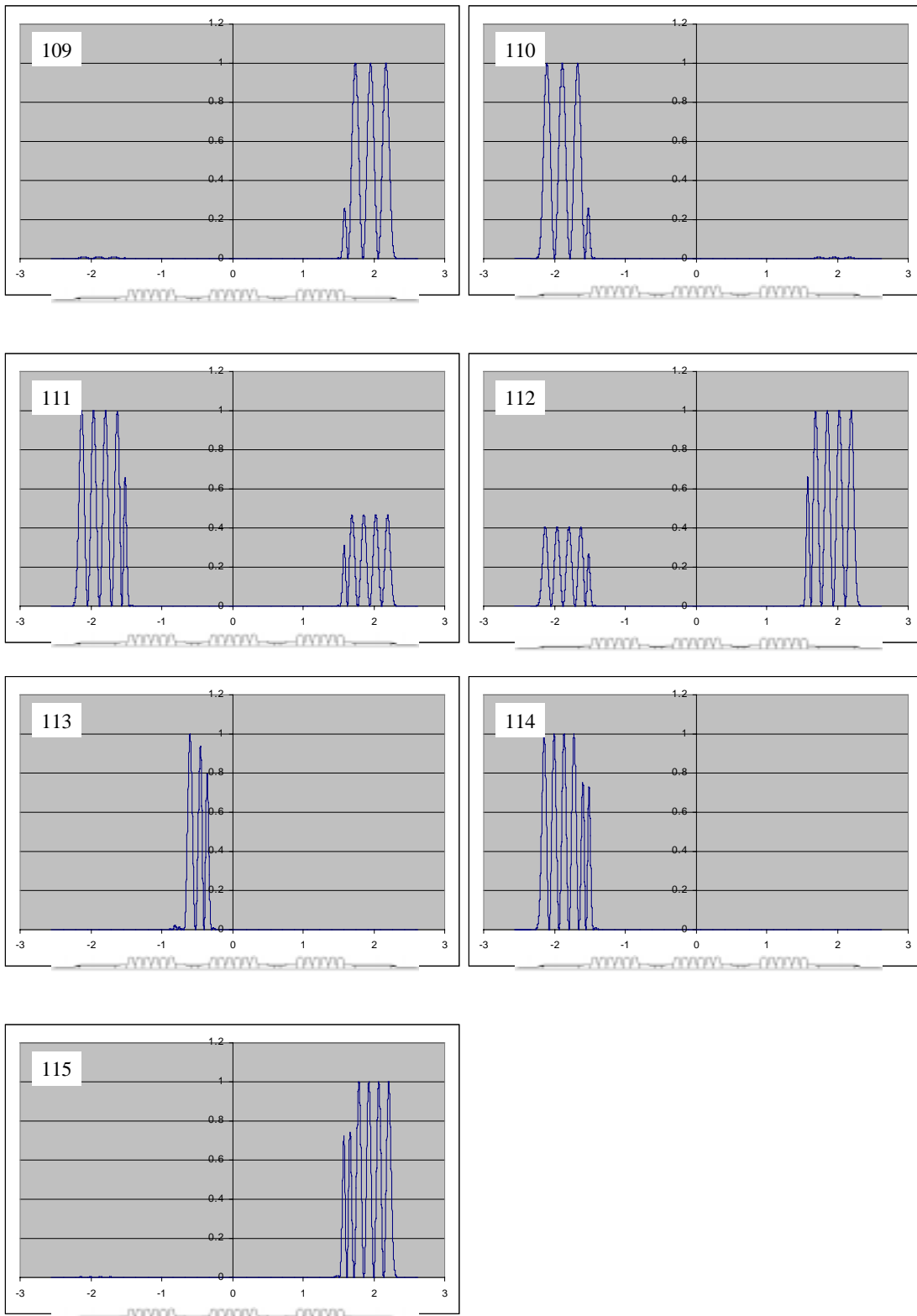


Figure B-4. E_z^2 on the axis of each TM monopoles (continue...)

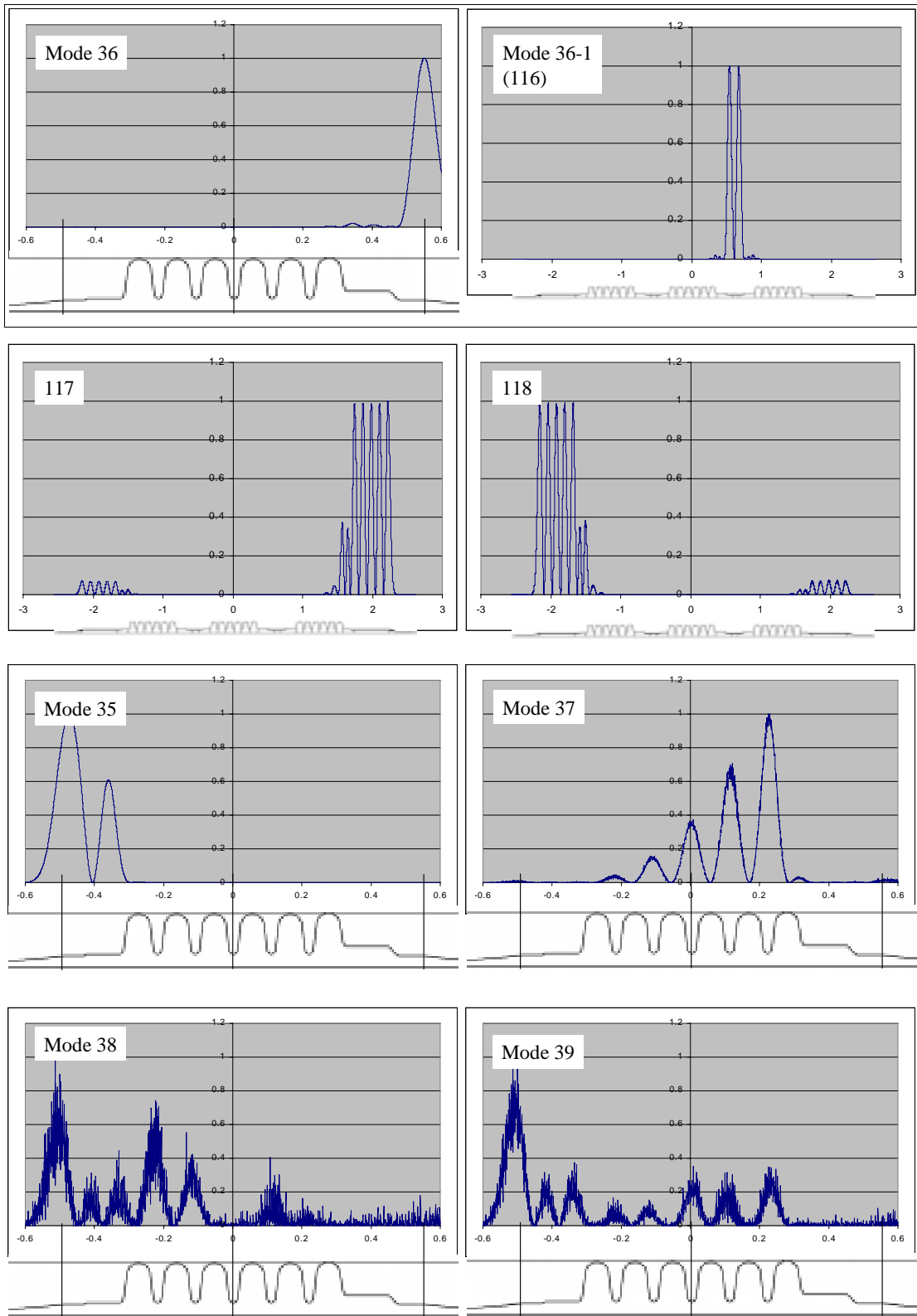


Figure B-4. E_z^2 on the axis of each TM monopoles

Table B-4. TE monopoles.

mode no.	frequency, Hz						
1	2.08157E+09	5	2.16827E+09	9	2.78167E+09	13	2.92836E+09
2	2.16271E+09	6	2.16991E+09	10	2.78697E+09	14	3.15724E+09
3	2.16431E+09	7	2.68210E+09	11	2.79190E+09		
4	2.16640E+09	8	2.77775E+09	12	2.79677E+09		

Table B-5. Dipoles and R/Q as a function of the particle velocity (medium beta, Single cavity)

mode no.	frequency, Hz	R/Q at beta=							
		0.55	0.57	0.59	0.61	0.63	0.65	0.67	0.69
mode 1	1.11712E+09	5.293143	7.150375	9.365545	11.92866	14.8139	17.98069	21.37658	24.9407
mode 2	1.13793E+09	0.064754	0.16994	1.462054	5.084551	12.04908	22.92991	37.7297	55.9157
mode 3	1.14359E+09	6.195654	15.51973	29.07102	44.84854	59.98147	71.71786	78.16995	78.62726
mode 4	1.15214E+09	28.61056	38.90714	44.31834	43.50094	37.26964	27.84179	17.7943	9.249702
mode 5	1.16179E+09	22.17664	17.36008	10.71275	4.851749	1.336121	0.418377	1.424198	3.319905
mode 6	1.16955E+09	1.619243	0.279445	0.238914	0.860774	1.492589	1.765167	1.625947	1.224963
mode 7	1.34599E+09	4.785271	5.159096	5.307374	5.297421	5.18948	5.021393	4.814926	4.585741
mode 8	1.45814E+09	19.33117	20.02721	17.90187	14.23456	10.21966	6.596939	3.726027	1.729833
mode 9	1.50250E+09	1.715144	0.014238	1.718948	5.934801	10.62637	14.21952	16.04893	16.07211
mode 10	1.56286E+09	0.028538	0.725009	1.607982	1.35957	0.40754	0.061221	1.101405	3.438381
mode 11	1.62394E+09	0.200534	0.721208	0.602124	0.143681	0.208664	0.710441	0.937157	0.622688
mode 12	1.66988E+09	0.22197	0.255347	0.03214	0.066647	0.237853	0.183576	0.03035	0.107077
mode 13	1.71948E+09	0.151668	0.071486	0.001505	0.023881	0.026692	0.015894	0.050624	0.088792
mode 14	1.93725E+09	0.605236	0.58776	0.663385	0.460702	0.250424	0.182557	0.135122	0.064882
mode 15	1.97603E+09	1.233417	0.937887	0.214085	0.041882	0.263277	0.250972	0.071731	0.000793
mode 16	2.02147E+09	0.668655	0.755616	0.999719	0.946648	0.403856	0.026597	0.05285	0.1176
mode 17	2.06218E+09	0.09488	0.267444	0.407437	0.493717	0.675902	0.687038	0.374699	0.069706
mode 18	2.09318E+09	0.055375	0.039099	0.055999	0.120944	0.15837	0.225693	0.349068	0.354793
mode 19	2.11337E+09	0.02995	0.036077	0.024279	0.005629	0.007039	0.007305	0.002881	0.047656
mode 20	2.12418E+09	0.089124	0.06598	0.035414	0.010052	0.003433	0.038095	0.125866	0.267725
mode 21	2.19634E+09	0.032632	0.034971	0.029314	0.017493	0.005088	0.001419	0.018684	0.069992
mode 22	2.24083E+09	0.002695	0.002717	0.006115	0.011123	0.022796	0.038858	0.041525	0.066818
mode 23	2.24965E+09	0.00444	0.009203	0.009154	0.013865	0.017833	0.052241	0.312397	1.061284
mode 24	2.26555E+09	0.008379	0.002165	0.00522	0.01686	0.11424	0.533969	1.382606	2.256074
mode 25	2.28785E+09	0.001668	0.009371	0.016696	0.099428	0.486034	1.187999	1.59925	1.296494
mode 26	2.31482E+09	0.022928	0.011412	0.029763	0.285631	0.873489	1.037311	0.498155	0.06833
mode 27	2.34074E+09	0.006568	0.004961	0.119905	0.567295	0.639161	0.142745	0.035301	0.226114
mode 28	2.36812E+09	0.000963	0.035549	0.350763	0.52804	0.202579	0.110209	0.167214	0.044435
mode 29	2.41053E+09	0.00599	0.14685	0.411721	0.269766	0.040789	0.042887	0.032113	0.044114
mode 30	2.42991E+09	0.009474	0.017438	0.006697	0.002523	0.031096	0.050153	0.042991	0.05597
mode 31	2.45469E+09	0.031221	0.148823	0.179876	0.059352	0.022561	0.042978	0.043488	0.051927
mode 32	2.46507E+09	0.016587	0.015499	0.002475	0.001923	0.004324	0.005054	0.018601	0.055227
mode 33	2.46669E+09	0.000567	7.53E-05	0.000964	0.000802	0.000448	0.000727	0.000468	0.000383
mode 34	2.47234E+09	0.002649	0.013147	0.016129	0.024342	0.065665	0.149595	0.211892	0.182506
mode 35	2.47574E+09	0.007222	0.014453	0.042763	0.048953	0.0413	0.02877	0.012853	0.060263
mode 36	2.48555E+09	0.001927	0.019585	0.038676	0.014994	0.024743	0.085153	0.195423	0.329734
mode 37	2.52833E+09	0.020846	0.088596	0.11721	0.030288	0.005517	0.031362	0.034823	0.069956
mode 38	2.57639E+09	0.034201	0.069603	0.100829	0.015999	0.014646	0.031306	0.004546	0.016497
mode 39	2.63383E+09	0.020019	0.077579	0.121823	0.014736	0.026973	0.028119	0.000226	0.030958
mode 40	2.69575E+09	0.011955	0.102429	0.117958	0.010208	0.053831	0.026843	0.004372	0.021318

Table B-6. Quadrupoles and R/Q's as a function of the particle velocity.
(medium beta, Single cavity)

mode no.	frequency	R/Q (Ohm/cm^2) at beta=							
		0.55	0.57	0.59	0.61	0.63	0.65	0.67	0.69
mode 1	1.51744E+09	0.012439	0.019637	0.02998	0.043765	0.061205	0.082405	0.107418	0.136132
mode 2	1.55603E+09	0.000139	0.000262	0.000328	0.000371	0.000399	0.001348	0.003787	0.006985
mode 3	1.55720E+09	0.000516	0.000739	0.001278	0.003771	0.007806	0.009624	0.0063	0.002271
mode 4	1.55878E+09	0.000926	0.003532	0.007763	0.007424	0.00375	0.015568	0.073777	0.204134
mode 5	1.56026E+09	0.014972	0.010088	0.003305	0.029585	0.120729	0.277825	0.466764	0.634414
mode 6	1.56122E+09	0.035697	0.101238	0.194813	0.286798	0.342627	0.345023	0.296782	0.21759
mode 7	1.94871E+09	0.010264	0.01577	0.022906	0.031732	0.042217	0.054322	0.067914	0.082773
mode 8	2.07281E+09	4.01E-05	0.000525	0.001117	0.000445	0.00077	0.013737	0.058688	0.152131
mode 9	2.07960E+09	0.000953	0.000556	0.000705	0.015345	0.064589	0.151475	0.248121	0.309689
mode 10	2.08869E+09	1.89E-05	0.005355	0.032634	0.086506	0.141442	0.160487	0.129112	0.069282
mode 11	2.09736E+09	0.007057	0.03019	0.060073	0.070583	0.051784	0.021039	0.002127	0.003047
mode 12	2.10317E+09	0.01694	0.023025	0.016785	0.005823	0.000347	0.001751	0.004656	0.004751
mode 13	2.32915E+09	0.005673	0.009696	0.012917	0.014196	0.013305	0.010878	0.00791	0.005335
mode 14	2.46636E+09	0.024264	0.039379	0.055782	0.069262	0.08011	0.089422	0.095329	0.096492
mode 15	2.47653E+09	0.017433	0.074372	0.155919	0.2316	0.263803	0.238404	0.182003	0.123571
mode 16	2.48333E+09	0.094395	0.122061	0.087256	0.02467	0.00125	0.047418	0.117494	0.162391
mode 17	2.49272E+09	0.076091	0.029606	0.000892	0.009831	0.022951	0.010123	0.000438	0.023122
mode 18	2.50333E+09	0.009519	0.000397	0.007722	0.006882	0.000204	0.005997	0.012528	0.00619
mode 19	2.51293E+09	0.000902	0.002787	0.000968	0.000364	0.003071	0.002205	0.000143	0.002163
mode 20	2.54108E+09	0.001263	0.002117	0.004211	0.00715	0.009309	0.010372	0.010686	0.009776
mode 21	2.56694E+09	2.29E-05	5.87E-06	0.000334	0.000507	0.000256	0.000583	0.000715	0.000957
mode 22	2.58399E+09	0.002996	7.67E-05	0.000353	0.000196	0.001124	0.001456	0.001884	0.002459
mode 23	2.60272E+09	0.004238	0.001836	9.04E-05	0.001571	0.001254	0.001428	0.002138	0.004953
mode 24	2.61892E+09	0.000126	0.000572	0.0002	0.001609	0.006291	0.007759	0.014008	0.047116
mode 25	2.62850E+09	0.000529	0.000275	8.66E-05	0.000913	0.008551	0.03197	0.067411	0.096248
mode 26	2.71646E+09	0.000317	0.000634	0.000751	0.000567	0.000257	0.000208	0.000837	0.002418
mode 27	2.76014E+09	0.00233	0.001397	0.000297	1.74E-05	8.6E-05	6.47E-05	2.78E-05	2.3E-05
mode 28	2.76229E+09	0.001567	0.00397	0.004393	0.002066	0.000292	2.02E-05	0.000154	0.000248
mode 29	2.76571E+09	4.35E-05	0.000662	0.003803	0.006895	0.005641	0.002449	0.000593	8.14E-05
mode 30	2.77015E+09	0.000101	0.000119	5.29E-05	0.001578	0.004948	0.006805	0.006077	0.004449

Table B-7. Sextupoles and R/Q as a function of the particle velocity (medium beta, Single cavity)

mode no.	frequency	R/Q (Ohm/cm^4) at beta=							
		0.55	0.57	0.59	0.61	0.63	0.65	0.67	0.69
mode 1	1.89045E+09	0.000125	9.8E-05	7.86E-05	7.34E-05	8.94E-05	0.000132	0.000208	0.000319
mode 2	1.93433E+09	0.00017	6.81E-05	2.08E-05	2.3E-06	5.22E-06	2.52E-05	6.08E-05	0.000115
mode 3	1.93453E+09	0.000274	7.69E-05	8.57E-06	2.5E-07	1.37E-06	1.29E-05	3.45E-05	4.38E-05
mode 4	1.93472E+09	0.000292	0.000198	5.86E-05	1.03E-06	1E-05	1.03E-05	3.1E-06	6.11E-05
mode 5	1.93494E+09	3.03E-05	5.96E-05	3.79E-05	4.98E-07	4.94E-05	0.000208	0.000358	0.00035
mode 6	1.93513E+09	1.78E-06	8.81E-08	2.61E-06	1.61E-07	1.7E-05	0.000149	0.000544	0.001314
mode 7	2.31760E+09	2.35E-05	2.78E-05	4.14E-05	6.74E-05	0.000108	0.000166	0.00024	0.000332
mode 8	2.38305E+09	9.32E-08	5.43E-08	1.41E-07	1.54E-07	3.04E-06	8.48E-06	8.54E-06	9.34E-07
mode 9	2.38357E+09	2.73E-07	9.52E-09	2.33E-06	8.58E-06	6.08E-06	1.07E-06	5.79E-05	0.000277
mode 10	2.38422E+09	5.06E-06	1.22E-06	2.63E-06	2.81E-06	6.81E-05	0.000275	0.000614	0.000966
mode 11	2.38476E+09	3.86E-06	2.96E-06	5.36E-05	0.000174	0.000317	0.000404	0.000387	0.000282
mode 12	2.39201E+09	4.83E-06	2.4E-06	1.46E-05	4.56E-05	9.67E-05	0.000167	0.000254	0.000354
mode 13	2.78600E+09	2.44E-05	4.09E-05	6.27E-05	8.98E-05	0.000121	0.000156	0.000191	0.000226
mode 14	2.87809E+09	0.000246	0.000321	0.000413	0.000521	0.000644	0.000781	0.000932	0.001101

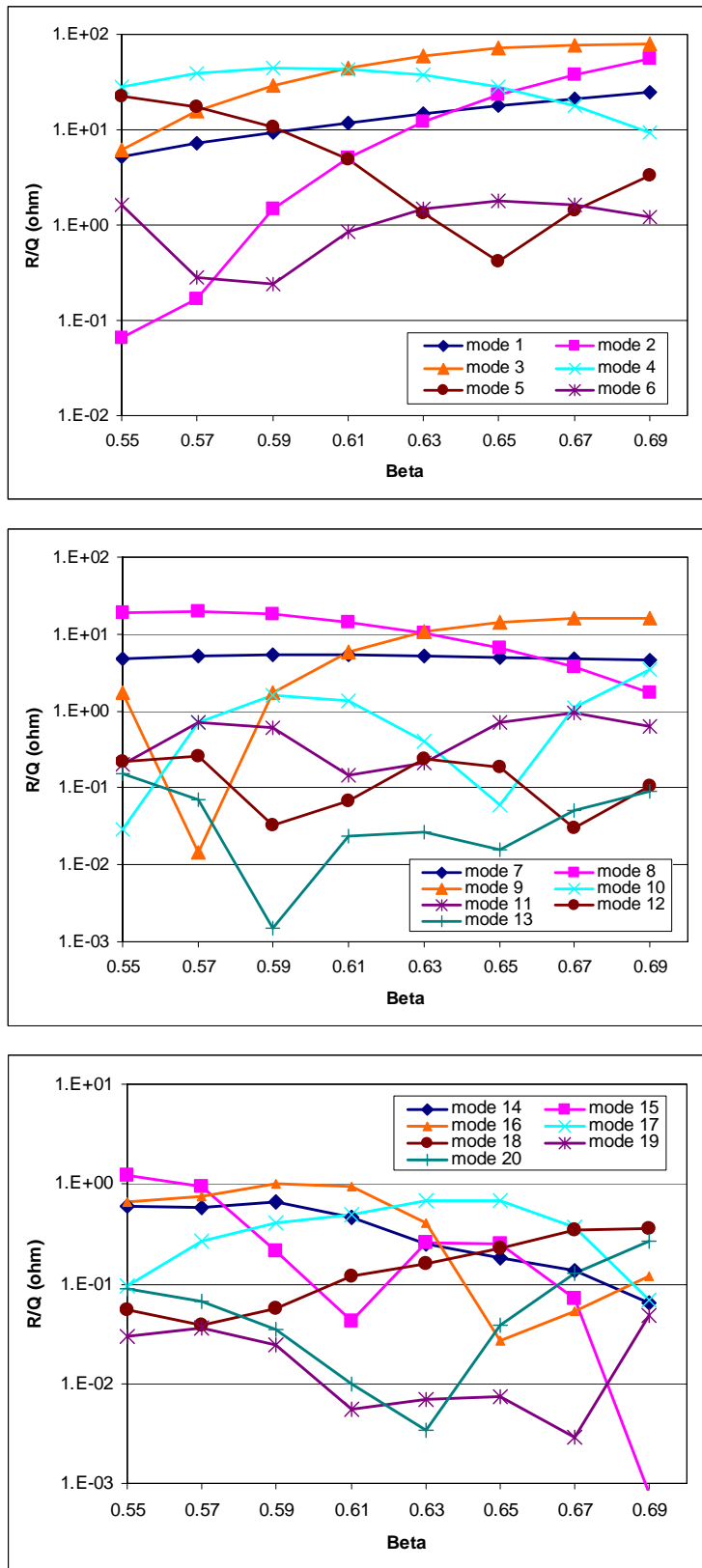


Figure B-5. R/Q 's of dipoles as a function of the particle velocity (medium beta, single cavity)

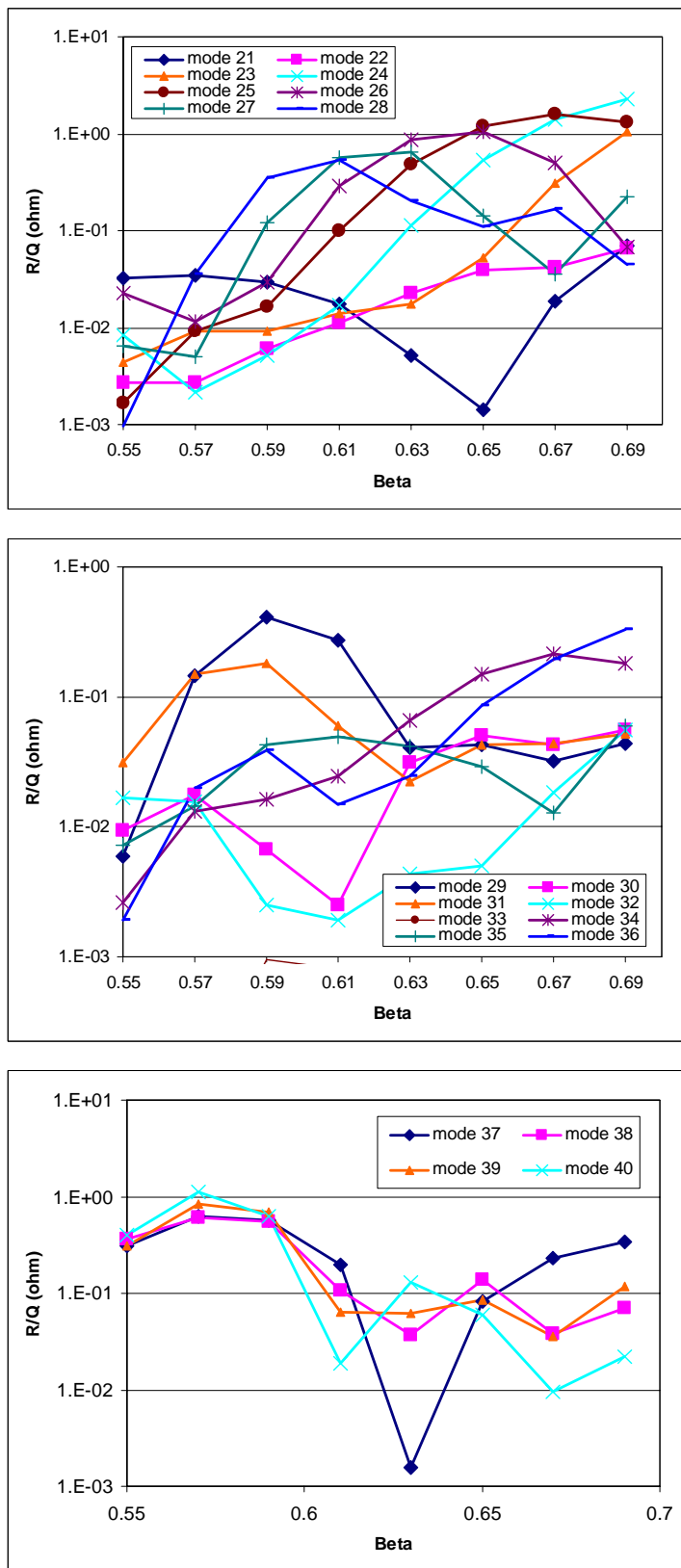


Figure B-5. R/Q 's of dipoles as a function of the particle velocity (medium beta, single cavity)

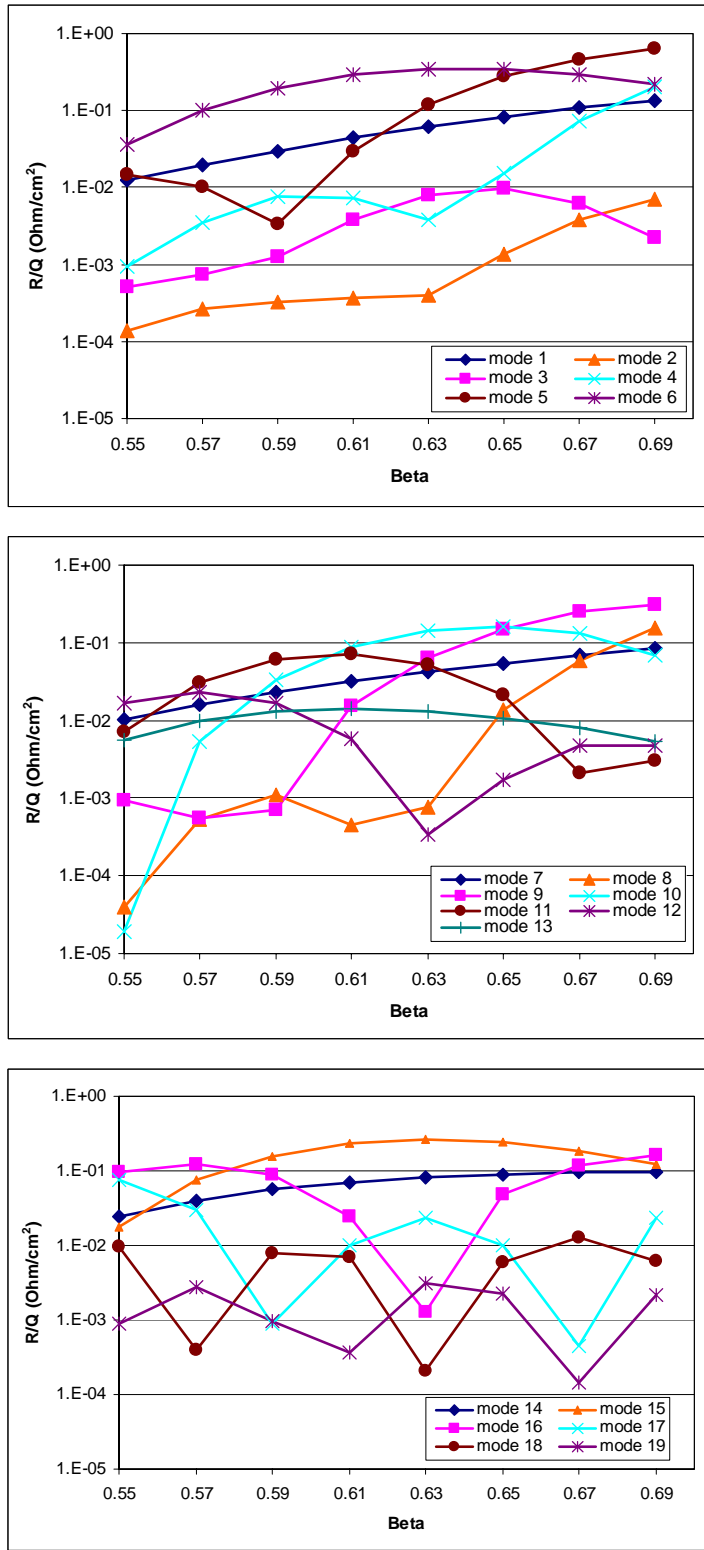


Figure B-6. R/Q 's of quadrupoles as a function of the particle velocity (medium beta, single cavity)

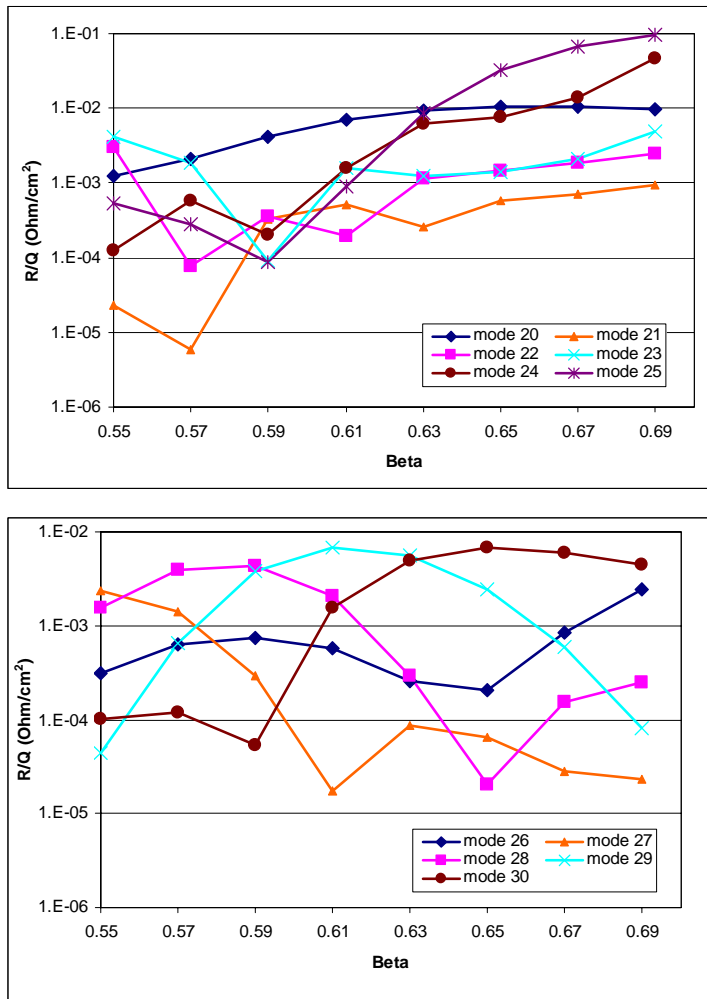


Figure B-6. R/Q's of quadrupoles as a function of the particle velocity (medium beta, single cavity)

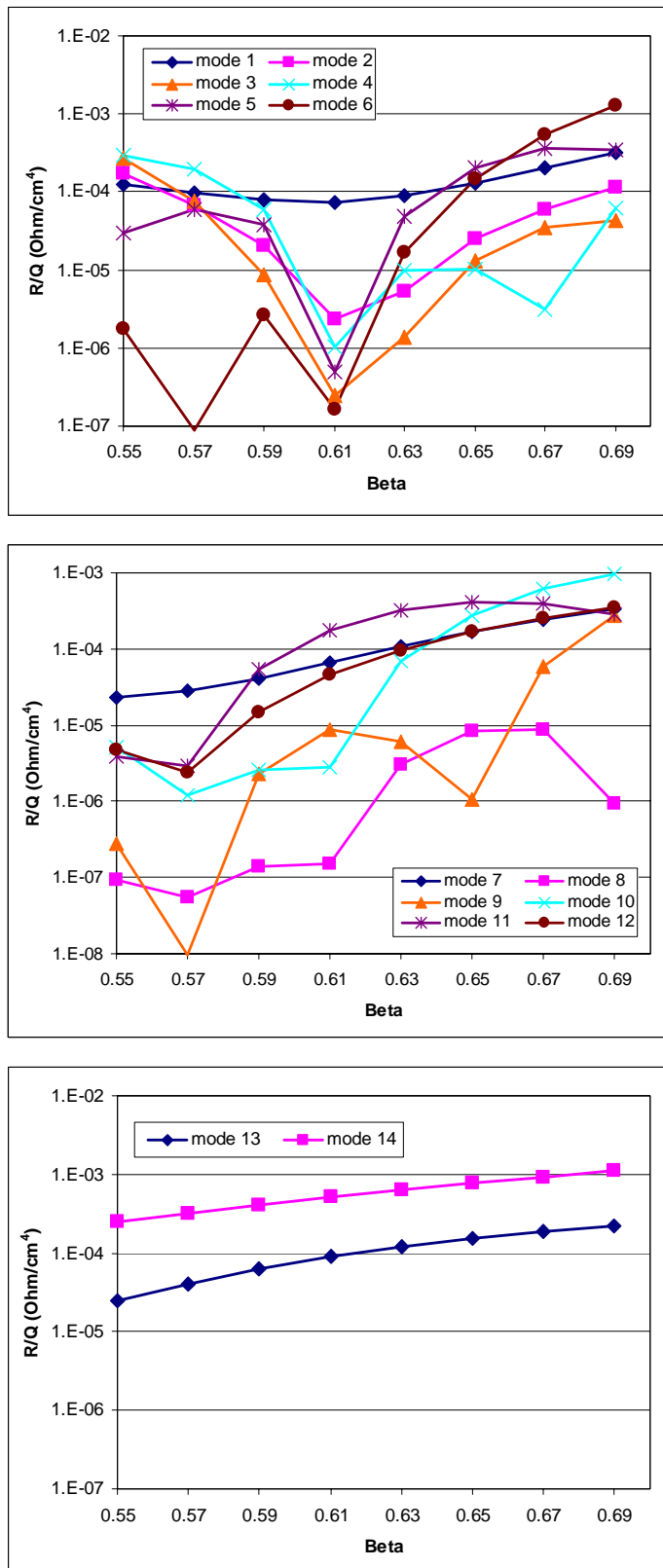


Figure B-7. R/Q 's of sextupoles as a function of the particle velocity (medium beta, single cavity)

Appendix C. SNS high beta cavity HOM and their properties.

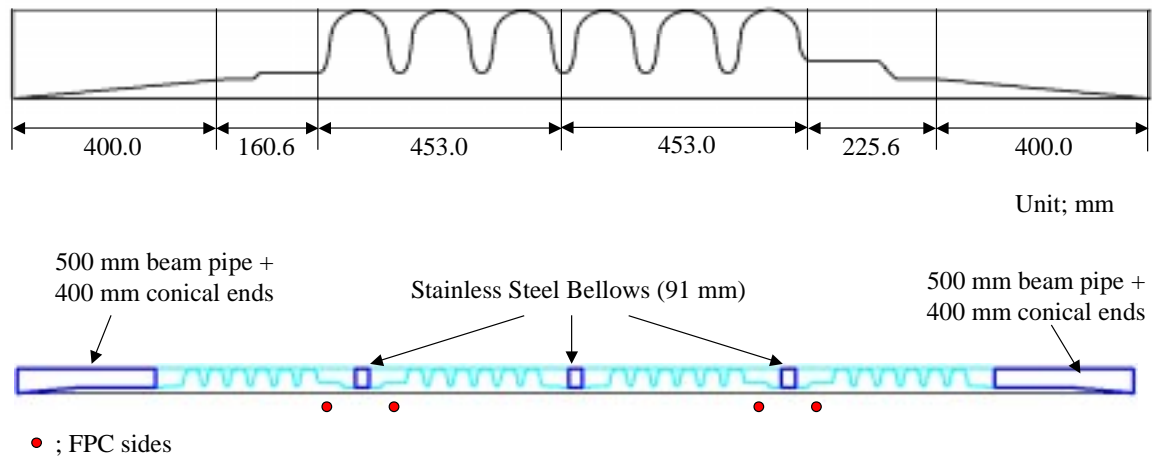


Figure C-1. MAFIA models of the single cavity with conical ends
and the super-structure (ref. SNS drawing)

Table C-1. TM monopoles and R/Q as a function of the particle velocity of high beta, single cavity (continue..)

mode no.	frequency Hz	R/Q (Ohm) at beta=									
		0.7	0.71	0.72	0.73	0.74	0.75	0.76	0.77	0.78	0.79
1	7.93629E+08	0.018	0.025	0.036	0.047	0.057	0.063	0.066	0.066	0.063	0.058
2	7.95869E+08	0.924	0.772	0.616	0.470	0.344	0.242	0.166	0.115	0.086	0.074
3	7.98919E+08	0.115	0.248	0.432	0.608	0.736	0.801	0.805	0.754	0.665	0.557
4	8.01954E+08	24.007	17.597	12.366	8.274	5.227	3.080	1.669	0.821	0.370	0.179
5	8.04172E+08	145.285	133.814	119.310	102.713	84.994	66.982	49.856	34.269	21.007	10.696
6	8.04979E+08	146.411	179.657	214.706	250.769	286.966	322.561	356.580	388.727	418.054	444.114
7	1.65457E+09	0.449	0.569	0.702	0.847	1.002	1.164	1.331	1.502	1.675	1.847
8	1.69962E+09	0.906	0.996	1.085	1.171	1.253	1.326	1.392	1.444	1.482	1.507
9	1.70749E+09	0.418	0.546	0.681	0.815	0.945	1.067	1.175	1.268	1.342	1.400
10	1.71052E+09	1.247	1.298	1.317	1.303	1.260	1.197	1.116	1.025	0.926	0.827
11	1.71370E+09	0.828	0.731	0.630	0.532	0.441	0.362	0.296	0.244	0.206	0.181
12	1.71563E+09	0.240	0.230	0.233	0.245	0.264	0.289	0.317	0.347	0.378	0.409
13	1.73695E+09	1.534	1.616	1.691	1.757	1.816	1.871	1.918	1.965	2.013	2.061
14	1.74926E+09	1.870	2.260	2.707	3.214	3.789	4.428	5.141	5.922	6.781	7.709
15	1.75522E+09	0.781	1.230	1.844	2.650	3.672	4.927	6.424	8.167	10.147	12.351
16	1.75780E+09	3.593	4.327	5.037	5.683	6.218	6.601	6.812	6.831	6.654	6.284
17	1.76088E+09	1.695	1.544	1.342	1.109	0.869	0.640	0.447	0.306	0.228	0.222
18	1.76567E+09	1.928	2.119	2.334	2.573	2.834	3.119	3.425	3.753	4.101	4.468
19	1.81342E+09	0.744	0.751	0.750	0.740	0.722	0.699	0.672	0.641	0.609	0.575
20	2.14631E+09	0.127	0.131	0.147	0.178	0.226	0.291	0.373	0.471	0.584	0.711
21	2.30243E+09	0.003	0.003	0.007	0.019	0.042	0.079	0.126	0.179	0.237	0.300
22	2.32069E+09	0.011	0.004	0.003	0.011	0.020	0.022	0.017	0.011	0.017	0.041
23	2.34716E+09	0.005	0.010	0.029	0.044	0.042	0.030	0.024	0.034	0.054	0.065
24	2.37932E+09	0.030	0.046	0.044	0.027	0.020	0.044	0.090	0.126	0.128	0.100
25	2.41457E+09	0.031	0.020	0.013	0.039	0.092	0.136	0.138	0.108	0.089	0.122
26	2.44580E+09	0.003	0.014	0.043	0.071	0.077	0.066	0.070	0.114	0.189	0.256
27	2.49981E+09	0.042	0.048	0.055	0.053	0.045	0.051	0.080	0.119	0.142	0.135
28	2.54140E+09	0.007	0.016	0.010	0.001	0.012	0.047	0.074	0.065	0.031	0.016
29	2.56249E+09	0.041	0.011	0.002	0.022	0.042	0.033	0.007	0.007	0.055	0.125
30	2.58186E+09	0.022	0.043	0.048	0.030	0.007	0.004	0.027	0.053	0.055	0.029
31	2.59817E+09	0.003	0.002	0.005	0.014	0.022	0.023	0.014	0.004	0.005	0.020
32	2.61004E+09	0.002	0.003	0.004	0.003	0.002	0.003	0.004	0.005	0.004	0.002
33	2.61678E+09	0.000	0.000	0.001	0.001	0.001	0.002	0.002	0.002	0.002	0.001
34	2.73812E+09	0.062	0.110	0.166	0.222	0.270	0.305	0.325	0.330	0.318	0.291
35	2.81596E+09	0.087	0.169	0.265	0.354	0.412	0.412	0.343	0.227	0.113	0.050
36	2.83079E+09	0.041	0.028	0.013	0.025	0.097	0.254	0.498	0.777	0.982	1.005
37	2.85801E+09	0.003	0.002	0.012	0.020	0.019	0.014	0.019	0.063	0.201	0.496
38	2.89410E+09	0.009	0.019	0.016	0.005	0.001	0.007	0.011	0.008	0.004	0.004
39	2.93447E+09	0.014	0.006	0.001	0.011	0.026	0.025	0.010	0.000	0.006	0.016
40	2.97638E+09	0.002	0.003	0.019	0.029	0.018	0.001	0.009	0.038	0.058	0.047

Table C-1. TM monopoles and R/Q as a function of the particle velocity of high beta, single cavity

mode	frequency (Hz)	R/Q (Ohm) at beta=									
		0.8	0.81	0.82	0.83	0.84	0.85	0.86	0.87	0.88	
1	7.93629E+08	0.051	0.043	0.035	0.027	0.021	0.015	0.010	0.006	0.003	
2	7.95869E+08	0.077	0.089	0.109	0.134	0.164	0.198	0.238	0.284	0.338	
3	7.98919E+08	0.446	0.345	0.265	0.208	0.177	0.166	0.169	0.180	0.189	
4	8.01954E+08	0.138	0.172	0.247	0.363	0.553	0.882	1.437	2.319	3.645	
5	8.04172E+08	3.823	0.730	1.614	6.547	15.468	28.207	44.510	64.018	86.320	
6	8.04979E+08	466.519	484.946	499.136	509.435	515.446	517.366	515.172	509.708	500.485	
7	1.65457E+09	2.015	2.176	2.331	2.474	2.602	2.721	2.827	2.917	2.994	
8	1.69962E+09	1.515	1.510	1.490	1.457	1.414	1.363	1.305	1.247	1.190	
9	1.70749E+09	1.441	1.461	1.468	1.457	1.431	1.390	1.334	1.266	1.183	
10	1.71052E+09	0.729	0.634	0.544	0.462	0.387	0.319	0.260	0.209	0.166	
11	1.71370E+09	0.168	0.165	0.171	0.186	0.207	0.235	0.268	0.306	0.347	
12	1.71563E+09	0.439	0.467	0.493	0.516	0.538	0.556	0.572	0.586	0.597	
13	1.73695E+09	2.114	2.174	2.246	2.334	2.435	2.557	2.702	2.872	3.072	
14	1.74926E+09	8.709	9.783	10.919	12.125	13.386	14.702	16.063	17.476	18.911	
15	1.75522E+09	14.760	17.349	20.089	22.949	25.890	28.871	31.861	34.814	37.697	
16	1.75780E+09	5.749	5.076	4.309	3.492	2.684	1.935	1.305	0.847	0.614	
17	1.76088E+09	0.289	0.423	0.617	0.857	1.127	1.408	1.684	1.937	2.153	
18	1.76567E+09	4.855	5.259	5.689	6.140	6.614	7.117	7.649	8.213	8.815	
19	1.81342E+09	0.544	0.517	0.499	0.492	0.498	0.522	0.566	0.634	0.732	
20	2.14631E+09	0.850	1.002	1.167	1.344	1.535	1.742	1.968	2.218	2.490	
21	2.30243E+09	0.372	0.452	0.531	0.593	0.621	0.599	0.525	0.410	0.276	
22	2.32069E+09	0.080	0.132	0.205	0.321	0.512	0.801	1.185	1.622	2.041	
23	2.34716E+09	0.058	0.040	0.028	0.035	0.059	0.090	0.122	0.184	0.339	
24	2.37932E+09	0.072	0.071	0.103	0.145	0.166	0.152	0.113	0.077	0.066	
25	2.41457E+09	0.207	0.300	0.347	0.326	0.259	0.198	0.188	0.239	0.319	
26	2.44580E+09	0.276	0.248	0.211	0.214	0.282	0.398	0.510	0.568	0.551	
27	2.49981E+09	0.115	0.116	0.163	0.248	0.335	0.380	0.367	0.314	0.269	
28	2.54140E+09	0.056	0.144	0.225	0.242	0.182	0.090	0.042	0.089	0.229	
29	2.56249E+09	0.160	0.127	0.054	0.007	0.042	0.156	0.291	0.364	0.332	
30	2.58186E+09	0.003	0.009	0.055	0.117	0.154	0.142	0.089	0.031	0.007	
31	2.59817E+09	0.041	0.054	0.050	0.032	0.013	0.006	0.018	0.042	0.065	
32	2.61004E+09	0.001	0.005	0.012	0.022	0.032	0.037	0.037	0.032	0.026	
33	2.61678E+09	0.001	0.000	0.000	0.001	0.003	0.005	0.007	0.007	0.005	
34	2.73812E+09	0.254	0.209	0.161	0.114	0.073	0.043	0.030	0.041	0.085	
35	2.81596E+09	0.056	0.104	0.149	0.158	0.131	0.093	0.070	0.070	0.083	
36	2.83079E+09	0.817	0.505	0.216	0.068	0.080	0.183	0.277	0.299	0.252	
37	2.85801E+09	0.949	1.455	1.825	1.893	1.621	1.117	0.588	0.211	0.056	
38	2.89410E+09	0.013	0.068	0.249	0.643	1.272	2.021	2.675	3.007	2.902	
39	2.93447E+09	0.016	0.008	0.003	0.001	0.002	0.037	0.188	0.561	1.203	
40	2.97638E+09	0.019	0.004	0.011	0.026	0.033	0.031	0.025	0.014	0.002	

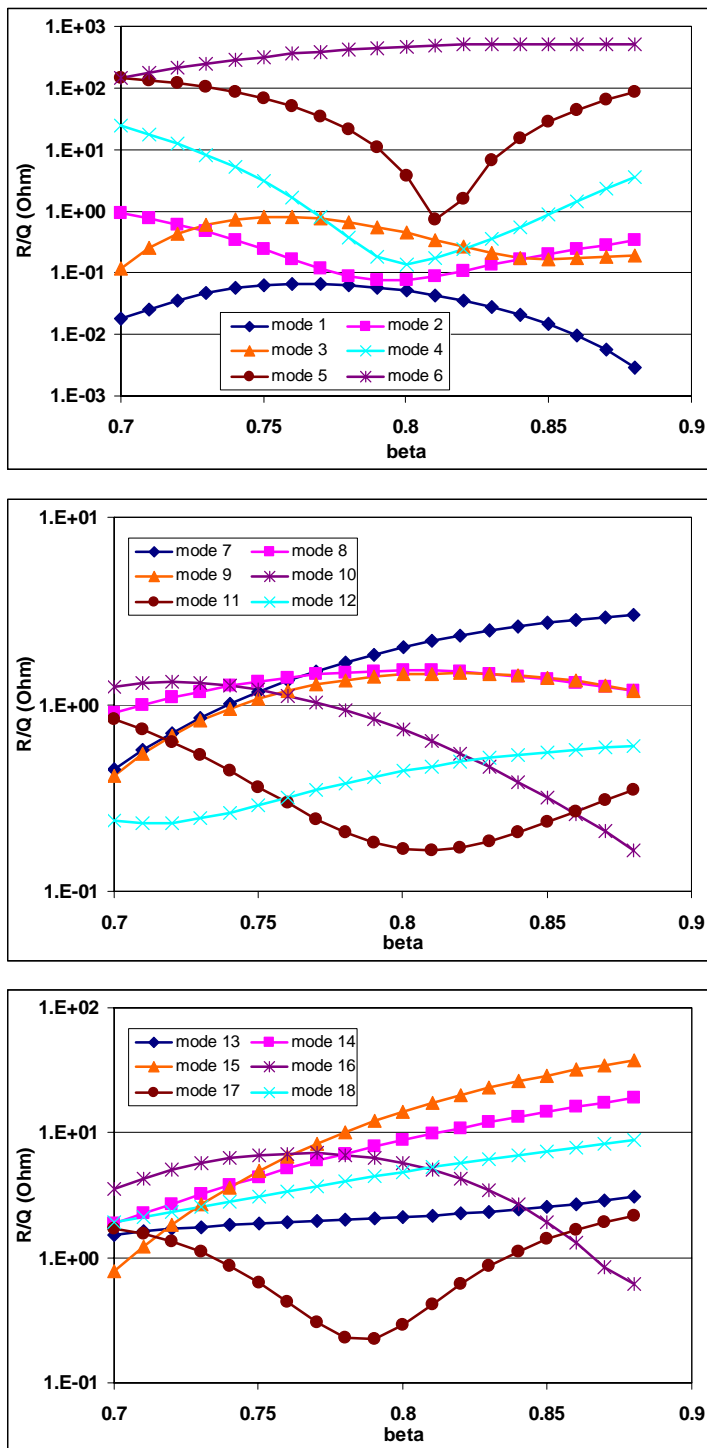


Figure C-2. R/Q 's of TM monopoles (high β) (continue...)

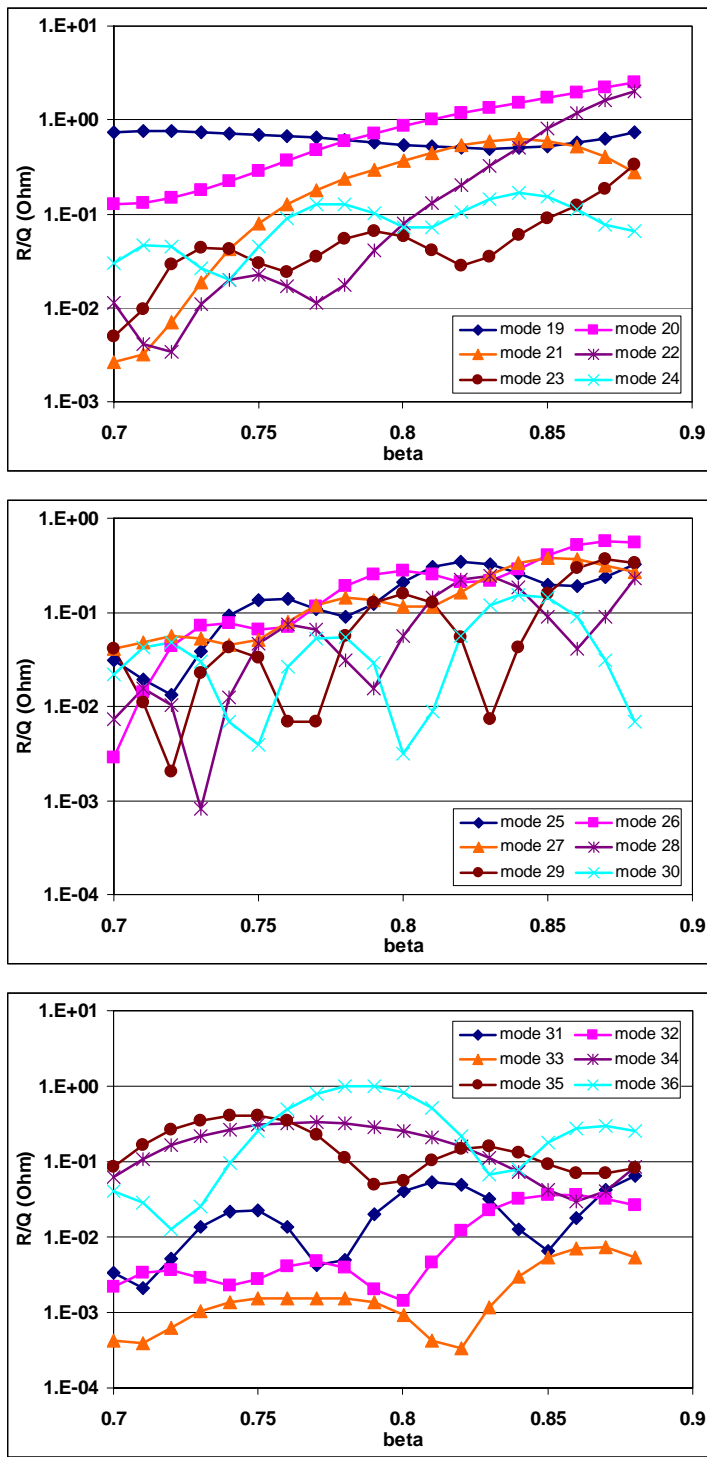


Figure C-2. R/Q 's of TM monopoles (high beta) (continue...)

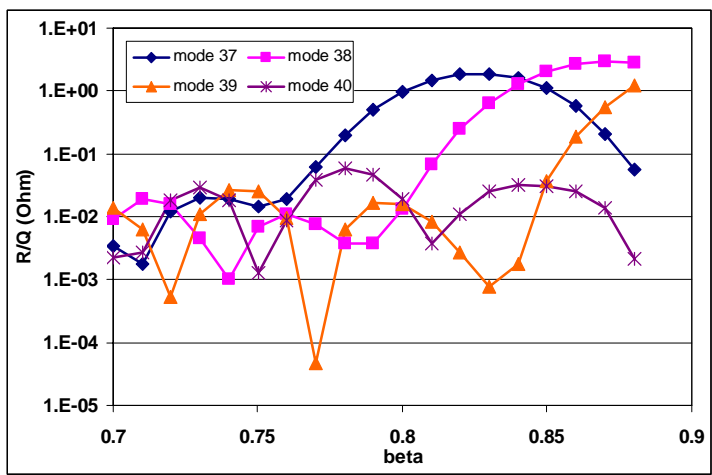


Figure C-2. R/Q's of TM monopoles (high beta)

Table C-2. mode comparisons between the results from the single cavity modeling and the super-structure modeling (continue...)

Single cavity	4-cavity superstructure	Single cavity	4-cavity superstructure
1.654573E+09	7 25 1.654529E+09	21 81 2.301809E+09 26 1.654331E+09 27 1.654378E+09 28 1.654352E+09	81 2.301809E+09
	26 1.654331E+09		82 2.301035E+09
	27 1.654378E+09		83 2.301214E+09
	28 1.654352E+09		84 2.301153E+09
1.699617E+09	8 29 1.699278E+09	22 85 2.318723E+09 30 1.699429E+09 31 1.699382E+09 32 1.699349E+09	85 2.318723E+09
	30 1.699429E+09		86 2.319914E+09
	31 1.699382E+09		87 2.318874E+09
	32 1.699349E+09		88 2.319785E+09
1.707494E+09	9 33 1.707014E+09	23 89 2.346086E+09 34 1.707097E+09 35 1.707451E+09 36 1.707406E+09	89 2.346086E+09
	34 1.707097E+09		90 2.346262E+09
	35 1.707451E+09		91 2.346572E+09
	36 1.707406E+09		92 2.346490E+09
1.710520E+09	10 37 1.710406E+09	24 93 2.378835E+09 38 1.710189E+09 39 1.710097E+09 40 1.710016E+09	93 2.378835E+09
	38 1.710189E+09		94 2.377665E+09
	39 1.710097E+09		95 2.378281E+09
	40 1.710016E+09		96 2.377870E+09
1.713700E+09	11 41 1.713202E+09	25 97 2.413887E+09 42 1.713289E+09 43 1.713501E+09 44 1.713400E+09	97 2.413887E+09
	42 1.713289E+09		98 2.414064E+09
	43 1.713501E+09		99 2.413944E+09
	44 1.713400E+09		100 2.413265E+09
1.715630E+09	12 45 1.715466E+09	26 101 2.444244E+09 46 1.715250E+09 47 1.715277E+09 48 1.715048E+09	101 2.444244E+09
	46 1.715250E+09		102 2.444877E+09
	47 1.715277E+09		103 2.445032E+09
	48 1.715048E+09		104 2.445190E+09
1.736947E+09	13 49 1.736545E+09	27 105 2.498771E+09 50 1.736597E+09 51 1.736651E+09 52 1.736619E+09	105 2.498771E+09
	50 1.736597E+09		106 2.499328E+09
	51 1.736651E+09		107 2.499388E+09
	52 1.736619E+09		108 2.499724E+09
1.749261E+09	14 53 1.748965E+09	28 109 2.540710E+09 54 1.748903E+09 55 1.748840E+09 56 1.748742E+09	109 2.540710E+09
	54 1.748903E+09		110 2.541109E+09
	55 1.748840E+09		111 2.541189E+09
	56 1.748742E+09		112 2.540851E+09
1.755221E+09	15 57 1.754649E+09	29 113 2.561369E+09 58 1.754685E+09 59 1.754926E+09 60 1.754841E+09	113 2.561369E+09
	58 1.754685E+09		114 2.562144E+09
	59 1.754926E+09		115 2.562012E+09
	60 1.754841E+09		116 2.561921E+09
1.757800E+09	16 61 1.757287E+09	30 117 2.581624E+09 62 1.757468E+09 63 1.757741E+09 64 1.757599E+09	117 2.581624E+09
	62 1.757468E+09		118 2.581070E+09
	63 1.757741E+09		119 2.581305E+09
	64 1.757599E+09		120 2.582023E+09
1.760878E+09	17 65 1.760836E+09	31 121 2.597697E+09 66 1.760645E+09 67 1.760625E+09 68 1.760326E+09	121 2.597697E+09
	66 1.760645E+09		122 2.597893E+09
	67 1.760625E+09		123 2.597851E+09
	68 1.760326E+09		124 2.598008E+09
1.765671E+09	18 69 1.765869E+09	32 125 2.609883E+09 70 1.765986E+09 71 1.765632E+09 72 1.765696E+09	125 2.609883E+09
	70 1.765986E+09		126 2.609875E+09
	71 1.765632E+09		127 2.616886E+09
	72 1.765696E+09		128 2.616472E+09
1.813416E+09	19 73 1.813407E+09	33 129 2.616500E+09 74 1.813252E+09 75 1.813295E+09 76 1.813306E+09	129 2.616500E+09
	74 1.813252E+09		130 2.616719E+09
	75 1.813295E+09		131 2.610040E+09
	76 1.813306E+09		132 2.609932E+09
2.146308E+09	20 77 2.146338E+09	34 133 2.738060E+09 78 2.146299E+09 79 2.146265E+09 80 2.146290E+09	133 2.738060E+09
	78 2.146299E+09		134 2.738157E+09
	79 2.146265E+09		135 2.738330E+09
	80 2.146290E+09		136 2.738233E+09

Table C-2. mode comparisons between the results from the single cavity modeling and the super-structure modeling.

Single cavity	4-cavity superstructure	Single cavity	4-cavity superstructure
2.815962E+09	35 137 2.815396E+09		193 3.205823E+09
	138 2.815756E+09		194 3.202782E+09
	139 2.815551E+09		195 3.199340E+09
	140 2.815557E+09		196 3.218204E+09
2.830789E+09	36 141 2.830641E+09		197 3.221692E+09
	142 2.830461E+09		198 3.224910E+09
	143 2.830155E+09		199 3.228823E+09
	144 2.830081E+09		200 3.236084E+09
2.858007E+09	37 145 2.857820E+09		201 3.237031E+09
	146 2.857520E+09		202 3.273635E+09
	147 2.857185E+09		203 3.271329E+09
	148 2.857304E+09		204 3.274610E+09
2.894103E+09	38 149 2.893636E+09		205 3.299244E+09
	150 2.893393E+09		206 3.303694E+09
	151 2.893367E+09		207 3.306632E+09
	152 2.893745E+09		208 3.323452E+09
2.934472E+09	39 153 2.933839E+09		209 3.325351E+09
	154 2.933911E+09		210 3.333060E+09
	155 2.933505E+09		
	156 2.934144E+09		
2.976384E+09	40 157 2.974896E+09		
	158 2.975482E+09		
	159 2.976038E+09		
	160 2.975554E+09		
	41 161 3.009258E+09		
	162 3.008418E+09		
	163 3.007412E+09		
	164 3.008017E+09		
	165 3.039023E+09		
	166 3.039053E+09		
	42 167 3.047501E+09		
	168 3.048577E+09		
	169 3.051231E+09		
	170 3.050124E+09		
	171 3.069041E+09		
	172 3.068907E+09		
	173 3.077395E+09		
	174 3.076179E+09		
	175 3.089962E+09		
	176 3.086862E+09		
	177 3.097807E+09		
	178 3.095657E+09		
	179 3.114688E+09		
	180 3.117457E+09		
	181 3.114697E+09		
	182 3.128209E+09		
	183 3.132314E+09		
	184 3.133776E+09		
	185 3.142129E+09		
	186 3.161733E+09		
	187 3.160180E+09		
	188 3.172646E+09		
	189 3.165232E+09		
	190 3.183652E+09		
	191 3.184364E+09		
	192 3.193465E+09		

Table C-3. Q's only from the damping on the normal conducting beam pipes or bellows in the super-structure modeling.

mode no. (single cavity)	mode no. (super structure)	frequency (Hz)	Qo	mode no. (single cavity)	mode no. (super structure)	frequency (Hz)	Qo
34 1	133	2.73806E+09	1.459E+07	172	172	3.06891E+09	6.882E+03
34 2	134	2.73816E+09	1.393E+07	173	173	3.07740E+09	1.557E+04
34 3	135	2.73833E+09	2.671E+07	174	174	3.07618E+09	1.605E+04
34 4	136	2.73823E+09	1.882E+07	175	175	3.08996E+09	9.422E+04
35 1	137	2.81540E+09	7.942E+06	176	176	3.08686E+09	4.340E+04
35 2	138	2.81576E+09	4.206E+06	177	177	3.09781E+09	2.838E+04
35 3	139	2.81555E+09	4.314E+06	178	178	3.09566E+09	2.330E+04
35 4	140	2.81556E+09	2.772E+06	179	179	3.11469E+09	1.625E+04
36 1	141	2.83064E+09	5.508E+06	180	180	3.11746E+09	1.048E+04
36 2	142	2.83046E+09	2.655E+06	181	181	3.11470E+09	1.630E+04
36 3	143	2.83016E+09	2.086E+06	182	182	3.12821E+09	6.464E+04
36 4	144	2.83008E+09	2.224E+06	183	183	3.13231E+09	2.406E+04
37 1	145	2.85782E+09	5.526E+06	184	184	3.13378E+09	3.017E+04
37 2	146	2.85752E+09	2.505E+06	185	185	3.14213E+09	3.279E+04
37 3	147	2.85719E+09	2.482E+06	186	186	3.16173E+09	3.771E+04
37 4	148	2.85730E+09	1.734E+06	187	187	3.16018E+09	6.366E+04
38 1	149	2.89364E+09	2.133E+06	188	188	3.17265E+09	4.940E+04
38 2	150	2.89339E+09	1.461E+06	189	189	3.16523E+09	6.240E+04
38 3	151	2.89337E+09	2.113E+06	190	190	3.18365E+09	1.319E+04
38 4	152	2.89375E+09	5.034E+06	191	191	3.18436E+09	1.263E+04
39 1	153	2.93384E+09	1.425E+06	192	192	3.19347E+09	5.224E+04
39 2	154	2.93391E+09	1.449E+06	193	193	3.20582E+09	3.827E+04
39 3	155	2.93351E+09	1.005E+06	194	194	3.20278E+09	2.370E+04
39 4	156	2.93414E+09	3.653E+06	195	195	3.19934E+09	2.495E+04
40 1	157	2.97490E+09	4.774E+05	196	196	3.21820E+09	7.124E+04
40 2	158	2.97548E+09	6.019E+05	197	197	3.22169E+09	4.646E+04
40 3	159	2.97604E+09	1.859E+06	198	198	3.22491E+09	8.157E+04
40 4	160	2.97555E+09	7.171E+05	199	199	3.22882E+09	8.731E+04
41 1	161	3.00926E+09	9.746E+05	200	200	3.23608E+09	8.859E+04
41 2	162	3.00842E+09	3.376E+05	201	201	3.23703E+09	9.300E+04
41 3	163	3.00741E+09	2.392E+05	202	202	3.27364E+09	2.840E+04
41 4	164	3.00802E+09	2.546E+05	203	203	3.27133E+09	9.461E+03
	165	3.03902E+09	6.111E+03	204	204	3.27461E+09	1.510E+04
	166	3.03905E+09	6.303E+04	205	205	3.29924E+09	9.376E+04
42 1	167	3.04750E+09	6.109E+03	206	206	3.30369E+09	3.965E+05
42 2	168	3.04858E+09	5.003E+04	207	207	3.30663E+09	3.646E+05
42 3	169	3.05123E+09	1.564E+05	208	208	3.32345E+09	3.671E+05
42 4	170	3.05012E+09	6.957E+04	209	209	3.32535E+09	2.542E+05
	171	3.06904E+09	6.900E+03	210	210	3.33306E+09	4.723E+04

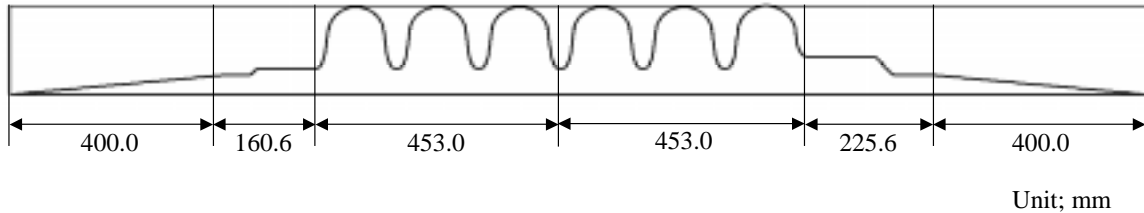


Figure C-3. MAFIA models of the single cavity (ref. SNS drawing).

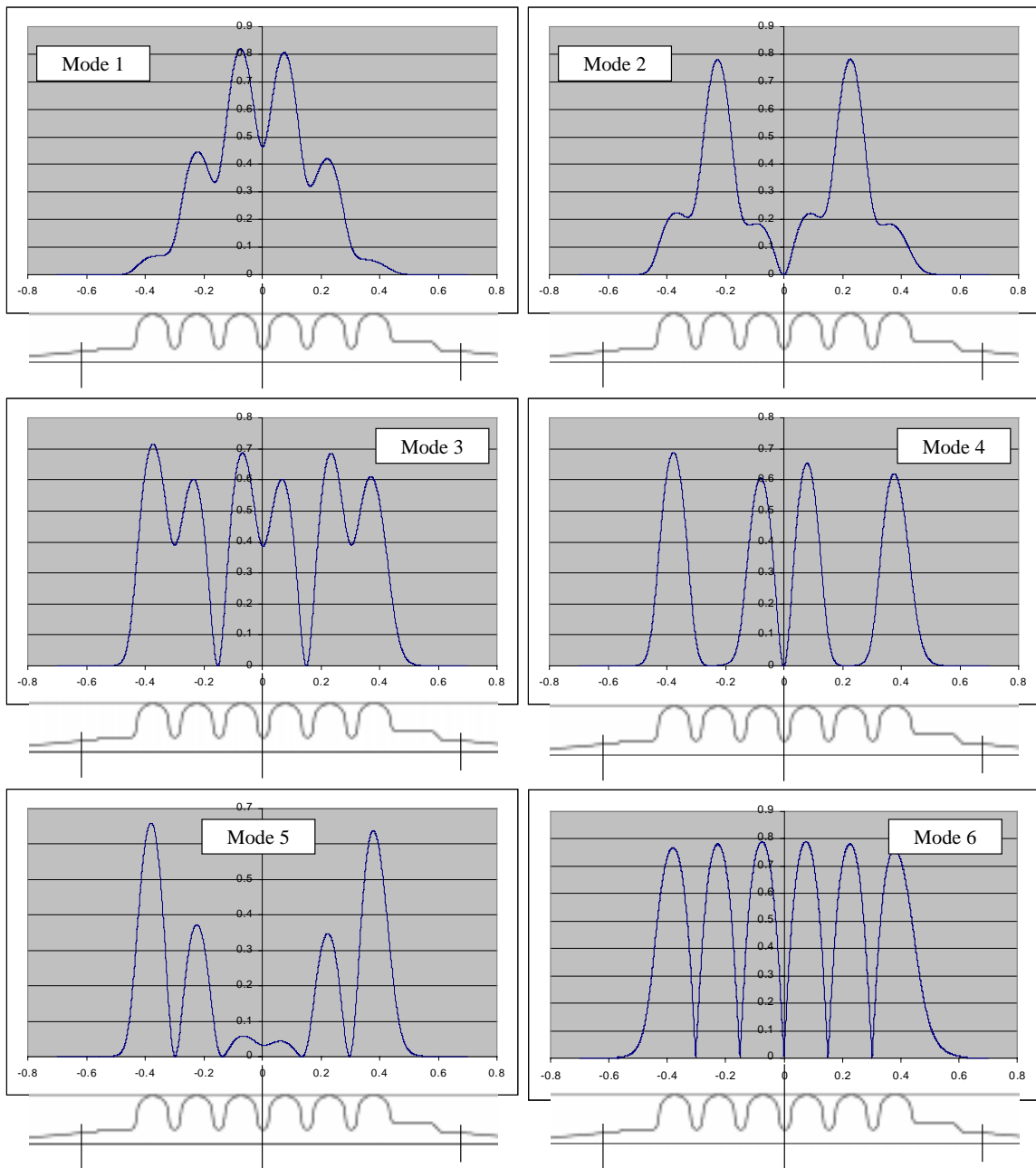


Figure C-4. E_z^2 on the axis of each TM monopoles from the single cavity modeling (continue...)

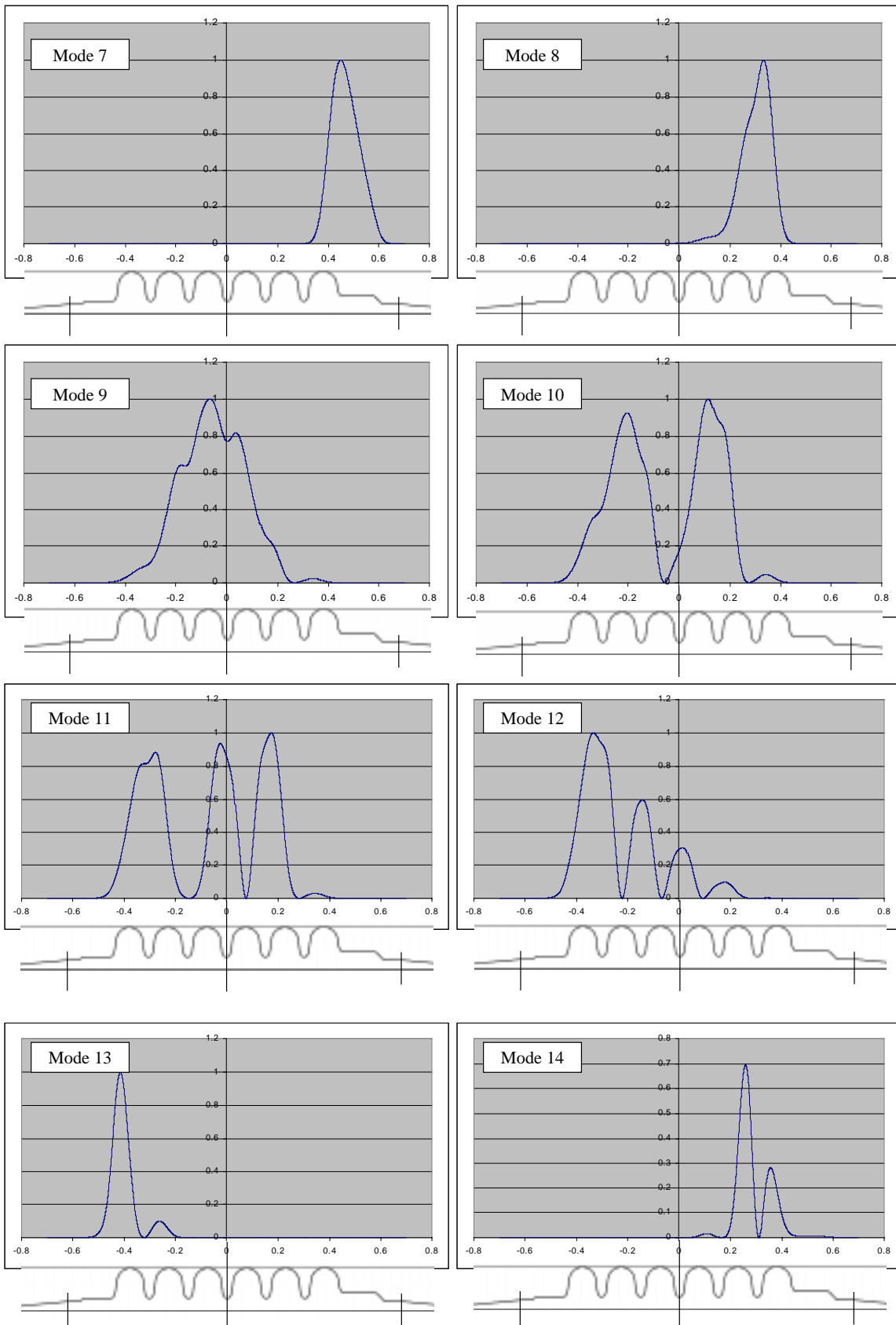


Figure C-4. Ez^2 on the axis of each TM monopoles from the single cavity modeling (continue...)

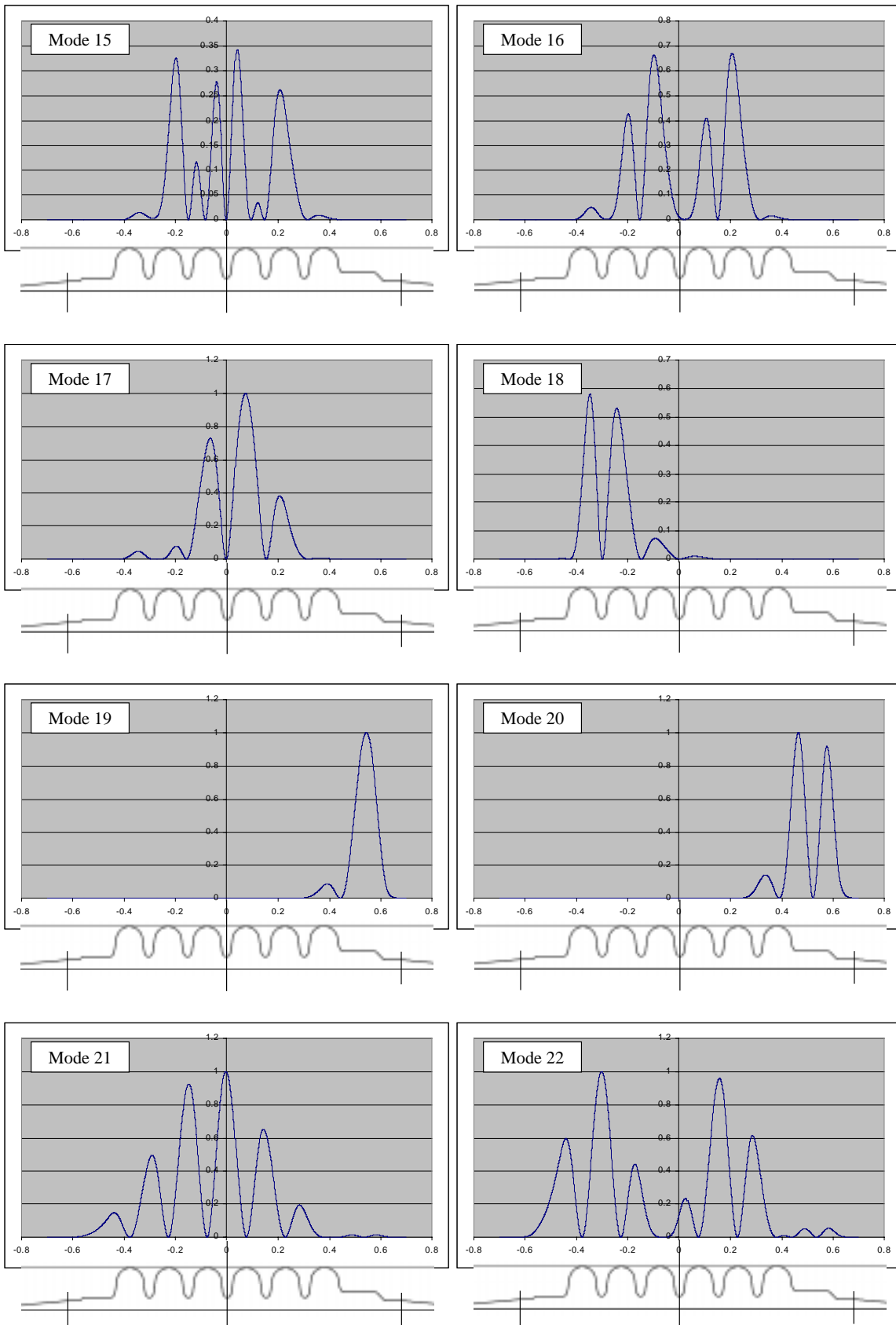


Figure C-4. Ez^2 on the axis of each TM monopoles from the single cavity modeling (continue...)

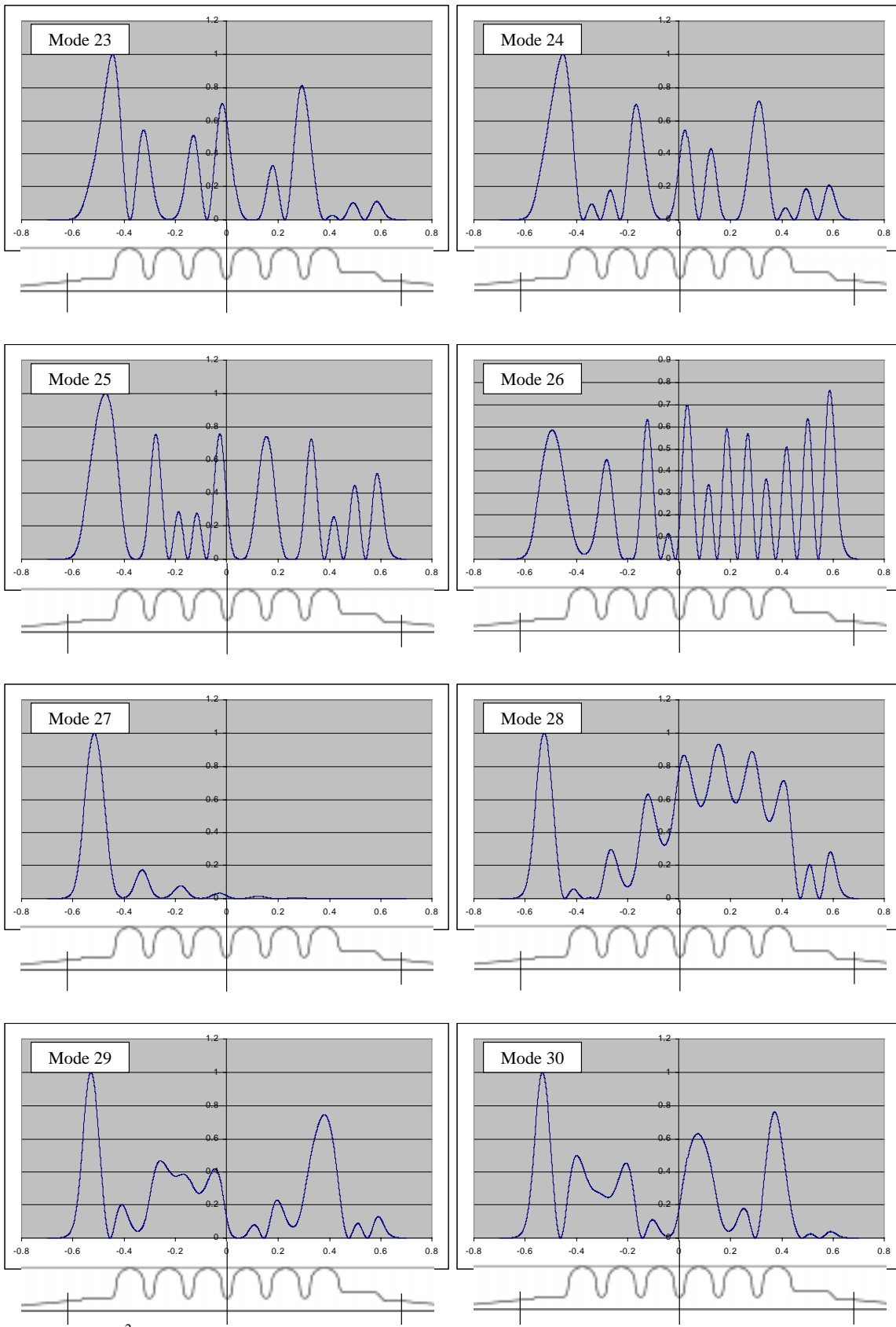


Figure C-4. Ez^2 on the axis of each TM monopoles from the single cavity modeling (continue...)

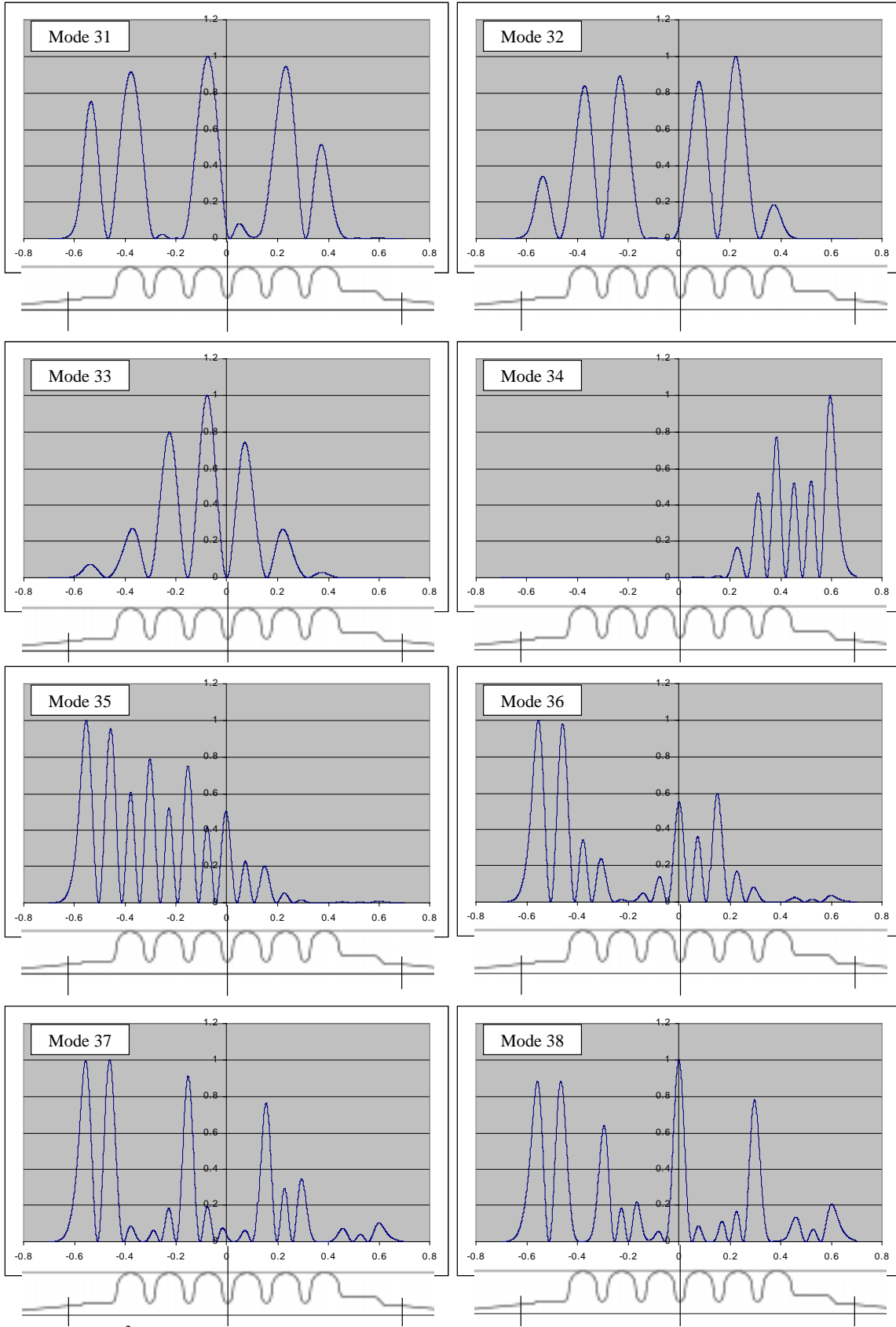


Figure C-4. Ez^2 on the axis of each TM monopoles from the single cavity modeling (continue...)

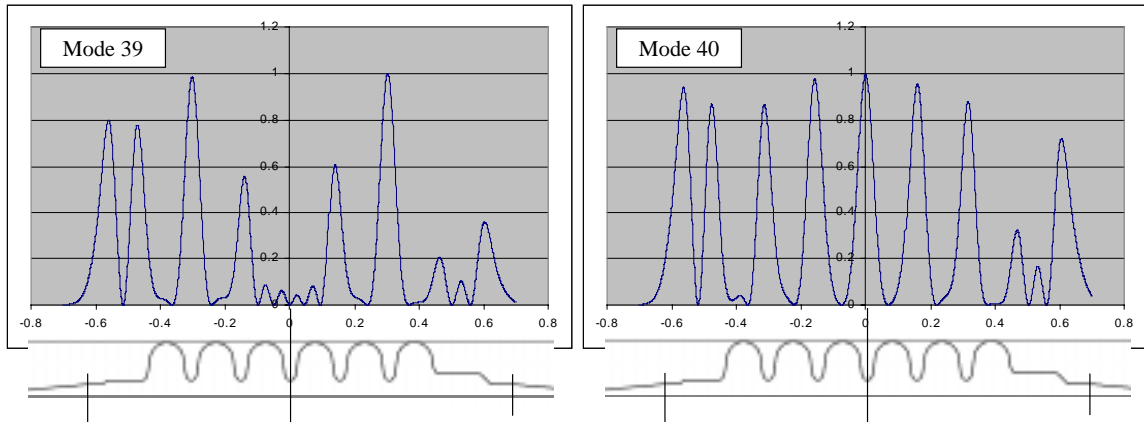


Figure C-4. E_z^2 on the axis of each TM monopoles from the single cavity modeling.

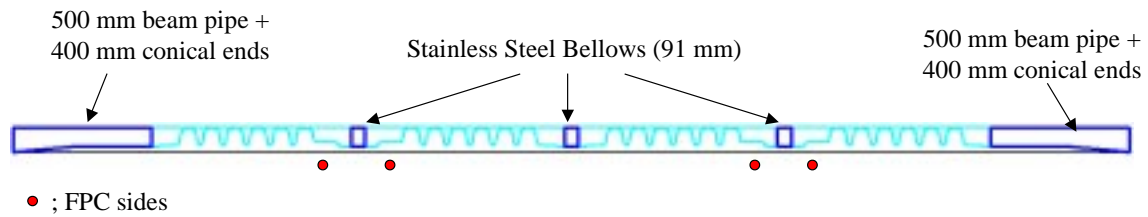


Figure C-5. MAFIA models of the super-structure (ref. SNS drawing).

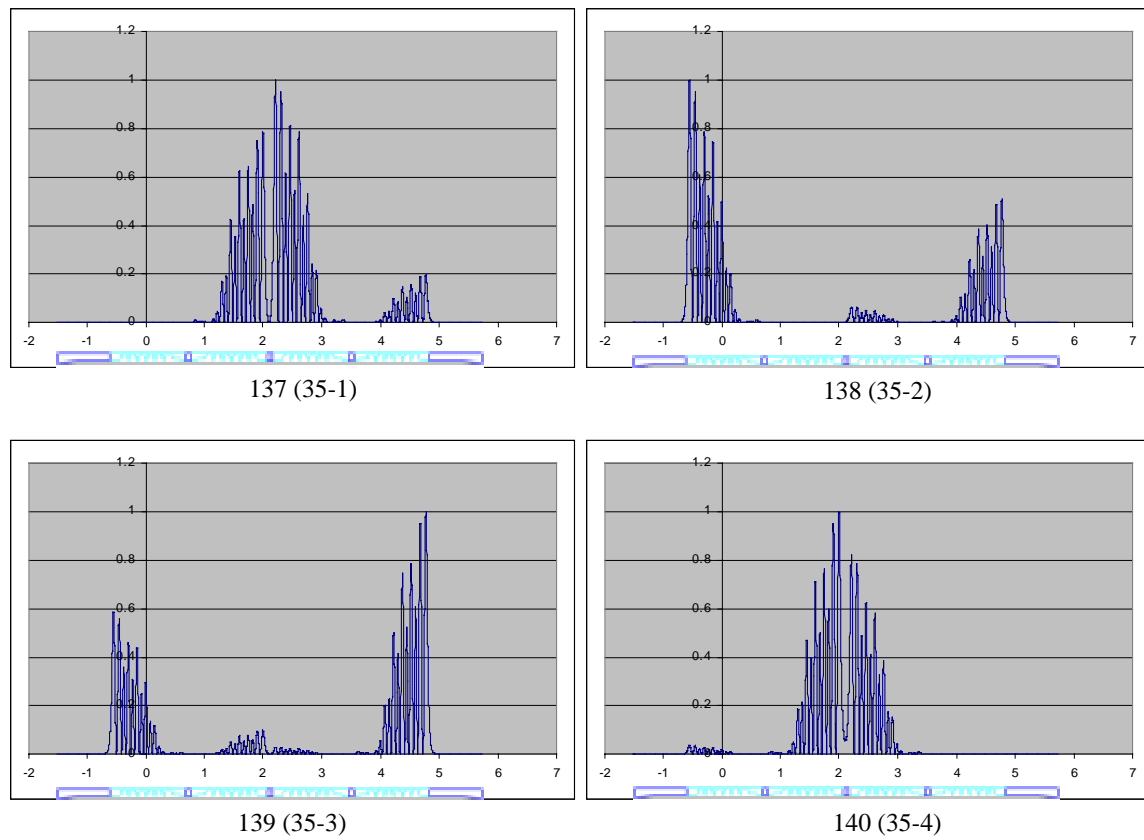


Figure C-6. E_z^2 on the axis of each TM monopoles (continue...)

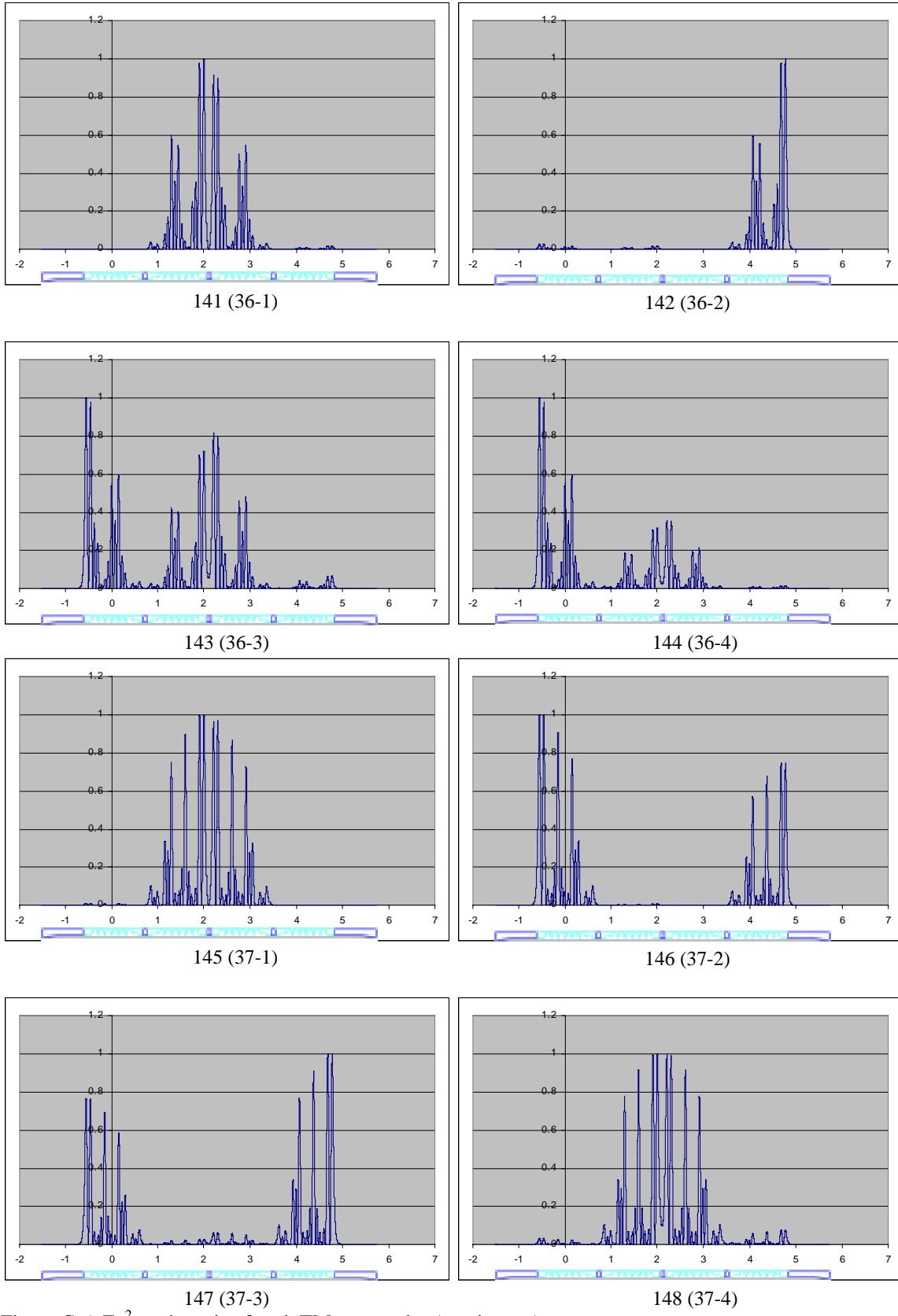


Figure C-6. Ez^2 on the axis of each TM monopoles (continue...)

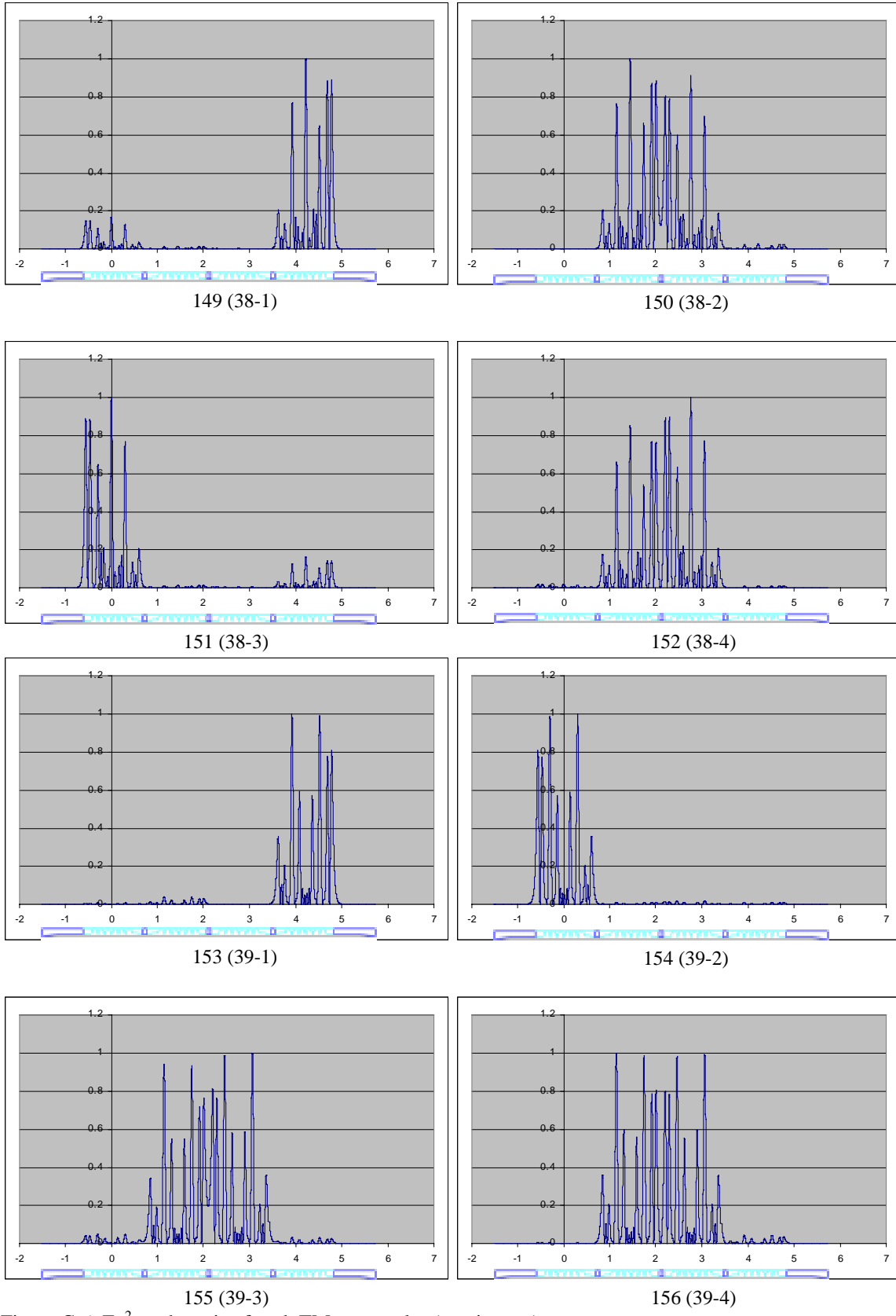


Figure C-6. Ez^2 on the axis of each TM monopoles (continue...)

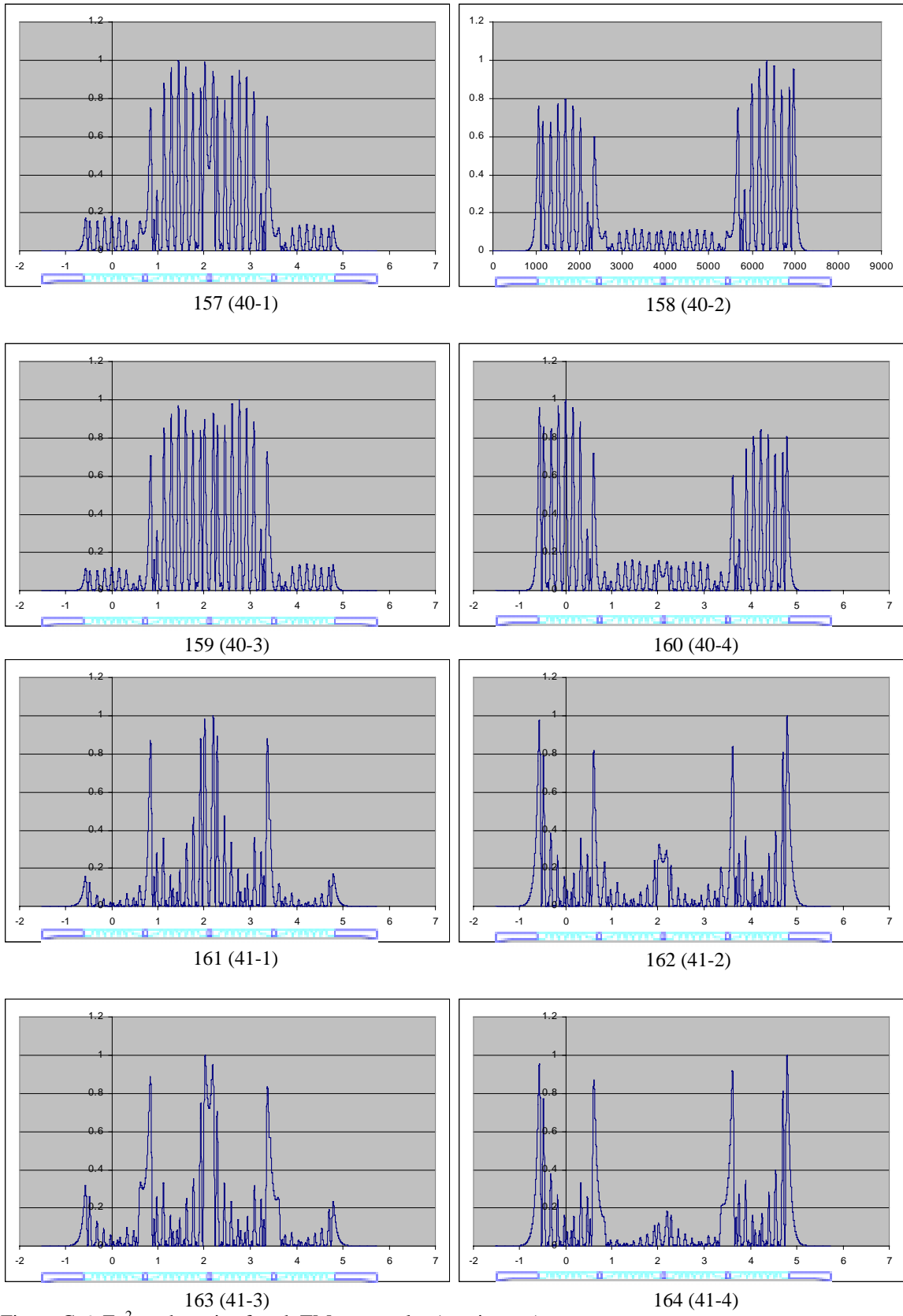
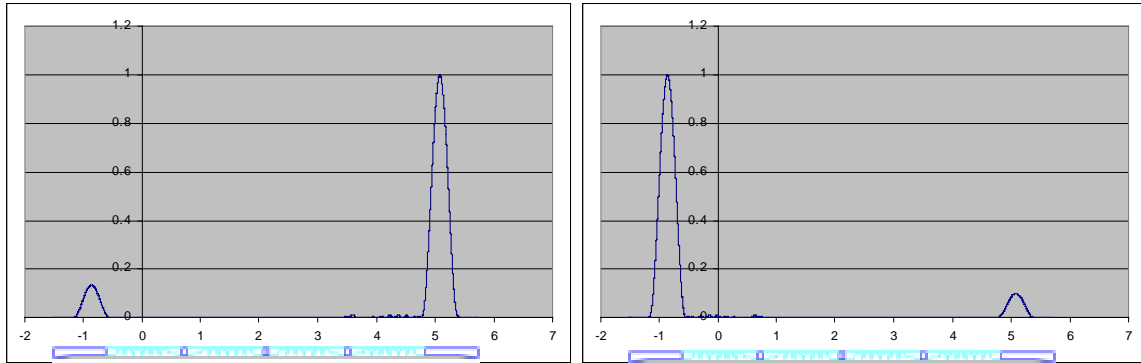
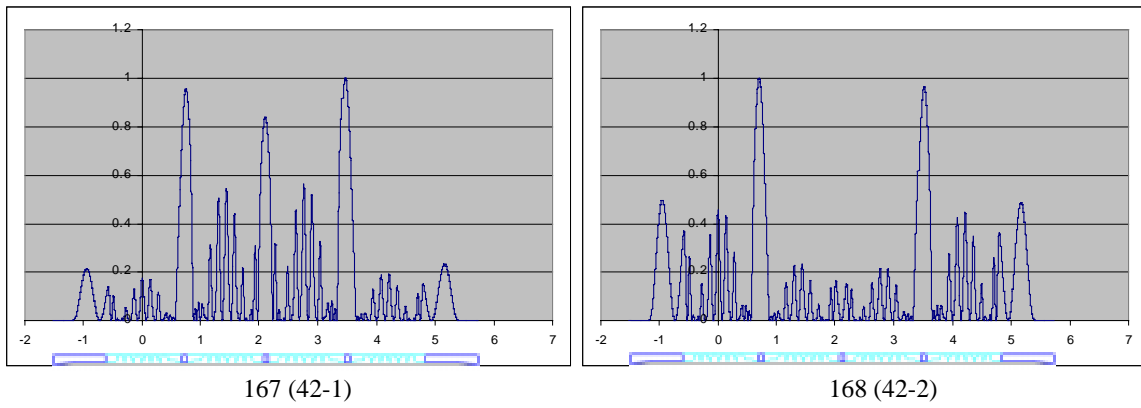


Figure C-6. Ez^2 on the axis of each TM monopoles (continue...)



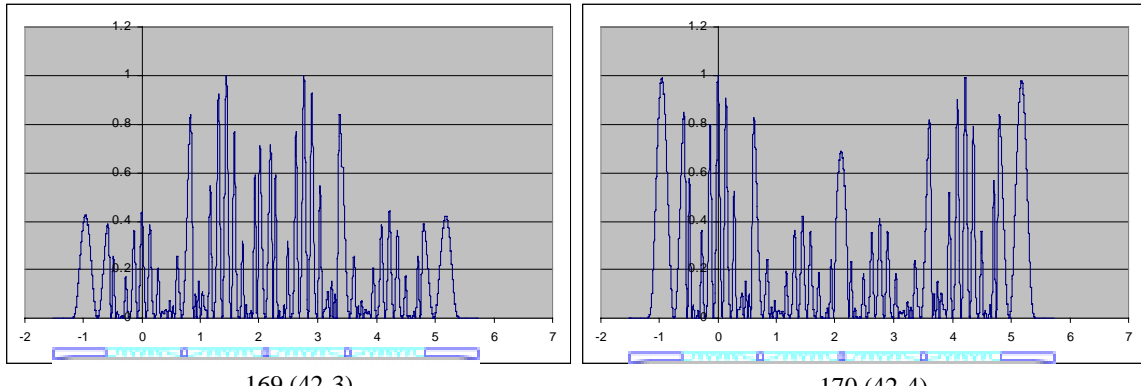
165

166



167 (42-1)

168 (42-2)



169 (42-3)

170 (42-4)

Figure C-6. E_z^2 on the axis of each TM monopoles (continue...)

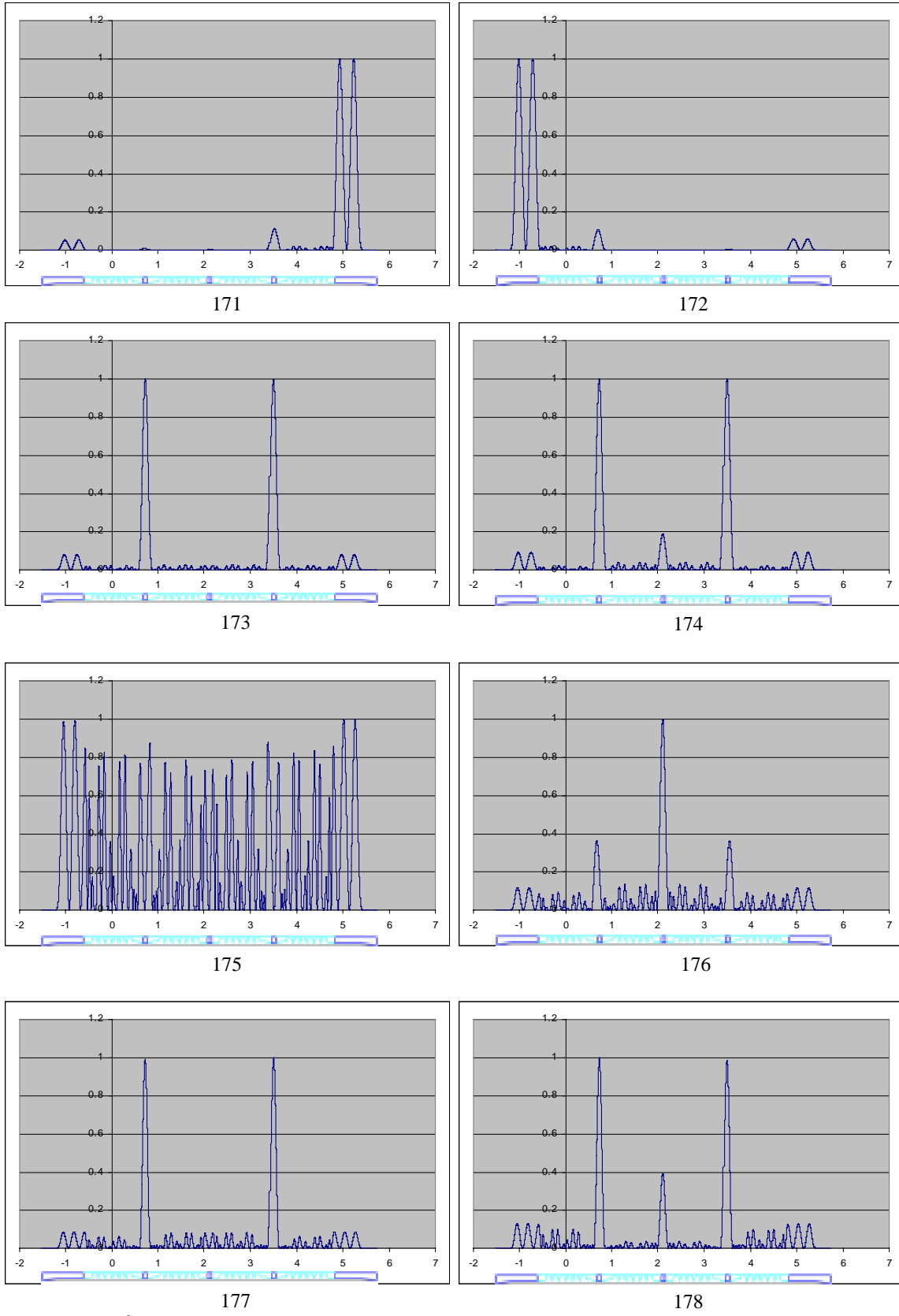


Figure C-6. Ez^2 on the axis of each TM monopoles (continue...)

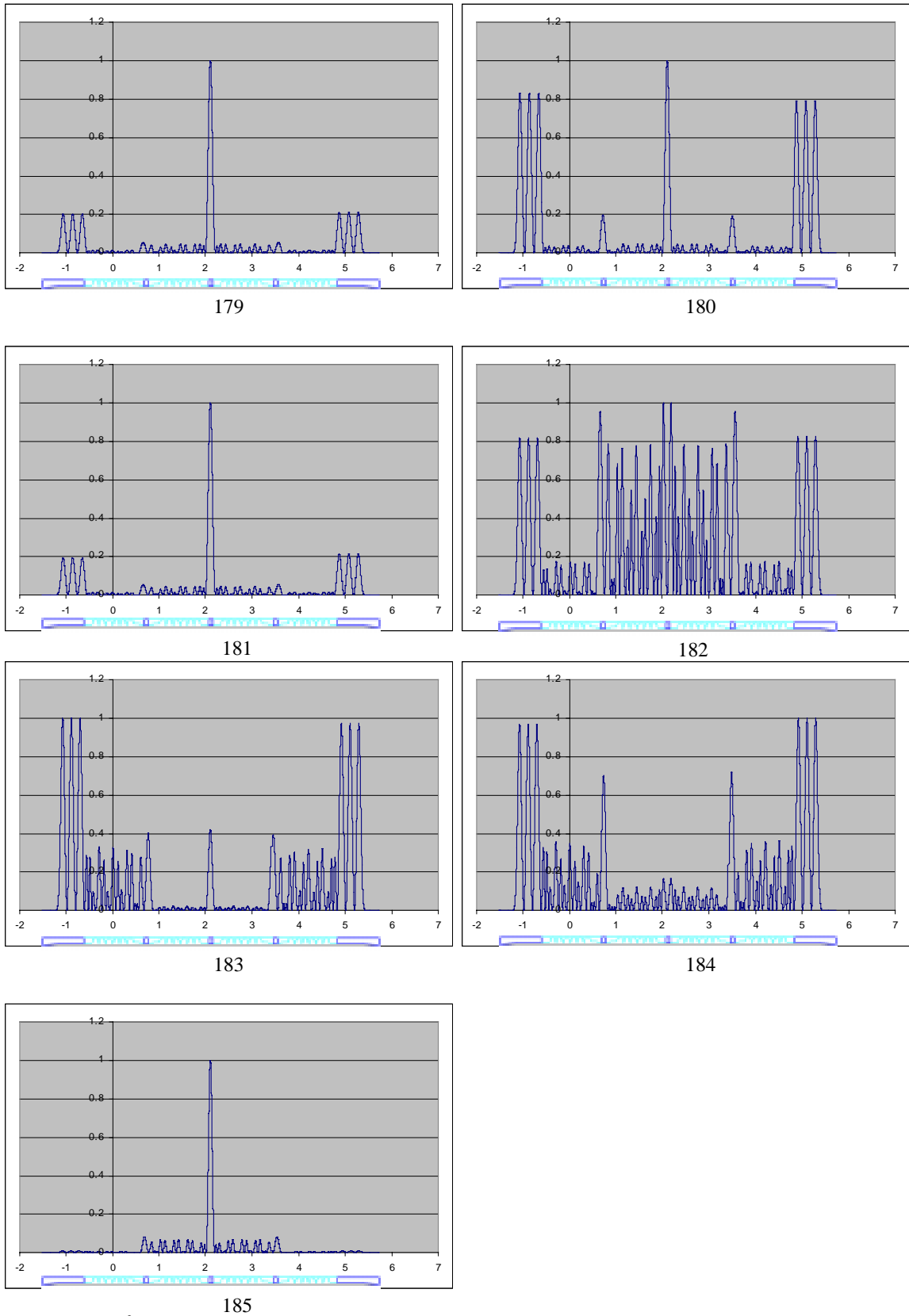
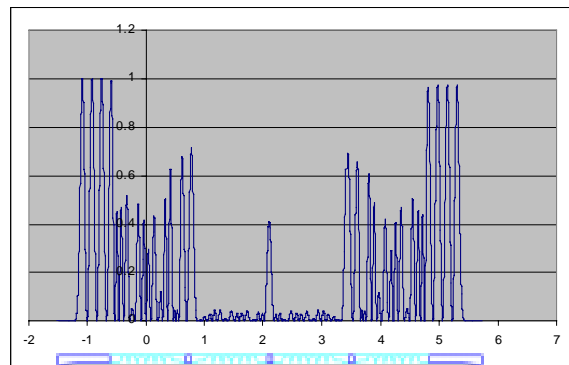
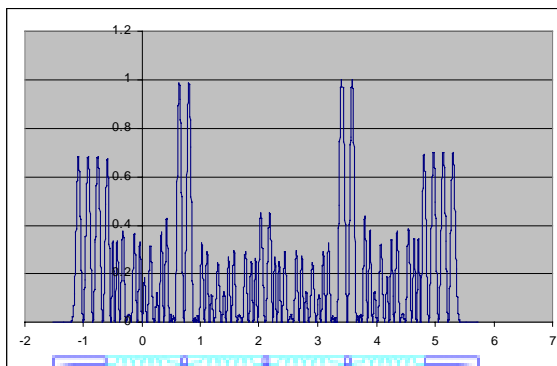


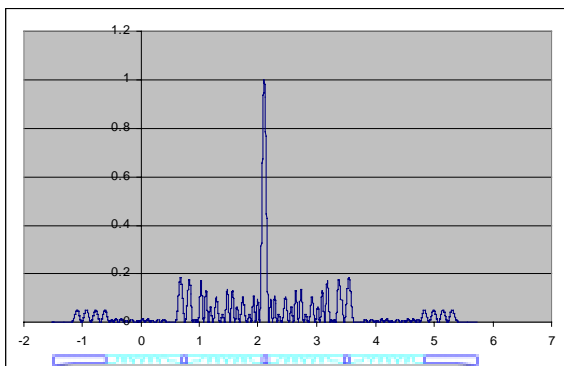
Figure C-6. Ez^2 on the axis of each TM monopoles (continue...)



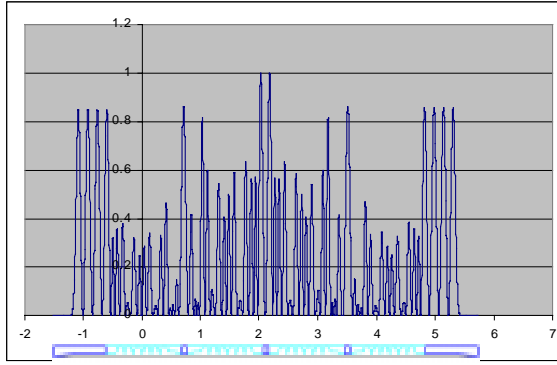
186



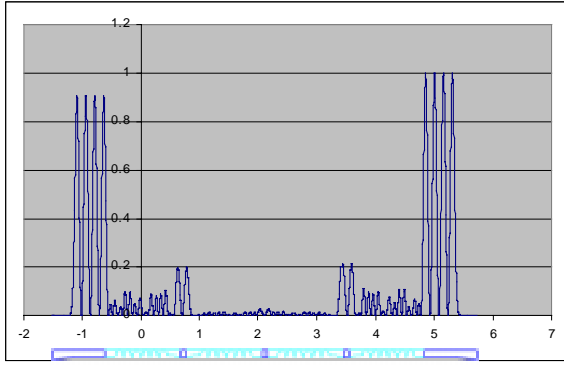
187



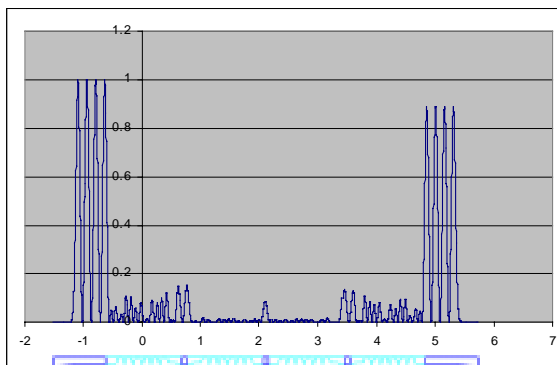
188



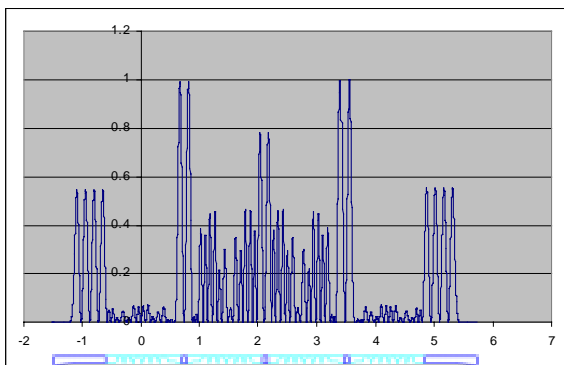
189



190



191



192

Figure C-6. Ez^2 on the axis of each TM monopoles (continue...)

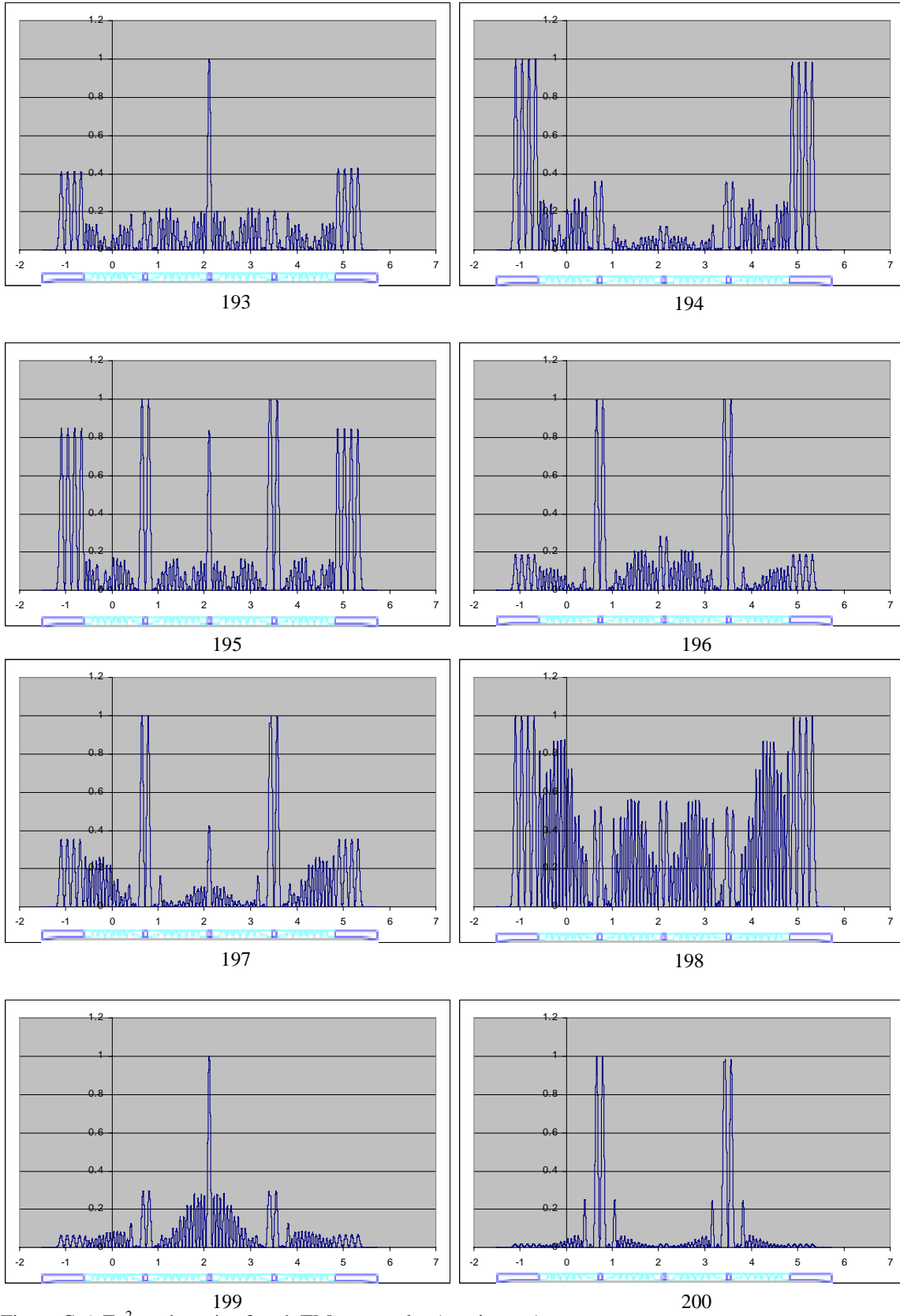


Figure C-6. Ez^2 on the axis of each TM monopoles (continue...)

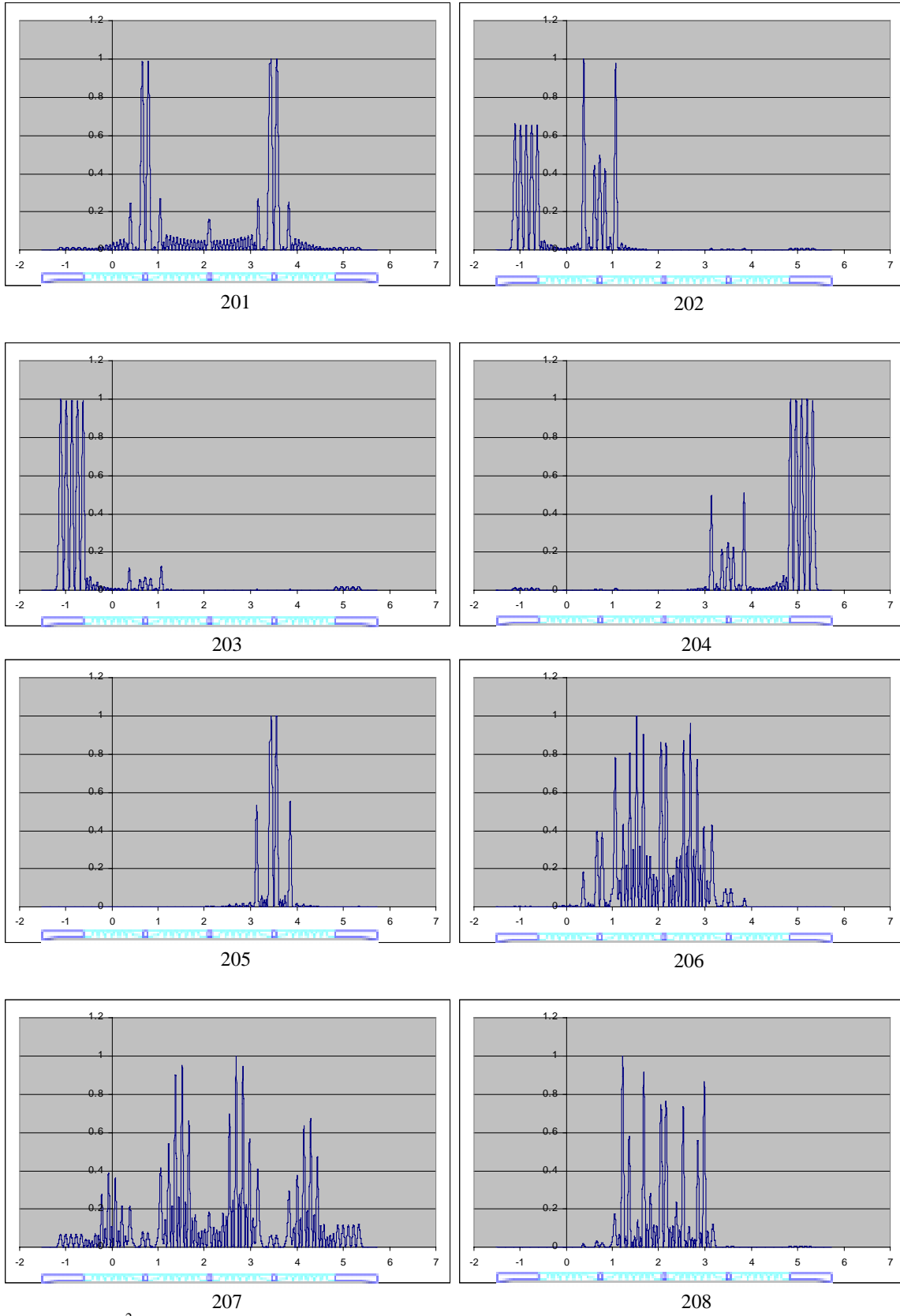


Figure C-6. Ez^2 on the axis of each TM monopoles (continue...)

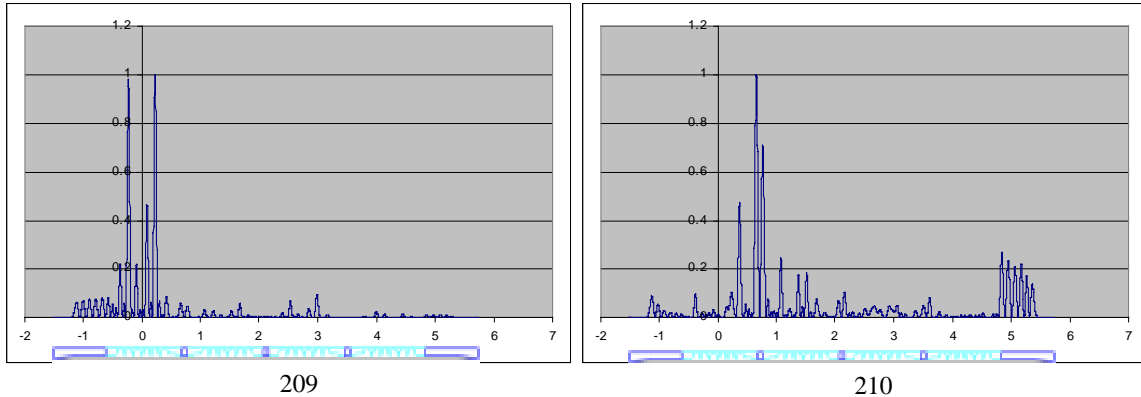


Figure C-6. E_z^2 on the axis of each TM monopoles.

Table C-4. TE monopoles.

mode	frequency/Hz	mode	frequency/Hz	mode	frequency/Hz
1	1.71141E+09	6	1.76314E+09	11	2.47768E+09
2	1.76228E+09	7	2.39996E+09	12	2.48567E+09
3	1.76512E+09	8	2.47138E+09	13	2.61434E+09
4	1.76424E+09	9	2.47402E+09	14	2.78118E+09
5	1.77147E+09	10	2.48104E+09	15	2.80812E+09

Table C-5. Dipoles and R/Q's as a function of the particle velocity (Single cavity). (continue..)

mode no.	frequency (Hz)	R/Q at beta=									
		0.7	0.71	0.72	0.73	0.74	0.75	0.76	0.77	0.78	0.79
1	1.10365E+09	5.5707	6.0063	6.4402	6.8800	7.3246	7.7634	8.2048	8.6480	9.0921	9.5308
2	1.13505E+09	0.6908	0.6746	0.6015	0.4837	0.3496	0.2457	0.2341	0.3934	0.8141	1.5954
3	1.13794E+09	0.9980	2.1666	4.1256	7.0348	11.0148	16.1392	22.4079	29.8398	38.2340	47.4997
4	1.14341E+09	26.7756	34.8365	43.4251	52.1429	60.6516	68.5323	75.4905	81.1832	85.3656	87.9103
5	1.15223E+09	53.8392	56.0591	56.5915	55.4706	52.8033	48.8705	43.9330	38.2771	32.3349	26.3246
6	1.16526E+09	22.3494	18.0033	13.6807	9.7321	6.3699	3.7424	1.9097	0.8642	0.5336	0.8033
7	1.18163E+09	0.8732	0.5132	0.5905	0.9797	1.5481	2.1682	2.7338	3.1674	3.4198	3.4738
8	1.21323E+09	3.7929	3.2524	2.7630	2.2998	1.8535	1.4280	1.0337	0.6880	0.4057	0.1990
9	1.24628E+09	5.1191	5.5911	5.8904	6.0311	6.0345	5.9225	5.7149	5.4331	5.0924	4.7069
10	1.28416E+09	0.1286	0.0325	0.0607	0.2220	0.5123	0.9160	1.4123	1.9749	2.5767	3.1908
11	1.32158E+09	0.2240	0.3274	0.4139	0.4689	0.4862	0.4645	0.4087	0.3281	0.2351	0.1436
12	1.35039E+09	0.0977	0.0769	0.0533	0.0318	0.0162	0.0091	0.0112	0.0224	0.0410	0.0649
13	1.48482E+09	0.6215	0.5951	0.5654	0.5342	0.5003	0.4661	0.4304	0.3948	0.3589	0.3241
14	1.75515E+09	0.3653	0.4195	0.4748	0.5163	0.5384	0.5435	0.5363	0.5262	0.5255	0.5435
15	1.77015E+09	2.1573	1.3017	0.7005	0.3416	0.1847	0.1853	0.2963	0.4705	0.6648	0.8380
16	1.78903E+09	8.1979	8.1629	7.6267	6.7396	5.6603	4.5211	3.4202	2.4293	1.5930	0.9460
17	1.80276E+09	2.5160	4.0186	5.6487	7.2126	8.5584	9.5800	10.2344	10.5239	10.4758	10.1254
18	1.81014E+09	0.0292	0.0049	0.1004	0.3843	0.9002	1.6592	2.6427	3.8176	5.1421	6.5817
19	1.81755E+09	0.7571	0.9181	1.0879	1.2625	1.4397	1.6212	1.8068	1.9973	2.1900	2.3805
20	1.83628E+09	0.7471	0.9048	1.0831	1.2823	1.5009	1.7381	1.9942	2.2646	2.5506	2.8464
21	1.94169E+09	0.5593	0.3747	0.2413	0.1520	0.0984	0.0721	0.0646	0.0677	0.0738	0.0776
22	1.96390E+09	0.6124	0.6789	0.6817	0.6434	0.5809	0.5029	0.4145	0.3224	0.2377	0.1722
23	1.99773E+09	0.0583	0.0679	0.1322	0.2201	0.3027	0.3689	0.4253	0.4824	0.5444	0.6032
24	2.02792E+09	0.0868	0.1144	0.1119	0.0857	0.0564	0.0429	0.0530	0.0848	0.1326	0.1941
25	2.04903E+09	0.0565	0.0465	0.0351	0.0269	0.0288	0.0443	0.0710	0.1008	0.1238	0.1334
26	2.06394E+09	0.0315	0.0282	0.0300	0.0384	0.0481	0.0521	0.0461	0.0326	0.0187	0.0131
27	2.08002E+09	0.0039	0.0178	0.0424	0.0762	0.1171	0.1625	0.2093	0.2543	0.2941	0.3256
28	2.09126E+09	0.1262	0.1749	0.2199	0.2585	0.2895	0.3112	0.3219	0.3201	0.3048	0.2771
29	2.09477E+09	0.0010	0.0050	0.0231	0.0554	0.1003	0.1579	0.2297	0.3168	0.4163	0.5194
30	2.10097E+09	0.0168	0.0170	0.0146	0.0118	0.0120	0.0167	0.0247	0.0340	0.0453	0.0652
31	2.10712E+09	0.0129	0.0145	0.0116	0.0070	0.0036	0.0020	0.0018	0.0031	0.0067	0.0125
32	2.11612E+09	0.1254	0.1083	0.0945	0.0826	0.0701	0.0564	0.0427	0.0308	0.0215	0.0148
33	2.12431E+09	0.0227	0.0190	0.0220	0.0320	0.0494	0.0742	0.1060	0.1442	0.1878	0.2358
34	2.18652E+09	0.1084	0.1645	0.2167	0.2527	0.2651	0.2522	0.2193	0.1754	0.1314	0.0966
35	2.19460E+09	0.1239	0.1216	0.0964	0.0604	0.0300	0.0159	0.0179	0.0267	0.0313	0.0260
36	2.20486E+09	0.0671	0.0363	0.0120	0.0094	0.0255	0.0440	0.0503	0.0428	0.0301	0.0219
37	2.22790E+09	0.0310	0.0213	0.0521	0.0915	0.1027	0.0788	0.0440	0.0290	0.0452	0.0806
38	2.26830E+09	0.0301	0.0889	0.1239	0.1031	0.0557	0.0362	0.0703	0.1342	0.1804	0.1799
39	2.32420E+09	0.0639	0.0878	0.0621	0.0262	0.0340	0.0917	0.1529	0.1671	0.1286	0.0791
40	2.39484E+09	0.0493	0.0456	0.0153	0.0147	0.0668	0.1288	0.1415	0.0979	0.0536	0.0734
41	2.44540E+09	0.0427	0.0125	0.0020	0.0362	0.0749	0.0696	0.0290	0.0122	0.0623	0.1571
42	2.49867E+09	0.0399	0.0018	0.0128	0.0444	0.0514	0.0254	0.0011	0.0128	0.0552	0.0892
43	2.55012E+09	0.0924	0.0907	0.0937	0.0811	0.0439	0.0072	0.0069	0.0492	0.0997	0.1140
44	2.59501E+09	0.0866	0.1198	0.1085	0.0597	0.0189	0.0270	0.0771	0.1207	0.1174	0.0741
45	2.63305E+09	0.0051	0.0086	0.0388	0.0908	0.1352	0.1403	0.0993	0.0398	0.0042	0.0166

Table C-5. Dipoles and R/Q's as a function of the particle velocity (Single cavity).

mode no	Frequency, Hz	R/Q at beta=									
		0.8	0.81	0.82	0.83	0.84	0.85	0.86	0.87	0.88	
1	1.10365E+09	9.9743	10.4107	10.8506	11.2876	11.7212	12.1567	12.5938	13.0259	13.4587	
2	1.13505E+09	2.8399	4.6516	7.1311	10.3633	14.4297	19.4045	25.3035	32.1231	39.9618	
3	1.13794E+09	57.4010	67.7048	78.1411	88.4852	98.3444	107.5453	115.8463	123.1043	128.9224	
4	1.14341E+09	88.7416	87.9103	85.4399	81.5459	76.4015	70.2740	63.3743	56.0457	48.4929	
5	1.15223E+09	20.6084	15.4234	10.9155	7.2292	4.4248	2.5120	1.4522	1.1675	1.5516	
6	1.16526E+09	1.5319	2.5646	3.7497	4.9499	6.0492	6.9580	7.6158	7.9922	8.0780	
7	1.18163E+09	3.3341	3.0328	2.6088	2.1118	1.5938	1.1007	0.6738	0.3435	0.1310	
8	1.21323E+09	0.0754	0.0353	0.0730	0.1778	0.3340	0.5237	0.7291	0.9312	1.1138	
9	1.24628E+09	4.2875	3.8454	3.3902	2.9315	2.4809	2.0460	1.6361	1.2602	0.9260	
10	1.28416E+09	3.7933	4.3604	4.8756	5.3229	5.6940	5.9794	6.1780	6.2895	6.3146	
11	1.32158E+09	0.0686	0.0238	0.0218	0.0730	0.1849	0.3620	0.6057	0.9145	1.2842	
12	1.35039E+09	0.0915	0.1176	0.1408	0.1581	0.1679	0.1689	0.1609	0.1442	0.1206	
13	1.48482E+09	0.2895	0.2564	0.2246	0.1945	0.1666	0.1408	0.1176	0.0971	0.0792	
14	1.75515E+09	0.5871	0.6577	0.7509	0.8594	0.9723	1.0779	1.1664	1.2343	1.2784	
15	1.77015E+09	0.9620	1.0177	1.0059	0.9374	0.8380	0.7349	0.6567	0.6271	0.6582	
16	1.78903E+09	0.5047	0.2746	0.2451	0.3878	0.6606	1.0105	1.3804	1.7168	1.9760	
17	1.80276E+09	9.5135	8.6827	7.6703	6.5276	5.3115	4.0874	2.9299	1.9088	1.0909	
18	1.81014E+09	8.1081	9.6965	11.3291	12.9840	14.6511	16.2794	17.8473	19.3351	20.6310	
19	1.81755E+09	2.5617	2.7259	2.8647	2.9712	3.0432	3.0783	3.0820	3.0595	3.0195	
20	1.83628E+09	3.1527	3.4667	3.7832	4.1048	4.4239	4.7386	5.0498	5.3536	5.6486	
21	1.94169E+09	0.0763	0.0703	0.0619	0.0544	0.0506	0.0521	0.0587	0.0690	0.0802	
22	1.96390E+09	0.1345	0.1266	0.1429	0.1728	0.2035	0.2240	0.2278	0.2140	0.1867	
23	1.99773E+09	0.6435	0.6493	0.6126	0.5378	0.4384	0.3358	0.2510	0.2006	0.1934	
24	2.02792E+09	0.2726	0.3740	0.5026	0.6558	0.8222	0.9838	1.1186	1.2067	1.2339	
25	2.04903E+09	0.1299	0.1219	0.1241	0.1544	0.2289	0.3590	0.5474	0.7894	1.0715	
26	2.06394E+09	0.0207	0.0413	0.0701	0.1008	0.1292	0.1559	0.1879	0.2380	0.3219	
27	2.08002E+09	0.3464	0.3554	0.3519	0.3370	0.3124	0.2801	0.2432	0.2047	0.1682	
28	2.09126E+09	0.2396	0.1964	0.1524	0.1117	0.0770	0.0500	0.0305	0.0177	0.0099	
29	2.09477E+09	0.6124	0.6799	0.7098	0.6957	0.6398	0.5513	0.4440	0.3328	0.2309	
30	2.10097E+09	0.1046	0.1749	0.2808	0.4164	0.5643	0.6992	0.7952	0.8321	0.8022	
31	2.10712E+09	0.0189	0.0223	0.0202	0.0132	0.0066	0.0087	0.0281	0.0695	0.1312	
32	2.11612E+09	0.0094	0.0049	0.0015	0.0001	0.0016	0.0064	0.0142	0.0238	0.0344	
33	2.12431E+09	0.2876	0.3420	0.3977	0.4525	0.5052	0.5539	0.5958	0.6297	0.6547	
34	2.18652E+09	0.0771	0.0757	0.0915	0.1220	0.1633	0.2110	0.2617	0.3116	0.3585	
35	2.19460E+09	0.0140	0.0044	0.0059	0.0219	0.0482	0.0754	0.0938	0.0973	0.0862	
36	2.20486E+09	0.0197	0.0176	0.0102	0.0011	0.0056	0.0445	0.1328	0.2696	0.4341	
37	2.22790E+09	0.1132	0.1281	0.1247	0.1105	0.0917	0.0685	0.0397	0.0121	0.0083	
38	2.26830E+09	0.1406	0.0971	0.0818	0.1038	0.1477	0.1871	0.2037	0.1951	0.1717	
39	2.32420E+09	0.0710	0.1235	0.2100	0.2794	0.2919	0.2444	0.1687	0.1100	0.1004	
40	2.39484E+09	0.1694	0.2884	0.3527	0.3206	0.2174	0.1175	0.0961	0.1827	0.3457	
41	2.44540E+09	0.2259	0.2131	0.1296	0.0455	0.0394	0.1398	0.3048	0.4487	0.4947	
42	2.49867E+09	0.0824	0.0410	0.0046	0.0117	0.0673	0.1394	0.1824	0.1695	0.1099	
43	2.55012E+09	0.0797	0.0265	0.0008	0.0278	0.0932	0.1556	0.1769	0.1461	0.0837	
44	2.59501E+09	0.0384	0.0539	0.1214	0.1987	0.2349	0.2081	0.1392	0.0745	0.0531	
45	2.63305E+09	0.0652	0.1141	0.1323	0.1154	0.0850	0.0685	0.0786	0.1055	0.1269	

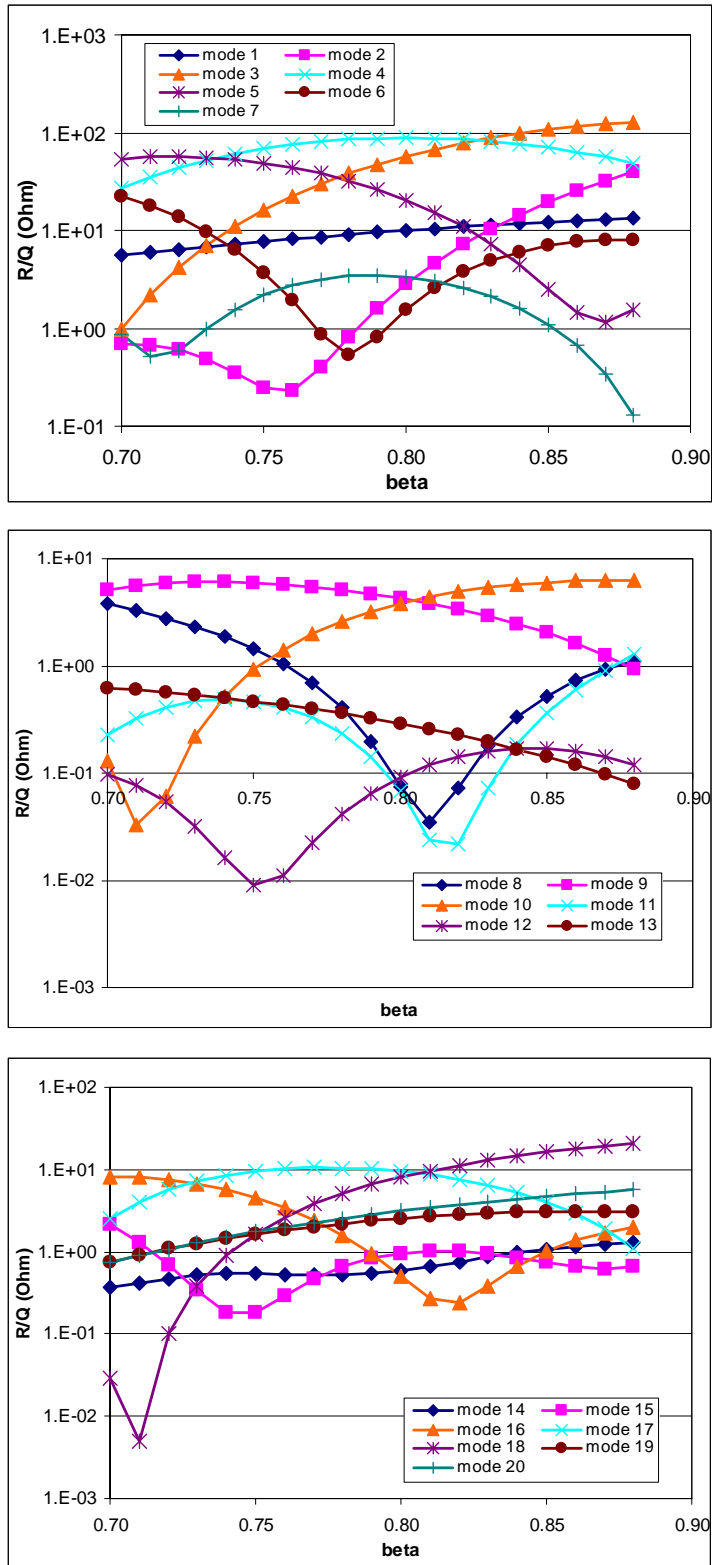


Figure C-7. R/Q 's of dipoles as a function of the particle velocity (single cavity modeling). (continue..)

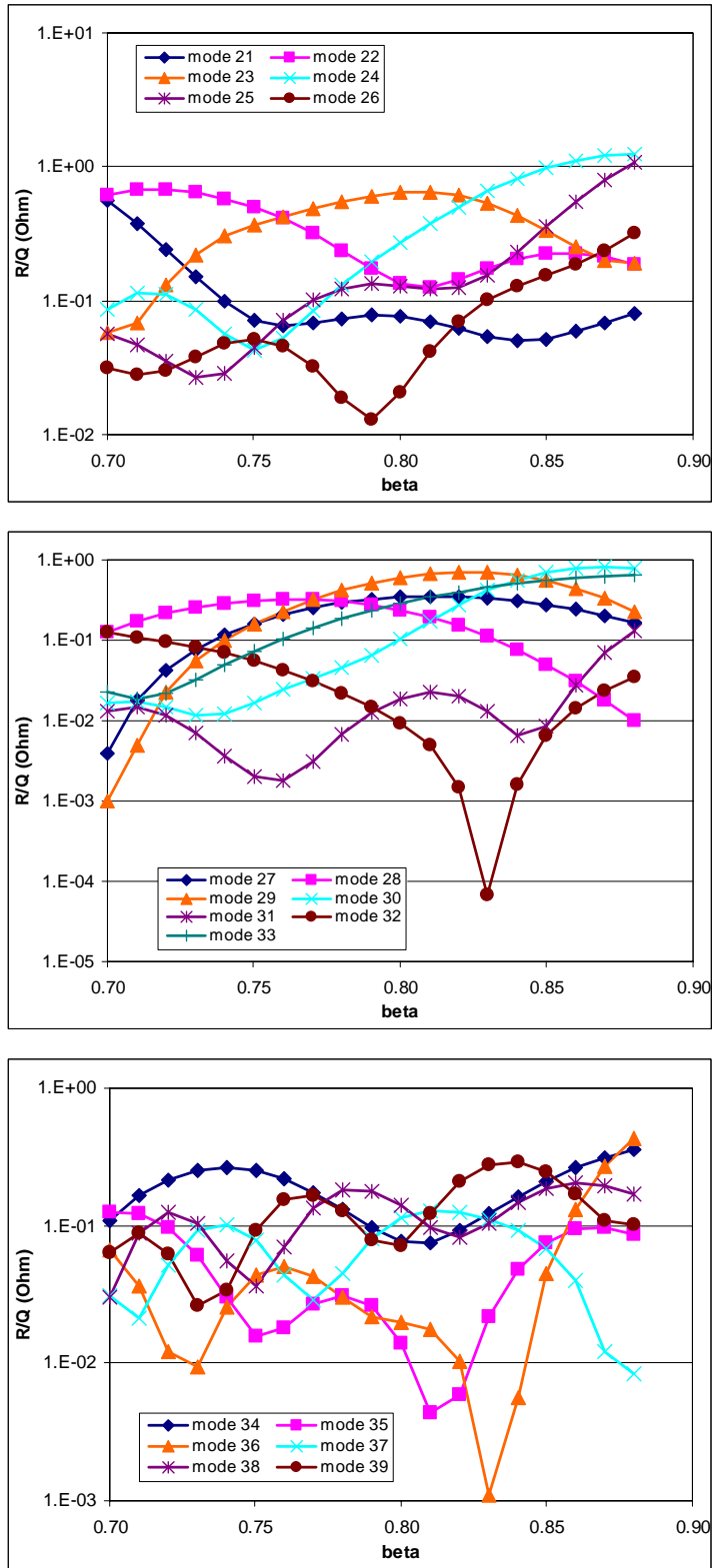


Figure C-7. R/Q 's of dipoles as a function of the particle velocity (single cavity modeling). (continue..)

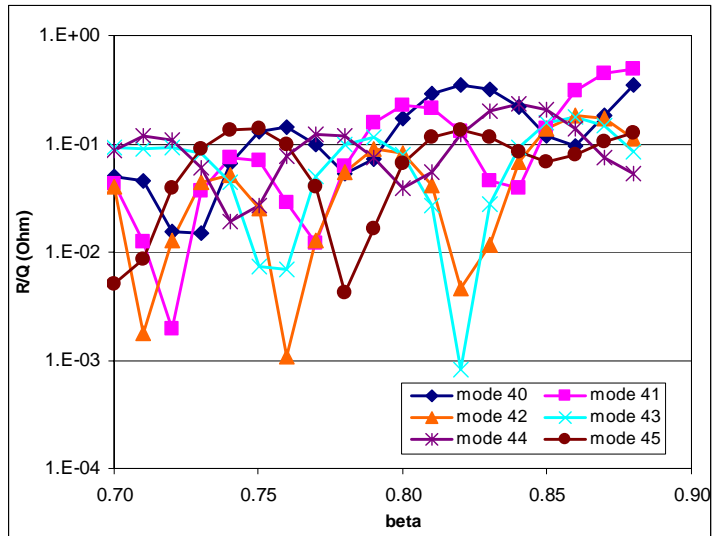


Figure C-7. R/Q's of dipoles as a function of the particle velocity (single cavity modeling).

Table C-6. Quadrupoles and R/Q's as a function of the particle velocity (Single cavity).(continue..)

mode no.	frequency Hz	R/Q at beta=										
			0.7	0.71	0.72	0.73	0.74	0.75	0.76	0.77	0.78	0.79
1	1.52443E+09	0.00196	0.00360	0.00580	0.00861	0.01204	0.01613	0.02090	0.02635	0.03250	0.03937	
2	1.55870E+09	0.00003	0.00007	0.00013	0.00020	0.00027	0.00035	0.00042	0.00047	0.00051	0.00053	
3	1.56025E+09	0.00026	0.00034	0.00044	0.00060	0.00080	0.00106	0.00140	0.00187	0.00255	0.00352	
4	1.56235E+09	0.00117	0.00190	0.00242	0.00282	0.00331	0.00408	0.00515	0.00639	0.00750	0.00820	
5	1.56441E+09	0.00663	0.01232	0.01833	0.02339	0.02649	0.02737	0.02667	0.02599	0.02776	0.03492	
6	1.56571E+09	0.00592	0.01374	0.02715	0.04768	0.07637	0.11351	0.15854	0.21019	0.26579	0.32325	
7	1.60687E+09	0.05894	0.06597	0.07340	0.08113	0.08909	0.09725	0.10550	0.11383	0.12211	0.13029	
8	1.66181E+09	0.02809	0.04832	0.07602	0.11155	0.15446	0.20375	0.25791	0.31522	0.37280	0.42891	
9	1.66544E+09	0.15513	0.18380	0.20594	0.21946	0.22283	0.21521	0.19745	0.17144	0.13987	0.10585	
10	1.67000E+09	0.08931	0.07435	0.05665	0.03865	0.02269	0.01055	0.00331	0.00125	0.00392	0.01026	
11	1.67395E+09	0.00168	0.00090	0.00202	0.00445	0.00744	0.01025	0.01230	0.01321	0.01290	0.01150	
12	1.67829E+09	0.02623	0.02760	0.02881	0.02992	0.03097	0.03203	0.03316	0.03446	0.03590	0.03749	
13	2.07735E+09	0.00334	0.00419	0.00517	0.00633	0.00774	0.00945	0.01152	0.01403	0.01705	0.02065	
14	2.18356E+09	0.00016	0.00028	0.00034	0.00029	0.00018	0.00009	0.00015	0.00051	0.00127	0.00240	
15	2.19212E+09	0.00043	0.00020	0.00030	0.00099	0.00227	0.00393	0.00546	0.00624	0.00572	0.00388	
16	2.20491E+09	0.00112	0.00269	0.00397	0.00435	0.00360	0.00211	0.00130	0.00394	0.01428	0.03779	
17	2.21929E+09	0.00156	0.00252	0.00499	0.00966	0.01886	0.03638	0.06672	0.11383	0.17970	0.26351	
18	2.23043E+09	0.00438	0.01311	0.03013	0.05718	0.09392	0.13803	0.18532	0.23045	0.26821	0.29261	
19	2.24853E+09	0.02662	0.02996	0.03426	0.03997	0.04754	0.05715	0.06838	0.08041	0.09219	0.10272	
20	2.37723E+09	0.00787	0.01002	0.01207	0.01375	0.01477	0.01489	0.01403	0.01227	0.00994	0.00741	
21	2.39157E+09	0.02362	0.03185	0.04727	0.07392	0.11565	0.17459	0.24927	0.33382	0.41866	0.49154	
22	2.40195E+09	0.06091	0.10196	0.15560	0.21807	0.28225	0.33904	0.38146	0.40361	0.40811	0.39785	
23	2.40810E+09	0.12910	0.16383	0.18711	0.19372	0.18214	0.15546	0.12055	0.08537	0.05619	0.03666	
24	2.41004E+09	0.00744	0.00644	0.00595	0.00564	0.00521	0.00448	0.00348	0.00239	0.00139	0.00065	
25	2.43010E+09	0.00638	0.00736	0.00848	0.00944	0.00956	0.00830	0.00595	0.00364	0.00289	0.00468	
26	2.43350E+09	0.00077	0.00015	0.00018	0.00240	0.00855	0.01916	0.03269	0.04593	0.05556	0.05982	
27	2.44405E+09	0.03603	0.06942	0.11056	0.14945	0.17408	0.17631	0.15506	0.11776	0.07516	0.03845	
28	2.46073E+09	0.14616	0.16598	0.16274	0.13671	0.09653	0.05452	0.02187	0.00404	0.00012	0.00493	
29	2.47580E+09	0.08325	0.05704	0.03047	0.01084	0.00131	0.00052	0.00425	0.00813	0.00954	0.00813	
30	2.48470E+09	0.00364	0.00027	0.00034	0.00174	0.00277	0.00270	0.00178	0.00071	0.00007	0.00008	

Table C-6. Quadrupoles and R/Q's as a function of the particle velocity (Single cavity).

mode no.	frequency Hz	R/Q at beta=									
		0.8	0.81	0.82	0.83	0.84	0.85	0.86	0.87	0.88	
1	1.52443E+09	0.04699	0.05527	0.06437	0.07412	0.08466	0.09591	0.10785	0.12050	0.13384	
2	1.55870E+09	0.00053	0.00053	0.00058	0.00072	0.00101	0.00150	0.00222	0.00318	0.00435	
3	1.56025E+09	0.00479	0.00633	0.00799	0.00956	0.01078	0.01138	0.01120	0.01018	0.00850	
4	1.56235E+09	0.00832	0.00804	0.00796	0.00919	0.01336	0.02249	0.03886	0.06485	0.10271	
5	1.56441E+09	0.05052	0.07736	0.11750	0.17210	0.24092	0.32333	0.41611	0.51671	0.62113	
6	1.56571E+09	0.37904	0.43032	0.47418	0.50782	0.53133	0.54195	0.53995	0.52672	0.50331	
7	1.60687E+09	0.13831	0.14616	0.15376	0.16109	0.16807	0.17475	0.18111	0.18713	0.19277	
8	1.66181E+09	0.48096	0.52715	0.56533	0.59498	0.61482	0.62487	0.62537	0.61633	0.59941	
9	1.66544E+09	0.07250	0.04300	0.02000	0.00556	0.00098	0.00679	0.02281	0.04820	0.08163	
10	1.67000E+09	0.01885	0.02815	0.03669	0.04326	0.04704	0.04764	0.04510	0.03984	0.03261	
11	1.67395E+09	0.00937	0.00691	0.00460	0.00283	0.00190	0.00199	0.00311	0.00515	0.00791	
12	1.67829E+09	0.03924	0.04106	0.04290	0.04474	0.04652	0.04824	0.04985	0.05141	0.05293	
13	2.07735E+09	0.02491	0.02985	0.03555	0.04205	0.04937	0.05751	0.06644	0.07618	0.08674	
14	2.18356E+09	0.00372	0.00492	0.00557	0.00529	0.00396	0.00196	0.00039	0.00129	0.00764	
15	2.19212E+09	0.00154	0.00083	0.00540	0.02029	0.05157	0.10553	0.18758	0.30162	0.44838	
16	2.20491E+09	0.08040	0.14748	0.24189	0.36371	0.50880	0.66852	0.83157	0.98263	1.10729	
17	2.21929E+09	0.36073	0.46246	0.55856	0.63617	0.68480	0.69723	0.67072	0.60752	0.51576	
18	2.23043E+09	0.30066	0.29120	0.26506	0.22671	0.18200	0.13800	0.10101	0.07581	0.06455	
19	2.24853E+09	0.11138	0.11806	0.12306	0.12688	0.13000	0.13280	0.13528	0.13728	0.13857	
20	2.37723E+09	0.00510	0.00328	0.00209	0.00151	0.00141	0.00160	0.00188	0.00211	0.00219	
21	2.39157E+09	0.54420	0.56771	0.56179	0.52935	0.47665	0.41285	0.34564	0.28158	0.22536	
22	2.40195E+09	0.38084	0.36298	0.34852	0.33787	0.33028	0.32163	0.30859	0.28927	0.26222	
23	2.40810E+09	0.02747	0.02724	0.03371	0.04466	0.05837	0.07355	0.08910	0.10382	0.11640	
24	2.41004E+09	0.00024	0.00015	0.00030	0.00062	0.00102	0.00145	0.00185	0.00220	0.00247	
25	2.43010E+09	0.00893	0.01444	0.01941	0.02221	0.02200	0.01897	0.01414	0.00897	0.00480	
26	2.43350E+09	0.05951	0.05752	0.05745	0.06194	0.07150	0.08437	0.09734	0.10673	0.10970	
27	2.44405E+09	0.01379	0.00248	0.00213	0.00924	0.02144	0.03816	0.06006	0.08778	0.12033	
28	2.46073E+09	0.01225	0.01749	0.01875	0.01639	0.01193	0.00702	0.00294	0.00067	0.00108	
29	2.47580E+09	0.00512	0.00215	0.00036	0.00008	0.00099	0.00247	0.00394	0.00499	0.00542	
30	2.48470E+09	0.00054	0.00112	0.00151	0.00157	0.00133	0.00094	0.00054	0.00023	0.00006	

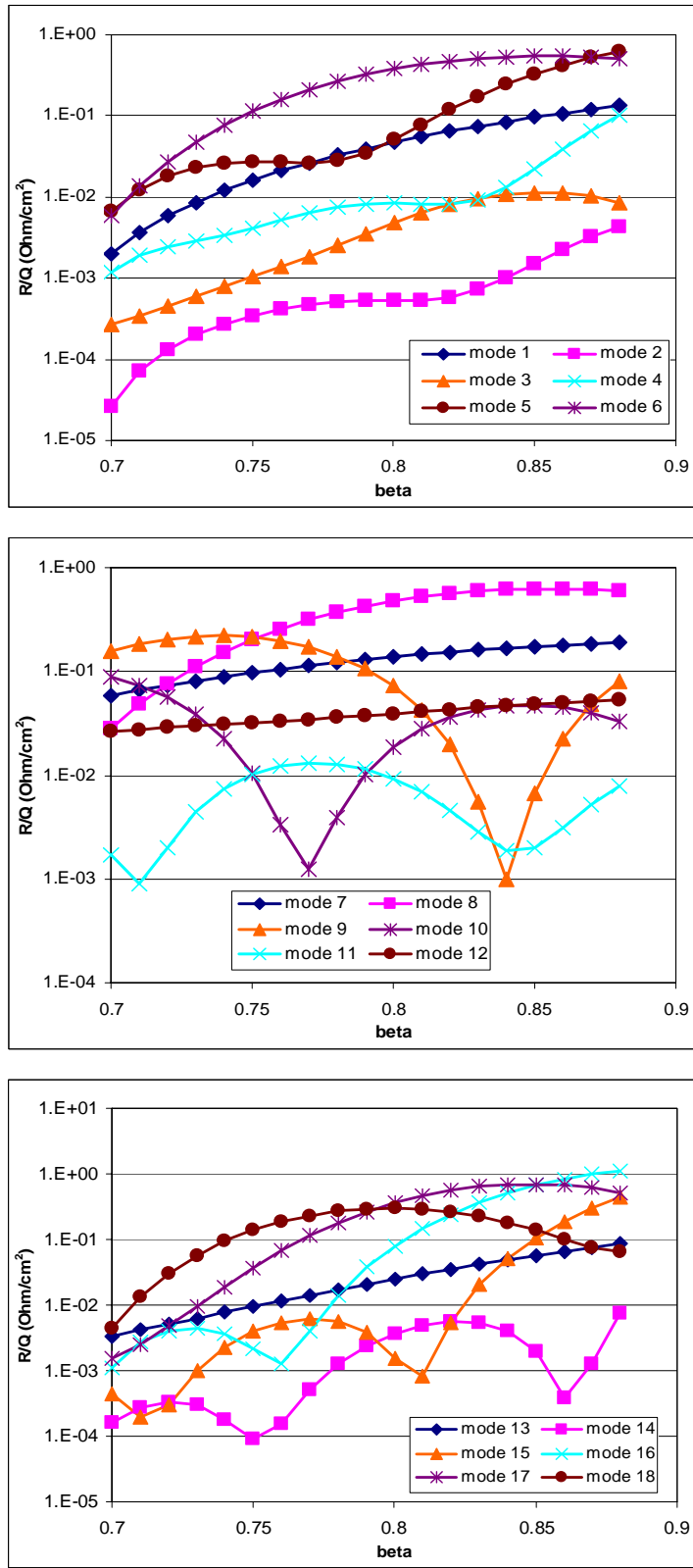


Figure C-8. R/Q 's of quadrupoles as a function of the particle velocity (single cavity modeling).
(continue..)

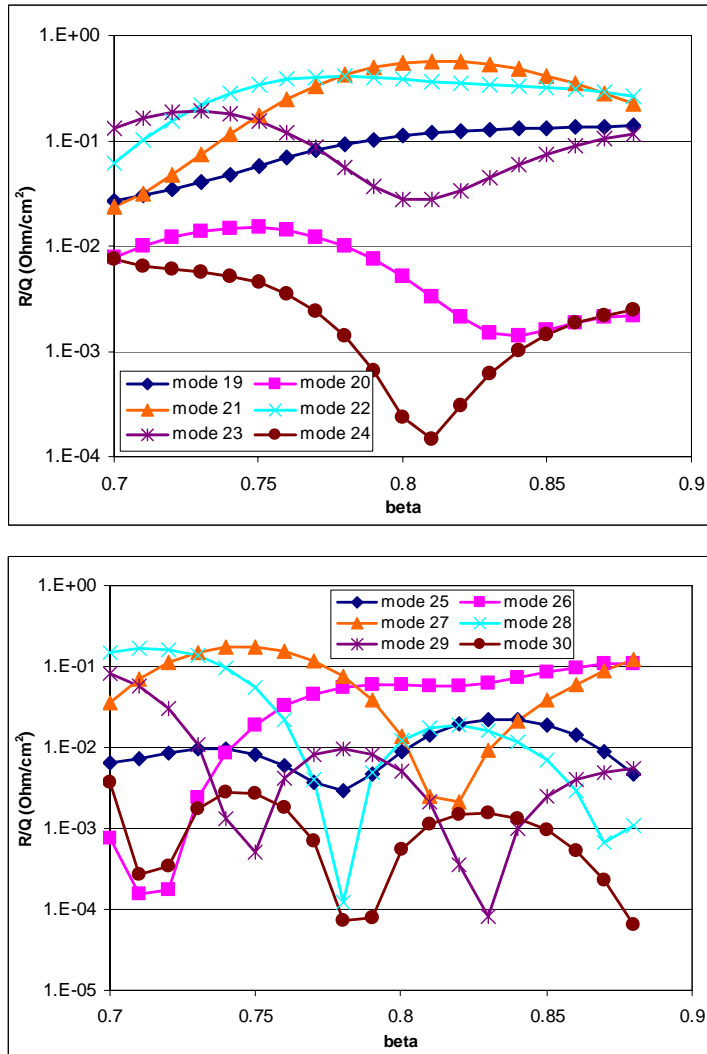


Figure C-8. R/Q's of quadrupoles as a function of the particle velocity (single cavity modeling).

Table C-7. Sextupoles and R/Q's as a function of the particle velocity (Single cavity).

mode no.	frequency Hz	R/Q at beta=									
		0.7	0.71	0.72	0.73	0.74	0.75	0.76	0.77	0.78	0.79
1	1.89049E+09	8.4E-05	8.1E-05	7.8E-05	7.7E-05	7.7E-05	7.9E-05	8.2E-05	8.7E-05	9.5E-05	0.00011
2	1.92253E+09	0.00034	0.00034	0.00034	0.00035	0.00035	0.00035	0.00036	0.00036	0.00037	0.00039
3	1.93809E+09	0.00098	0.00069	0.00046	0.00029	0.00017	9.3E-05	4.6E-05	2.1E-05	8.1E-06	2.8E-06
4	1.93837E+09	0.00074	0.00079	0.00077	0.00068	0.00055	0.00041	0.00028	0.00017	9.5E-05	4.3E-05
5	1.93872E+09	4.1E-06	3.1E-05	8.2E-05	0.00014	0.00018	0.0002	0.00019	0.00016	0.00011	6.2E-05
6	1.93901E+09	5.1E-05	4.1E-05	2.6E-05	1.2E-05	3.3E-06	7.1E-07	3.2E-06	7.8E-06	1.1E-05	1.1E-05
7	1.93969E+09	0.00023	0.00021	0.00018	0.00016	0.00013	0.00011	8.3E-05	6E-05	3.9E-05	2.1E-05
8	1.95007E+09	5.9E-06	7.8E-06	8.4E-06	7.2E-06	4.2E-06	1E-06	3.3E-07	6.6E-06	2.5E-05	6.3E-05
9	1.95035E+09	3.5E-07	2.1E-06	1.7E-05	5.2E-05	0.00012	0.00021	0.00035	0.00052	0.00072	0.00094
10	1.95068E+09	0.00016	0.00025	0.00037	0.0005	0.00062	0.00073	0.00081	0.00087	0.00088	0.00086
11	1.95094E+09	0.00031	0.00031	0.00031	0.00028	0.00025	0.0002	0.00016	0.00011	7.1E-05	3.9E-05
12	1.96177E+09	0.00012	0.00015	0.00018	0.00021	0.00025	0.00028	0.00032	0.00036	0.00041	0.00045
13	2.47881E+09	0.0001	8E-05	6.2E-05	4.9E-05	4.1E-05	4.1E-05	5E-05	6.9E-05	9.9E-05	0.00014
14	2.55441E+09	0.00019	8E-05	2.5E-05	5.1E-06	3.7E-07	7.4E-09	7.9E-09	4.8E-07	2.6E-06	6.9E-06
15	2.55631E+09	0.00045	0.00032	0.00018	7.4E-05	1.7E-05	1.1E-07	6.3E-06	1.6E-05	1.8E-05	1.1E-05
16	2.55873E+09	6.9E-05	9.9E-05	9.8E-05	6.6E-05	2.4E-05	3.6E-07	1.9E-05	8.9E-05	0.0002	0.00032
17	2.56077E+09	6.3E-06	8.7E-07	3.1E-07	1.9E-06	1.8E-06	4.4E-08	5.6E-06	3.9E-05	0.00013	0.00032
18	2.57335E+09	0.00013	9.2E-05	5.9E-05	3.1E-05	1.3E-05	6.2E-06	1.7E-05	4.9E-05	0.00011	0.0002
19	2.70096E+09	4.2E-05	5.7E-05	7.5E-05	9.4E-05	0.00012	0.00014	0.00016	0.00019	0.00022	0.00024
20	2.78130E+09	3.9E-05	4.6E-05	6.8E-05	8.8E-05	9.1E-05	7.5E-05	5.3E-05	4.3E-05	5.9E-05	0.00011

mode no.	frequency Hz	R/Q at beta=									
		0.8	0.81	0.82	0.83	0.84	0.85	0.86	0.87	0.88	
1	1.89049E+09	0.00012	0.00013	0.00015	0.00018	0.0002	0.00023	0.00026	0.0003	0.00034	
2	1.92253E+09	0.0004	0.00042	0.00045	0.00047	0.00051	0.00054	0.00058	0.00063	0.00068	
3	1.93809E+09	8.7E-07	3.3E-07	2.5E-07	4.3E-07	9.1E-07	1.8E-06	3E-06	4.5E-06	5.9E-06	
4	1.93837E+09	1.5E-05	2.5E-06	1.7E-07	2.1E-06	4.3E-06	5.1E-06	4E-06	2.2E-06	1.1E-06	
5	1.93872E+09	2.3E-05	2.1E-06	4E-06	2.9E-05	7.2E-05	0.00013	0.00018	0.00024	0.00028	
6	1.93901E+09	6.4E-06	1.3E-06	9.1E-07	1.3E-05	4.6E-05	0.00011	0.00021	0.00036	0.00056	
7	1.93969E+09	8.1E-06	1.5E-06	2.8E-06	1.4E-05	3.8E-05	7.8E-05	0.00013	0.00021	0.00031	
8	1.95007E+09	0.00013	0.00022	0.00036	0.00054	0.00076	0.00103	0.00134	0.00169	0.00206	
9	1.95035E+09	0.00117	0.00139	0.00159	0.00175	0.00187	0.00193	0.00193	0.00186	0.00175	
10	1.95068E+09	0.0008	0.00071	0.0006	0.00048	0.00035	0.00024	0.00015	7.4E-05	2.6E-05	
11	1.95094E+09	1.6E-05	3.8E-06	1.1E-08	3.5E-06	1.2E-05	2.3E-05	3.4E-05	4.4E-05	5.2E-05	
12	1.96177E+09	0.0005	0.00055	0.00059	0.00064	0.00069	0.00074	0.00079	0.00084	0.00089	
13	2.47881E+09	0.0002	0.00027	0.00035	0.00046	0.00058	0.00072	0.00088	0.00105	0.00125	
14	2.55441E+09	1.2E-05	1.6E-05	1.7E-05	1.5E-05	8.9E-06	3E-06	8.2E-07	6.5E-06	2.3E-05	
15	2.55631E+09	2E-06	3.1E-06	2.5E-05	7.1E-05	0.00014	0.00021	0.00028	0.00031	0.0003	
16	2.55873E+09	0.00042	0.00047	0.00044	0.00034	0.0002	6.2E-05	3.2E-06	0.0001	0.00044	
17	2.56077E+09	0.00064	0.00112	0.00177	0.0026	0.0036	0.00471	0.00589	0.00708	0.00821	
18	2.57335E+09	0.00033	0.00049	0.0007	0.00095	0.00124	0.00158	0.00195	0.00236	0.00279	
19	2.70096E+09	0.00027	0.00031	0.00034	0.00037	0.0004	0.00044	0.00047	0.00051	0.00055	
20	2.78130E+09	0.00019	0.00029	0.0004	0.00047	0.00047	0.0004	0.00028	0.00017	7.7E-05	

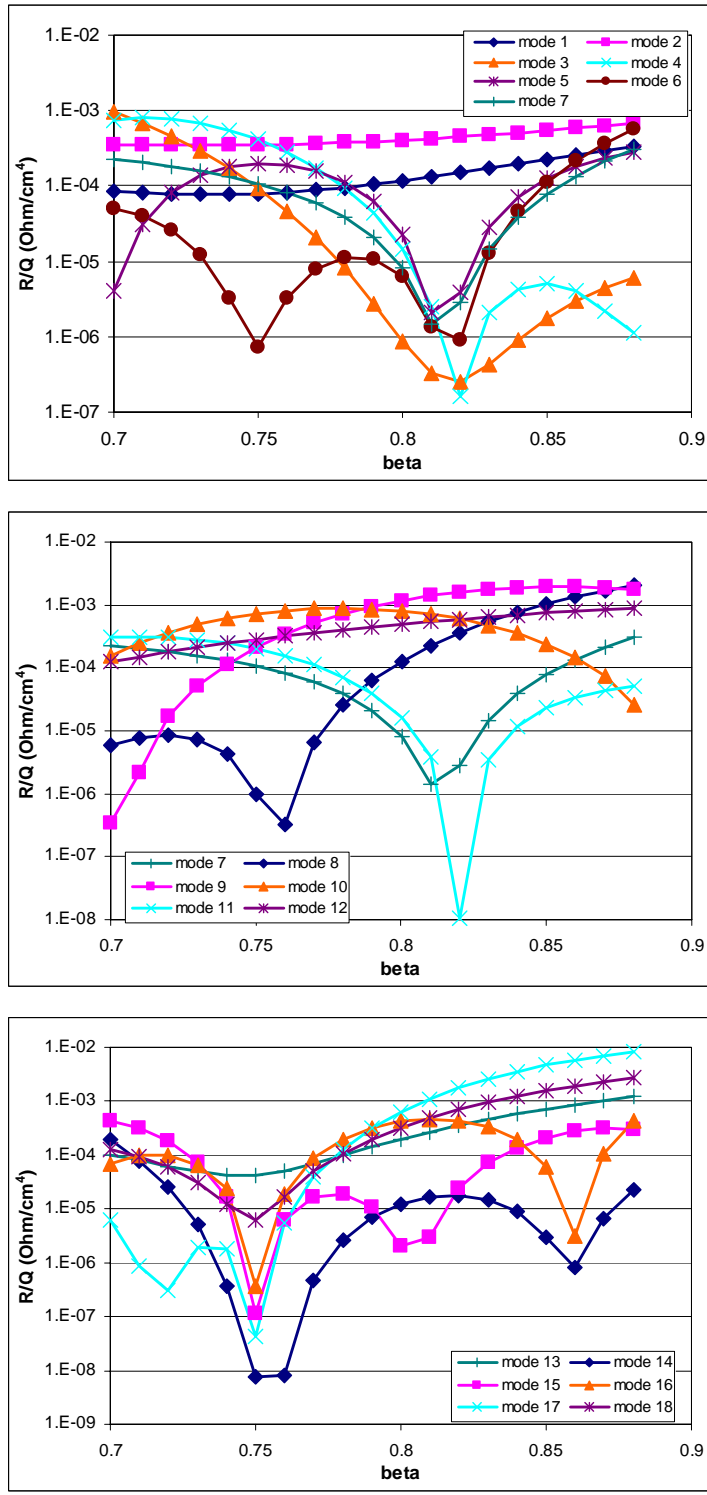


Figure C-9. R/Q 's of sextupoles as a function of the particle velocity (single cavity modeling).

Appendix D. Trapped mode finding

Table D-1. Stored energies at each end cell for the medium beta TM monopoles

mode	Frequency/Hz	right %	left %	total %
1	7.938028E+08	1.951734	2.539831	4.491565
2	7.960453E+08	7.452041	9.014796	16.46684
3	7.991052E+08	15.77017	17.26161	33.03178
4	8.020936E+08	25.70038	25.34067	51.04105
5	8.041902E+08	32.84035	29.70617	62.54652
6	8.050074E+08	16.29298	16.20341	32.49639
7	1.691105E+09	91.66194	0.00033	91.66227
8	1.716121E+09	1.274544	11.78856	13.0631
9	1.726082E+09	2.695113	29.08096	31.77608
10	1.740051E+09	2.65843	31.94767	34.6061
11	1.754807E+09	1.662046	20.81188	22.47393
12	1.766462E+09	0.514802	6.39529	6.910093
13	1.901688E+09	99.57727	1.97E-07	99.57727
14	2.135000E+09	95.45383	6.83E-05	95.45389
15	2.179097E+09	0.791271	6.656354	7.447624
16	2.191225E+09	1.666957	18.94783	20.61478
17	2.206089E+09	1.536183	27.81892	29.3551
18	2.219088E+09	0.804644	29.38241	30.18706
19	2.226949E+09	0.175627	17.08124	17.25687
20	2.350781E+09	99.70067	2.69E-08	99.70067
21	2.581959E+09	50.57462	0.133437	50.70806
22	2.590454E+09	6.730825	16.40128	23.13211
23	2.600957E+09	8.927433	29.9069	38.83433
24	2.616927E+09	8.978572	25.52912	34.50769
25	2.638303E+09	8.877955	17.74908	26.62703
26	2.665947E+09	14.75851	31.59481	46.35332
27	2.678655E+09	39.60369	11.73548	51.33917
28	2.718757E+09	24.78508	11.14923	35.93431
29	2.745414E+09	21.0534	19.53914	40.59254
30	2.774449E+09	10.84242	21.92504	32.76746
31	2.800984E+09	4.733005	14.83054	19.56355
32	2.820625E+09	1.323113	5.512661	6.835775
33	2.848210E+09	0.000752	94.03846	94.03921
34	3.042929E+09	99.35691	1.49E-08	99.35691
35	3.148941E+09	6.61E-08	99.98864	99.98864
36	3.200724E+09	100.0187	2.15E-07	100.0187
37	3.293018E+09	18.80777	1.22204	20.02981
38	3.303181E+09	14.12327	14.26899	28.39226
39	3.320184E+09	9.72503	44.10837	53.8334
40	3.337242E+09	7.646753	46.48052	54.12727

Gray colored modes are not realistic one.

Table D-2. Stored energies at each end cell for the medium beta TE monopoles

mode	frequency/hz	right %	left %	total %
1	2.0816E+09	9.99E+01	1.47E-13	9.99E+01
2	2.1627E+09	1.13E-02	1.52E-02	1.53E+00
3	2.1643E+09	3.16E-02	5.34E-02	5.38E+00
4	2.1664E+09	3.61E-02	9.34E-02	9.38E+00
5	2.1683E+09	1.79E-02	9.96E-02	9.98E+00
6	2.1699E+09	1.92E-04	7.39E-01	7.39E+01
7	2.6821E+09	9.99E+01	4.19E-12	9.99E+01
8	2.7777E+09	3.26E-02	1.26E-02	1.29E+00
9	2.7817E+09	9.33E-02	4.52E-02	4.61E+00
10	2.7870E+09	1.10E-01	8.24E-02	8.35E+00
11	2.7919E+09	5.60E-02	8.52E-02	8.58E+00
12	2.7968E+09	4.46E-04	7.75E-01	7.75E+01
13	2.9284E+09	9.99E+01	1.49E-10	9.99E+01
14	3.1572E+09	9.97E+01	8.52E-10	9.97E+01

Table D-3. Stored energies at each end cell for the medium beta dipoles

mode no.	frequency	right %	left %	total %
mode 1	1.11712E+09	9.66E+01	1.38E-06	9.66E+01
mode 2	1.13793E+09	5.14E-01	4.62E+00	5.13E+00
mode 3	1.14359E+09	1.29E+00	1.61E+01	1.74E+01
mode 4	1.15214E+09	1.48E+00	2.89E+01	3.03E+01
mode 5	1.16179E+09	1.01E+00	3.33E+01	3.43E+01
mode 6	1.16955E+09	3.15E-01	1.71E+01	1.74E+01
mode 7	1.34599E+09	9.08E+01	6.64E-04	9.08E+01
mode 8	1.45814E+09	1.95E+00	8.91E+00	1.09E+01
mode 9	1.50250E+09	5.76E+00	2.22E+01	2.79E+01
mode 10	1.56286E+09	1.30E+01	2.64E+01	3.95E+01
mode 11	1.62394E+09	3.76E+01	1.94E+01	5.71E+01
mode 12	1.66988E+09	4.40E+01	1.39E+01	5.79E+01
mode 13	1.71948E+09	9.91E+00	9.87E+00	1.98E+01
mode 14	1.93725E+09	5.07E+01	2.31E+00	5.30E+01
mode 15	1.97603E+09	1.68E+01	2.74E+01	4.43E+01
mode 16	2.02147E+09	1.58E+01	2.93E+01	4.52E+01
mode 17	2.06218E+09	1.33E+01	2.26E+01	3.58E+01
mode 18	2.09318E+09	1.15E+01	1.37E+01	2.52E+01
mode 19	2.11337E+09	1.41E+01	4.99E+00	1.91E+01
mode 20	2.12418E+09	7.51E+01	1.34E-01	7.52E+01
mode 21	2.19634E+09	5.80E-05	9.74E+01	9.74E+01
mode 22	2.24083E+09	9.83E+00	1.46E+00	1.13E+01
mode 23	2.24965E+09	1.45E+01	7.49E+00	2.20E+01
mode 24	2.26555E+09	1.52E+01	1.54E+01	3.06E+01
mode 25	2.28785E+09	1.64E+01	2.15E+01	3.80E+01
mode 26	2.31482E+09	2.43E+01	2.18E+01	4.61E+01
mode 27	2.34074E+09	4.94E+01	1.52E+01	6.46E+01
mode 28	2.36812E+09	2.09E+01	3.27E+01	5.36E+01
mode 29	2.41053E+09	2.14E+01	2.59E+01	4.73E+01
mode 30	2.42991E+09	9.43E+01	1.78E+00	9.61E+01
mode 31	2.45469E+09	9.11E+00	1.49E+01	2.40E+01
mode 32	2.46507E+09	5.68E-01	1.42E+00	1.99E+00
mode 33	2.46669E+09	6.67E-02	1.89E-01	2.56E-01
mode 34	2.47234E+09	4.82E+00	2.92E+00	7.74E+00
mode 35	2.47574E+09	2.33E+00	7.87E+01	8.11E+01
mode 36	2.48555E+09	1.52E+01	3.10E+01	4.62E+01
mode 37	2.52833E+09	3.45E+01	2.81E+01	6.26E+01
mode 38	2.57639E+09	3.43E+01	2.97E+01	6.40E+01
mode 39	2.63383E+09	2.90E+01	3.00E+01	5.90E+01
mode 40	2.69575E+09	3.48E+01	2.67E+01	6.14E+01

Table D-4. Stored energies at each end cell for the medium beta quadrupoles.

mode no.	frequency	right %	left %	total %
mode 1	1.51744E+09	9.99E+01	2.14E-07	9.99E+01
mode 2	1.55720E+09	4.74E-02	1.50E+01	1.50E+01
mode 3	1.55603E+09	1.68E-02	4.23E+00	4.24E+00
mode 4	1.55878E+09	5.66E-02	2.79E+01	2.80E+01
mode 5	1.56026E+09	3.51E-02	3.44E+01	3.44E+01
mode 6	1.56122E+09	9.49E-03	1.85E+01	1.85E+01
mode 7	1.94871E+09	9.94E+01	4.49E-09	9.94E+01
mode 8	2.07281E+09	7.80E-02	5.56E+00	5.64E+00
mode 9	2.07960E+09	2.28E-01	1.83E+01	1.85E+01
mode 10	2.08869E+09	2.87E-01	2.98E+01	3.01E+01
mode 11	2.09736E+09	1.94E-01	3.11E+01	3.13E+01
mode 12	2.10317E+09	5.46E-02	1.52E+01	1.52E+01
mode 13	2.32915E+09	9.97E+01	1.38E-05	9.97E+01
mode 14	2.46636E+09	8.00E+01	4.63E-03	8.00E+01
mode 15	2.47653E+09	3.38E+00	7.90E+00	1.13E+01
mode 16	2.48333E+09	6.06E+00	2.17E+01	2.78E+01
mode 17	2.49272E+09	6.68E+00	2.92E+01	3.59E+01
mode 18	2.50333E+09	6.20E+00	2.62E+01	3.24E+01
mode 19	2.51293E+09	3.23E+00	1.40E+01	1.72E+01
mode 20	2.54108E+09	8.29E+01	7.39E-02	8.30E+01
mode 21	2.56694E+09	4.10E+00	5.95E+00	1.01E+01
mode 22	2.58399E+09	4.43E+00	1.28E+01	1.72E+01
mode 23	2.60272E+09	2.91E+00	1.95E+01	2.24E+01
mode 24	2.61892E+09	1.24E+00	2.63E+01	2.76E+01
mode 25	2.62850E+09	1.29E-01	3.61E+01	3.62E+01
mode 26	2.71646E+09	1.00E+02	3.46E-07	1.00E+02
mode 27	2.76014E+09	2.74E-01	2.71E-01	5.45E-01
mode 28	2.76229E+09	6.48E-01	1.37E+00	2.02E+00
mode 29	2.76571E+09	9.23E-01	3.45E+00	4.37E+00
mode 30	2.77015E+09	5.73E-01	3.34E+00	3.91E+00

Table D-5. Stored energies at each end cell for the medium beta sextupoles

mode no.	frequency	right %	left %	total %
mode 1	1.89045E+09	1.00E+02	1.78E-12	1.00E+02
mode 6	1.93433E+09	1.01E-05	7.70E+01	7.70E+01
mode 5	1.93453E+09	1.60E-03	8.19E+00	8.20E+00
mode 4	1.93472E+09	3.01E-03	9.03E+00	9.03E+00
mode 3	1.93494E+09	2.54E-03	4.64E+00	4.64E+00
mode 2	1.93513E+09	9.86E-04	1.01E+00	1.01E+00
mode 7	2.31760E+09	1.00E+02	4.98E-08	1.00E+02
mode 9	2.38305E+09	3.21E-03	5.87E-02	6.19E-02
mode 10	2.38357E+09	8.73E-03	1.62E-01	1.71E-01
mode 11	2.38422E+09	8.91E-03	1.79E-01	1.88E-01
mode 12	2.38476E+09	3.51E-03	7.35E-02	7.70E-02
mode 8	2.39201E+09	6.29E-08	9.95E+01	9.95E+01
mode 13	2.78600E+09	1.00E+02	5.06E-07	1.00E+02
mode 14	2.87809E+09	9.86E+01	2.18E-07	9.86E+01

Table D-6. Stored energies at each end cell for the high beta TM monopoles

mode no.	frequency	right %	left %	total %
1	7.9363E+08	2.08E+00	2.46E+00	4.54E+00
2	7.9587E+08	7.91E+00	9.08E+00	1.70E+01
3	7.9892E+08	1.64E+01	1.77E+01	3.41E+01
4	8.0195E+08	2.55E+01	2.55E+01	5.10E+01
5	8.0417E+08	3.16E+01	2.98E+01	6.14E+01
6	8.0498E+08	1.65E+01	1.55E+01	3.20E+01
7	1.6545E+09	1.00E+02	1.15E-08	1.00E+02
8	1.6996E+09	6.58E+01	1.20E-04	6.58E+01
9	1.7075E+09	9.98E-01	2.33E+00	3.33E+00
10	1.7105E+09	1.47E+00	7.91E+00	9.38E+00
11	1.7137E+09	7.82E-01	1.39E+01	1.47E+01
12	1.7156E+09	7.69E-02	2.25E+01	2.26E+01
13	1.7369E+09	8.82E-09	9.00E+01	9.00E+01
14	1.7493E+09	2.94E+01	5.30E-06	2.94E+01
15	1.7552E+09	4.75E-01	7.25E-01	1.20E+00
16	1.7578E+09	8.56E-01	2.44E+00	3.29E+00
17	1.7609E+09	4.59E-01	2.87E+00	3.33E+00
18	1.7657E+09	1.32E-03	5.74E+01	5.74E+01
19	1.8143E+09	9.99E+01	2.96E-08	9.99E+01
20	2.1522E+09	9.92E+01	4.29E-08	9.92E+01
21	2.3025E+09	1.47E+00	8.57E+00	1.00E+01
22	2.3210E+09	5.32E+00	2.62E+01	3.15E+01
23	2.3478E+09	1.08E+01	3.32E+01	4.40E+01
24	2.3805E+09	1.82E+01	2.39E+01	4.21E+01
25	2.4167E+09	2.82E+01	1.31E+01	4.12E+01
26	2.4485E+09	3.50E+01	4.30E+00	3.93E+01
27	2.5065E+09	9.30E-01	7.30E+01	7.39E+01
28	2.5439E+09	2.47E+01	9.53E+00	3.42E+01
29	2.5655E+09	3.66E+01	1.35E+01	5.01E+01
30	2.5843E+09	2.54E+01	2.06E+01	4.60E+01
31	2.5999E+09	1.16E+01	2.95E+01	4.11E+01
32	2.6110E+09	3.84E+00	2.97E+01	3.36E+01
33	2.6171E+09	7.02E-01	1.46E+01	1.53E+01
34	2.7487E+09	8.95E+01	3.10E-05	8.95E+01
35	2.8188E+09	1.03E+00	1.69E+01	1.79E+01
36	2.8372E+09	3.23E+00	3.70E+01	4.02E+01
37	2.8650E+09	6.38E+00	3.01E+01	3.64E+01
38	2.9007E+09	1.08E+01	2.04E+01	3.12E+01
39	2.9410E+09	1.62E+01	1.85E+01	3.47E+01
40	2.9842E+09	2.58E+01	2.11E+01	4.69E+01

Table D-7. Stored energies at each end cell for the high beta TE monopoles

mode no.	frequency	right %	left %	total %
1	1.71141E+09	1.00E+02	3.87E-11	1.00E+02
2	1.76228E+09	7.57E-03	1.57E-01	1.64E-01
3	1.76424E+09	2.12E-02	5.28E-01	5.49E-01
4	1.76512E+09	8.28E-03	2.45E-01	2.53E-01
5	1.76314E+09	2.04E-02	4.49E-01	4.70E-01
6	1.77147E+09	2.25E-09	9.86E+01	9.86E+01
7	2.39996E+09	9.99E+01	2.98E-07	9.99E+01
8	2.47138E+09	3.25E-02	8.98E-01	9.31E-01
9	2.47402E+09	9.38E-02	3.18E+00	3.27E+00
10	2.47768E+09	1.11E-01	5.42E+00	5.53E+00
11	2.48104E+09	5.42E-02	4.63E+00	4.69E+00
12	2.48567E+09	1.08E-04	8.59E+01	8.59E+01
13	2.61434E+09	9.94E+01	5.19E-08	9.94E+01
14	2.78118E+09	9.75E+01	5.06E-04	9.75E+01
15	2.80812E+09	1.21E+00	1.52E+01	1.64E+01

Table D-8. Stored energies at each end cell for the high beta dipoles

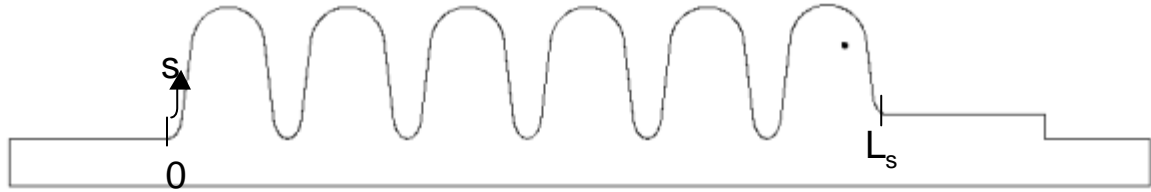
mode no.	frequency	right %	left %	total %
1	1.1037E+09	9.97E+01	1.26E-08	9.97E+01
2	1.1350E+09	2.69E+00	1.99E+00	4.68E+00
3	1.1379E+09	7.31E+00	8.84E+00	1.61E+01
4	1.1434E+09	1.06E+01	1.99E+01	3.05E+01
5	1.1522E+09	1.24E+01	2.90E+01	4.13E+01
6	1.1653E+09	1.29E+01	3.04E+01	4.33E+01
7	1.1816E+09	2.77E+01	8.14E+00	3.58E+01
8	1.2132E+09	9.32E+00	1.61E+01	2.54E+01
9	1.2463E+09	8.61E+00	2.29E+01	3.15E+01
10	1.2842E+09	6.54E+00	2.75E+01	3.40E+01
11	1.3216E+09	3.88E+00	2.45E+01	2.84E+01
12	1.3504E+09	1.23E+00	1.06E+01	1.19E+01
13	1.4848E+09	9.74E+01	9.58E-05	9.74E+01
14	1.7552E+09	2.94E+01	1.93E+00	3.13E+01
15	1.7701E+09	1.71E+01	1.39E+01	3.10E+01
16	1.7890E+09	8.33E+00	1.87E+01	2.70E+01
17	1.8028E+09	3.96E+00	1.19E+01	1.58E+01
18	1.8101E+09	1.91E+00	3.45E+00	5.36E+00
19	1.8176E+09	9.33E+01	8.99E-04	9.33E+01
20	1.8363E+09	2.47E-08	9.78E+01	9.78E+01
21	1.9417E+09	1.02E+01	3.17E+00	1.34E+01
22	1.9639E+09	1.93E+01	1.31E+01	3.24E+01
23	1.9977E+09	2.47E+01	2.03E+01	4.50E+01
24	2.0279E+09	3.93E+01	1.75E+01	5.68E+01
25	2.0490E+09	2.51E+01	2.08E+01	4.59E+01
26	2.0639E+09	3.63E+00	2.07E+01	2.44E+01
27	2.0800E+09	3.23E+01	3.03E-03	3.23E+01
28	2.0913E+09	3.01E-01	1.58E+00	1.88E+00
29	2.0948E+09	1.15E+00	1.08E+01	1.20E+01
30	2.1010E+09	1.47E+00	3.79E+01	3.94E+01
31	2.1071E+09	1.04E+00	2.45E+01	2.55E+01
32	2.1161E+09	2.37E-02	8.16E+01	8.16E+01
33	2.1243E+09	9.25E+01	7.75E-04	9.25E+01
34	2.1865E+09	4.63E+01	1.95E-03	4.64E+01
35	2.1946E+09	3.95E+00	8.31E+00	1.23E+01
36	2.2049E+09	9.89E+00	2.42E+01	3.41E+01
37	2.2279E+09	1.47E+01	2.95E+01	4.42E+01
38	2.2683E+09	1.70E+01	2.57E+01	4.27E+01
39	2.3242E+09	1.80E+01	2.31E+01	4.11E+01
40	2.3948E+09	2.81E+01	2.56E+01	5.37E+01
41	2.4454E+09	3.52E+01	2.89E+01	6.41E+01
42	2.4987E+09	3.17E+01	2.73E+01	5.89E+01
43	2.5501E+09	3.00E+01	2.89E+01	5.89E+01
44	2.5950E+09	4.06E+01	2.51E+01	6.57E+01
45	2.6330E+09	3.04E+01	2.64E+01	5.68E+01

Table D-9. Stored energies at each end cell for the high beta quadrupoles

mode no.	frequency	right %	left %	total %
1	1.52443E+09	9.99E+01	3.32E-09	9.99E+01
2	1.55870E+09	5.80E-02	2.38E+00	2.43E+00
3	1.56025E+09	1.74E-01	9.64E+00	9.82E+00
4	1.56235E+09	2.26E-01	2.07E+01	2.09E+01
5	1.56441E+09	1.49E-01	3.13E+01	3.14E+01
6	1.56571E+09	2.37E-02	3.59E+01	3.59E+01
7	1.60687E+09	9.88E+01	4.42E-07	9.88E+01
8	1.66181E+09	9.54E-02	1.57E+00	1.67E+00
9	1.66544E+09	2.46E-01	5.11E+00	5.35E+00
10	1.67000E+09	2.56E-01	7.99E+00	8.25E+00
11	1.67395E+09	1.15E-01	6.68E+00	6.79E+00
12	1.67829E+09	4.21E-04	7.86E+01	7.86E+01
13	2.07735E+09	9.98E+01	4.16E-07	9.98E+01
14	2.18356E+09	5.95E-01	1.84E+00	2.44E+00
15	2.19212E+09	2.12E+00	7.06E+00	9.18E+00
16	2.20491E+09	3.81E+00	1.50E+01	1.88E+01
17	2.21929E+09	4.22E+00	2.50E+01	2.92E+01
18	2.23043E+09	9.10E-01	5.09E+01	5.18E+01
19	2.24853E+09	8.83E+01	1.90E-02	8.84E+01
20	2.37723E+09	9.93E+01	2.78E-04	9.93E+01
21	2.39157E+09	5.98E+01	1.28E-01	5.99E+01
22	2.40195E+09	4.06E+00	3.24E+00	7.30E+00
23	2.40810E+09	1.17E+00	1.62E+01	1.73E+01
24	2.41004E+09	3.00E-01	3.31E-01	6.30E-01
25	2.43010E+09	2.80E+00	4.26E+01	4.54E+01
26	2.43350E+09	4.95E+00	6.02E+01	6.51E+01
27	2.44405E+09	1.06E+01	2.10E+01	3.16E+01
28	2.46073E+09	8.02E+00	2.58E+01	3.39E+01
29	2.47580E+09	3.67E+00	2.17E+01	2.54E+01
30	2.48470E+09	1.01E+00	7.50E+00	8.51E+00

Table D-10. Stored energies at each end cell for the high beta sextupoles

mode no.	frequency	right %	left %	total %
1	1.89049E+09	1.00E+02	1.09E-09	1.00E+02
2	1.92253E+09	9.99E+01	4.84E-07	9.99E+01
3	1.93809E+09	8.28E-03	3.04E-01	3.13E-01
4	1.93837E+09	2.17E-02	1.43E+00	1.45E+00
5	1.93872E+09	2.55E-02	2.68E+00	2.71E+00
6	1.93901E+09	1.27E-02	1.82E+00	1.84E+00
7	1.93969E+09	1.99E-06	9.36E+01	9.36E+01
8	1.95007E+09	4.20E-03	2.12E-02	2.54E-02
9	1.95035E+09	1.03E-02	5.23E-02	6.26E-02
10	1.95068E+09	9.41E-03	4.80E-02	5.74E-02
11	1.95094E+09	3.48E-03	1.68E-02	2.02E-02
12	1.96177E+09	2.67E-07	9.99E+01	9.99E+01
13	2.47881E+09	9.99E+01	4.41E-07	9.99E+01
14	2.55441E+09	1.75E-02	1.88E-01	2.05E-01
15	2.55631E+09	4.80E-02	5.67E-01	6.15E-01
16	2.55873E+09	5.20E-02	6.97E-01	7.49E-01
17	2.57335E+09	2.91E-06	9.82E+01	9.82E+01
18	2.56077E+09	2.13E-02	3.23E-01	3.45E-01



Deviations from the reference geometry = $\sum_{i=1}^{200} (a_i \cos(i\pi s / L_s) + b_i \sin(i\pi s / L_s))$
; normal to the surface

L_s ; total length along the cavity surface, ~1.9 m for high beta cavity
 a_i & b_i ; random coefficient with $\sigma=0.025$ mm

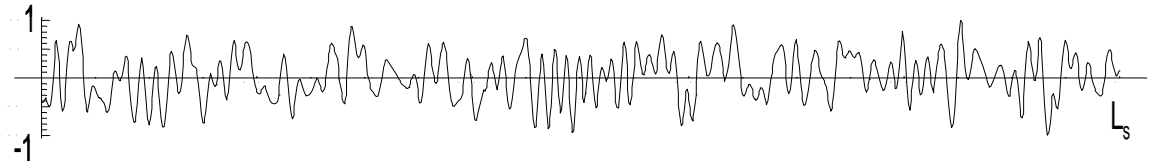


Figure D-1. An example of the random mechanical perturbation.

total deviation $s_t \sim 0.5$ mmPa little bit worse condition than real one

Ref.) A.Marziali et al, "Structure Fabrication and Control of Higher Order Modes," Proc. of 5th Workshop on RF superconductivity, pp802-822 (1992)

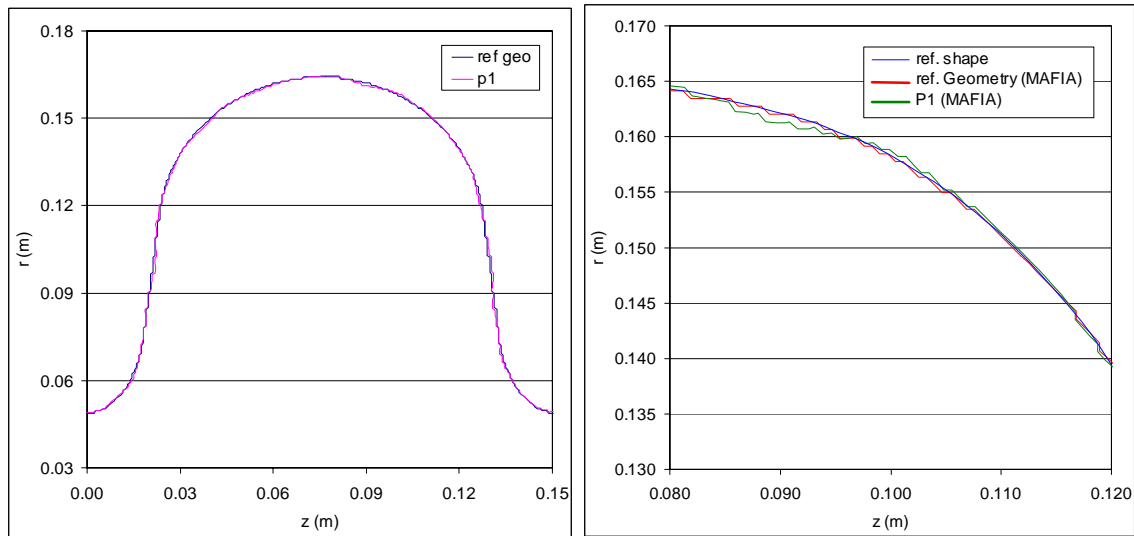


Figure D-2. Perturbed cavity geometry after applying a random mechanical perturbation.

Table D-11. Comparisons of stored energy at each end cell combined between the reference geometry and one of the random perturbed geometry (TM monopoles).

Ref. Geometry TM Monopoles

mode no.	frequency	total %
1	7.9341E+08	4.54E+00
2	7.9562E+08	1.70E+01
3	7.9862E+08	3.41E+01
4	8.0162E+08	5.10E+01
5	8.0379E+08	6.14E+01
6	8.0463E+08	3.20E+01
7	1.6545E+09	1.00E+02
8	1.6996E+09	6.58E+01
9	1.7075E+09	3.33E+00
10	1.7105E+09	9.38E+00
11	1.7137E+09	1.47E+01
12	1.7156E+09	2.26E+01
13	1.7369E+09	9.00E+01
14	1.7493E+09	2.94E+01
15	1.7552E+09	1.20E+00
16	1.7578E+09	3.29E+00
17	1.7609E+09	3.33E+00
18	1.7657E+09	5.74E+01
19	1.8143E+09	9.99E+01
20	2.1522E+09	9.92E+01
21	2.3025E+09	1.00E+01
22	2.3210E+09	3.15E+01
23	2.3478E+09	4.40E+01
24	2.3805E+09	4.21E+01
25	2.4167E+09	4.12E+01
26	2.4485E+09	3.93E+01
27	2.5065E+09	7.39E+01
28	2.5439E+09	3.42E+01
29	2.5655E+09	5.01E+01
30	2.5843E+09	4.60E+01
31	2.5999E+09	4.11E+01
32	2.6110E+09	3.36E+01
33	2.6171E+09	1.53E+01
34	2.7487E+09	8.95E+01
35	2.8188E+09	1.79E+01
36	2.8372E+09	4.02E+01
37	2.8650E+09	3.64E+01
38	2.9007E+09	3.12E+01
39	2.9410E+09	3.47E+01
40	2.9842E+09	4.69E+01

TM Monopoles P1

mode no.	frequency	total %
1	7.9345E+08	3.84E+00
2	7.9594E+08	1.73E+01
3	7.9879E+08	3.70E+01
4	8.0158E+08	5.13E+01
5	8.0394E+08	5.64E+01
6	8.0477E+08	3.43E+01
7	1.6540E+09	1.00E+02
8	1.6978E+09	6.56E+01
9	1.7083E+09	5.25E+00
10	1.7102E+09	7.74E+00
11	1.7141E+09	4.40E+00
12	1.7159E+09	2.81E+01
13	1.7369E+09	8.89E+01
14	1.7461E+09	3.12E+01
15	1.7546E+09	2.54E-01
16	1.7588E+09	8.91E-01
17	1.7625E+09	2.28E+00
18	1.7675E+09	6.58E+01
19	1.8147E+09	9.99E+01
20	2.1505E+09	9.92E+01
21	2.3036E+09	1.10E+01
22	2.3218E+09	3.20E+01
23	2.3489E+09	4.29E+01
24	2.3808E+09	4.31E+01
25	2.4170E+09	4.43E+01
26	2.4482E+09	3.55E+01
27	2.5059E+09	7.31E+01
28	2.5422E+09	3.26E+01
29	2.5642E+09	5.02E+01
30	2.5836E+09	4.31E+01
31	2.5994E+09	3.57E+01
32	2.6113E+09	3.19E+01
33	2.6156E+09	2.66E+01
34	2.7470E+09	9.03E+01
35	2.8175E+09	1.53E+01
36	2.8371E+09	3.74E+01
37	2.8650E+09	3.98E+01
38	2.8995E+09	3.13E+01
39	2.9420E+09	3.43E+01
40	2.9831E+09	4.70E+01

Table D-12. Comparisons of stored energy at each end cell between the reference geometry and one of the random perturbed geometry (Dipoles).

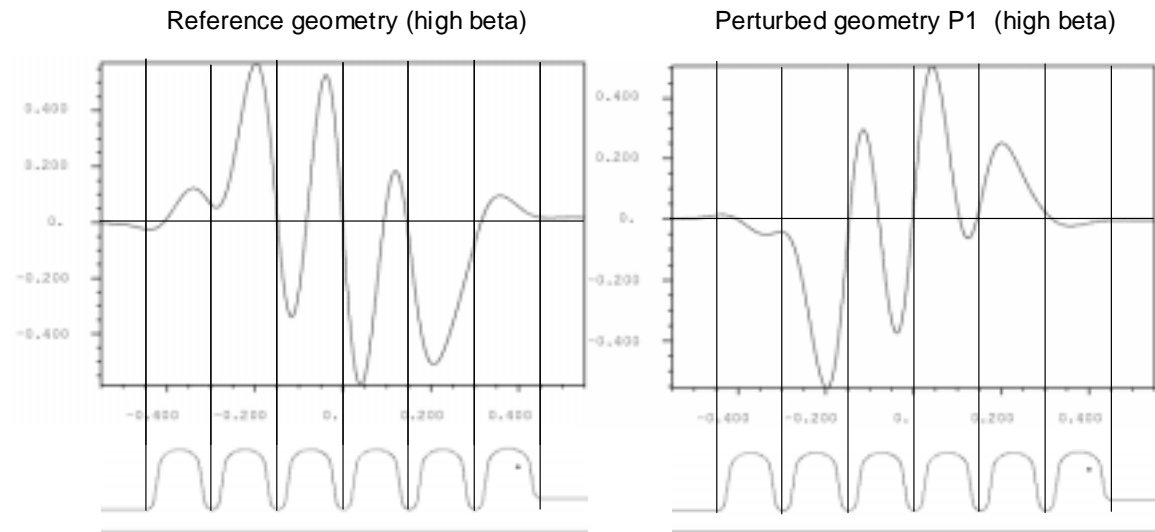
Ref. Geometry Dipoles

mode no.	frequency	right %	left %	total %
1	1.1037E+09	9.97E+01	1.26E-08	9.97E+01
13	1.4848E+09	9.74E+01	9.58E-05	9.74E+01
19	1.8176E+09	9.33E+01	8.99E-04	9.33E+01
20	1.8363E+09	2.47E-08	9.78E+01	9.78E+01
27	2.0800E+09	3.23E+01	3.03E-03	3.23E+01
28	2.0913E+09	3.01E-01	1.58E+00	1.88E+00
31	2.1071E+09	1.04E+00	2.45E+01	2.55E+01
32	2.1161E+09	2.37E-02	8.16E+01	8.16E+01
33	2.1243E+09	9.25E+01	7.75E-04	9.25E+01
34	2.1865E+09	4.63E+01	1.95E-03	4.64E+01

Perturbed geometry Dipoles (Example)

mode no.	frequency	right %	left %	total %
1	11.1026E+09	9.98E+01	2.60E-06	9.98E+01
13	1.4849E+09	9.75E+01	4.12E-04	9.75E+01
19	1.8180E+09	9.29E+01	6.72E-04	9.29E+01
20	1.8372E+09	5.40E-05	9.72E+01	9.72E+01
27	2.0813E+09	3.20E+01	4.18E-03	3.20E+01
28	2.0925E+09	1.53E-01	1.41E+00	1.56E+00
31	2.1077E+09	5.17E-01	3.10E+01	3.15E+01
32	2.1173E+09	7.41E-03	8.58E+01	8.58E+01
33	2.1243E+09	9.26E+01	5.28E-04	9.26E+01
34	2.1852E+09	4.60E+01	1.27E-03	4.60E+01

TM monopoles mode 15



TM monopoles mode 16

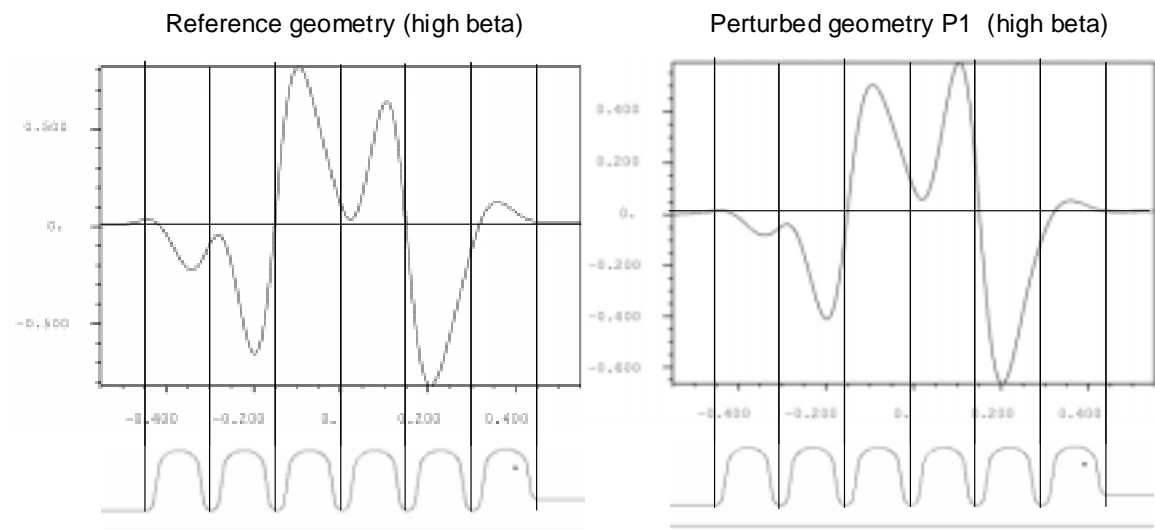


Figure D-3. Axial field profiles comparison between the reference geometry and the perturbed geometry. The modes 15 and 16 of the high beta TM monopoles are possible trapped modes. But these modes are far from the micro bunch resonance frequencies. That means the voltage development from these modes are very small even if these modes high the midi-pulse resonance frequencies.